LOCKHEED MARTIN ENERGY RESEARCH LIBRARIES
3 4456 0514321 6

CENTRAL RESEARCH LIBRARY
DOCUMENT COLLECTION

OAK RIDGE NATIONAL LABORATORY
operated by
UNION CARBIDE CORPORATION
for the
U.S. ATOMIC ENERGY COMMISSION

UNION CARBIDE

ORNL-TM-3212

cy. 1

ORNL NUCLEAR SAFETY RESEARCH AND DEVELOPMENT PROGRAM BIMONTHLY REPORT FOR SEPTEMBER-OCTOBER 1970

Wm. B. Cottrell

OAK RIDGE NATIONAL LABORATORY
CENTRAL RESEARCH LIBRARY
DOCUMENT COLLECTION
LIBRARY LOAN COPY
DO NOT TRANSFER TO ANOTHER PERSON
If you wish someone else to see this document, send in name with document and the library will arrange a loan.
UCN-7969
(3 3-67)

NOTICE This document contains information of a preliminary nature and was prepared primarily for internal use at the Oak Ridge National Laboratory. It is subject to revision or correction and therefore does not represent a final report.

This report was prepared as an account of work sponsored by the United States Government. Neither the United States nor the United States Atomic Energy Commission, nor any of their employees, nor any of their contractors, subcontractors, or their employees, makes any warranty, express or implied, or assumes any legal liability or responsibility for the accuracy, completeness or usefulness of any information, apparatus, product or process disclosed, or represents that its use would not infringe privately owned rights.

ORNL-TM-3212

Contract No. W-7405-eng-26

ORNL NUCLEAR SAFETY RESEARCH AND DEVELOPMENT PROGRAM BIMONTHLY REPORT FOR SEPTEMBER–OCTOBER 1970

Wm. B. Cottrell

JANUARY 1971

OAK RIDGE NATIONAL LABORATORY
Oak Ridge, Tennessee
operated by
UNION CARBIDE CORPORATION
for the
U.S. ATOMIC ENERGY COMMISSION

LOCKHEED MARTIN ENERGY RESEARCH LIBRARIES

3 4456 0514321 6

CONTENTS

	Activity No.	Page
LIST OF PREVIOUS REPORTS IN THIS SERIES		v
ABSTRACT		vii
SUMMARY		ix
1. FAILURE MODES OF ZIRCALOY-CLAD FUEL RODS		1
1.1 Program Objectives and Coordination	04 60 01 10 1	2
1.2 High-Temperature Properties and Metallurgical Evaluation of Zircaloy Cladding	04 60 01 10 1	4
1.3 Cladding Behavior in Loss-of-Coolant Accident Environment	04 60 01 10 1	8
1.4 Transient Tests of Zircaloy-Clad Fuel Rod Clusters in TREAT	04 60 01 10 1	11
1.5 Rupture Tests of Irradiated Fuel Rods	04 60 01 10 1	18
2. LMFBR SAFETY STUDIES		23
2.1 Program Coordination	04 60 01 09 1	24
2.2 Analytical Studies	04 60 01 09 1	27
2.3 Water-System Mockup of FFM Faciltiy	04 60 01 09 1	31
2.4 FFM Noise Analysis	04 60 01 09 1	34
2.5 FFM Facility Activities	04 60 01 09 1	35
3. SPRAY AND PRESSURE-SUPPRESSION TECHNOLOGY		41
3.1 Program Coordination	04 60 80 01 1	42
3.2 Search for Additives to Increase Absorption of CH_3I	04 60 80 01 1	44
3.3 Nuclear Safety Pilot Plant	04 60 80 01 1	48
3.4 Radiation and Thermal Stability of Spray Solutions	04 60 80 01 1	49
3.5 Corrosion Studies in Spray Solutions	04 60 80 01 1	52
4. HTGR SAFETY PROGRAM		53
4.1 Studies of Reactions of Graphite with Steam	04 60 10 01 1	54
4.2 Fuel Integrity and Fission-Product Release	04 60 10 01 1	60
4.3 Fission Products in HTGR Coolant Circuits	04 60 10 01 1	66

5. PRESSURE-VESSEL AND PIPING TECHNOLOGY 73

5.1 Heavy-Section Steel Technology Program 04 60 80 03 1 74

5.2 Experimental and Analytical Investigations of Nozzles 04 60 70 01 1 84

5.3 Design Criteria for Piping, Pumps, and Valves 04 60 80 03 1 98

6. RDT STANDARDS PROGRAM 107

6.1 Program Objectives and Activities 04 60 80 03 1 108

6.2 Reactor Coolant Systems and Equipment Standards 04 60 80 03 1 114

6.3 Instrumentation, Controls, and Electrical Equipment 04 60 80 03 1 117

6.4 Programmatic and Procedural Standards 04 60 80 03 1 119

6.5 Materials and Fabrication 04 60 80 03 1 121

7. GENERAL NUCLEAR SAFETY STUDIES 123

7.1 HTGR Safety Program Office 04 60 70 01 1 124

7.2 LOFT Assistance Program 04 60 60 05 1 125

7.3 Reactor Air-Cleaning Systems 02 04 20 90 131

7.4 Seismicity and the Seismic Resistance of Nuclear Power Plants 04 01 91 01 1 135

8. NUCLEAR SAFETY INFORMATION 137

8.1 Nuclear Safety Information Center 04 60 70 01 1 138

8.2 Technical Progress Review *Nuclear Safety* ... 14 02 01 141

Previous Reports in This Series

Period Covered	Report No.
September—October 1965	ORNL-CF-65-11-2
November—December 1965	ORNL-CF-66-1-41
January—February 1966	ORNL-CF-66-3-13
March—April 1966	ORNL-CF-66-5-20
May—June 1966	ORNL-CF-66-7-48
July—August 1966	ORNL-TM-1636
September—October 1966	ORNL-TM-1680
November—December 1966	ORNL-TM-1742
January—February 1967	ORNL-TM-1792
March—April 1967	ORNL-TM-1864
May—June 1967	ORNL-TM-1913
July—August 1967	ORNL-TM-1986
September—October 1967	ORNL-TM-2057
November—December 1967	ORNL-TM-2095
January—February 1968	ORNL-TM-2164
March—April 1968	ORNL-TM-2230
May—June 1968	ORNL-TM-2283
July—August 1968	ORNL-TM-2368
September—October 1968	ORNL-TM-2425
November—December 1968	ORNL-TM-2479
January—February 1969	ORNL-TM-2533
March—April 1969	ORNL-TM-2588
May—June 1969	ORNL-TM-2663
July—August 1969	ORNL-TM-2718
September—October 1969	ORNL-TM-2777
November—December 1969	ORNL-TM-2829
January—February 1970	ORNL-TM-2919
March—April 1970	ORNL-TM-2984
May—June 1970	ORNL-TM-3061
July—August 1970	ORNL-TM-3122

JOHN W. LANDIS TO PRESENT FEATURE ADDRESS AT ORNL NUCLEAR SAFETY PROGRAM ANNUAL INFORMATION MEETING

The next annual information meeting on the Nuclear Safety Program at ORNL will be held on Tuesday and Wednesday, February 16 and 17, 1971, in the Laboratory's main auditorium in Building 4500. The primary purpose of the meeting is to provide for management review and to keep ORNL staff members informed regarding the status of the multiple safety-oriented problems under study at ORNL.

So much interest has been evidenced in this series of meetings over the last several years, however, that the invitation to attend is extended to others engaged in nuclear safety research and development and to members of the nuclear industrial community at large, as well as to those in the Commission. Sessions are planned to cover the topics of Behavior of Accident-Released Fission Products, Spray and Pool Pressure-Suppression Program, Failure Modes of Zircaloy-Clad Fuel Rods, Filtration and Absorption Technology, Liquid-Metal Fast Breeder and Gas-Cooled Reactor Safety Studies, General Nuclear Safety Studies, and Pressure Vessel and Piping Technology. Questions and discussion will be invited from the audience.

A special feature of this year's meeting will be the dinner on Tuesday evening, February 16, at the Oak Ridge Country Club. John W. Landis, President of Gulf General Atomic and president-elect of the American Nuclear Society, will deliver the address on the subject "Impact of Environmental Critics of the Nuclear Power Industry."

Persons interested in attending the meeting should write to Wm. B. Cottrell, Oak Ridge National Laboratory, P. O. Box Y, Oak Ridge, Tennessee, so that prior clearance into the Laboratory may be arranged. The meeting is unclassified and a registration fee of $10 will be charged to cover the cost of the dinner and other incidental expenses associated with the meeting.

ABSTRACT

The accomplishments during the months of September and October in the research and development program under way at ORNL as part of the U.S. Atomic Energy Commission's Nuclear Safety Program are summarized. Much of this work is in general support of water-cooled power reactor technology, including LOFT and industry programs, and reflects current safety problems, such as measurements of prompt fuel element failure phenomena and the efficacy of containment-spray and filter systems for the removal of accident-released fission products and aerosols from gas streams. Several projects are also conducted in support of the high-temperature gas-cooled reactor (HTGR) and liquid-metal fast breeder reactor (LMFBR) programs. Other major projects include studies of primary piping, steel pressure-vessel technology, and seismic design consideration. Experimental work relative to pressure-vessel technology includes investigations of the attachment of nozzles to shells and the implementation of joint AEC-PVRC programs on heavy-section steel technology and nuclear piping, pumps, and valves. Several of the projects are directly related to another major undertaking; namely, the AEC's standards program, which entails development of engineering safeguards and the establishment of codes and standards for government-owned or -sponsored reactor facilities. The recent activities of NSIC and the *Nuclear Safety* journal in behalf of the nuclear community are also discussed. Of particular interest in both of these activities is the recent emphasis on environmental effects.

SUMMARY

1. Failure Modes of Zircaloy-Clad Fuel Rods

1.1 Program Objectives and Coordination

Several meetings were held recently on Idaho Nuclear Corporation programs that are relative to fuel rod failure areas of research. Some form of assistance on questions of the performance of the fuel rods in the LOFT core is being considered. The assessment of costs and expected program funding has resulted not only in the curtailment of planned bundle tests in both the furnace (argon environment) and in the blowdown facility (water-steam environment) but also the elimination of further bundle tests in TREAT.

1.2 High-Temperature Properties and Metallurgical Evaluation of Zircaloy Cladding

Specimens of annealed, BWR-size cladding are being prepared for transient burst testing for comparison with the results from similar tests on stress-relieved material. A transient burst test on a 32-rod, PWR-type bundle was conducted, but detailed results are not yet available. It is significant that the power supply was adequate to heat all rods and that the heaters constructed in-house operated perfectly. Both 16- and 32-rod experiments are scheduled during the next reporting period.

The pressure drop facility was calibrated with two 32-rod PWR bundles in series. Pressure taps were installed at several locations along the length of the downstream sleeve, and readings were taken at several flow rates from 74 to 575 gpm (4 to 32 ft/sec). The upstream sleeve and bundle are for flow development. The first test of a deformed bundle is scheduled during the next month.

Additional Zircaloy tubes were exposed to a high-temperature steam environment, and metallurgical examination of these specimens is under way. A testing device for impact compression of rings of steam-oxidized Zircaloy cladding was constructed, and experiments were begun to determine ductile-to-brittle transition temperatures as a function of oxidation exposure.

1.3 Cladding Behavior in Loss-of-Coolant Accident Environment

All construction and checkout of the modified loop system is complete. A seven-rod bundle of Zircaloy-clad heater rods is being assembled and will be tested during the coming period.

1.4 Transient Tests of Zircaloy-Clad Fuel Rod Clusters in TREAT

Prior to termination of this work, calculations relating to fuel rod cladding expansion and coolant channel blockage were made with data from the two TREAT experiments. Maximum expansion as a function of maximum pressure correlates well with out-of-pile, inert atmosphere, tube-burst test data. Maximum coolant channel blockage, averaged across the seven-rod bundle, was 48% in the first experiment and greater than 85% in the second experiment. Close examination of the decontaminated outer rods from experiment FRF-1 for locations of rod-to-rod contact allowed reconstruction of the rod orientation at the time of swelling and rupture. It was found that radiation cracking of UO_2 pellets in the irradiated center rod caused a form of fuel rod failure propagation between the center rod and an adjacent rod (H). The 13-rod PWR-size bundle that was to have been used in a TREAT fuel rod failure experiment will be used in a similar hot cell test. Equipment design and construction for the TREAT test to the time of its cancellation are described.

1.5 Rupture Tests of Irradiated Fuel Rods

Seven more BWR-diameter irradiated fuel rods were tested in the hot facility in this continuing program. The results of all valid tests of irradiated rods were analyzed and compared with results of previous tests of unirradiated tubes. The only effect of irradiation on the cladding behavior observed in these tests is a small and somewhat irregular loss in ductility. Equipment for conducting a hot cell test of 13 irradiated rods is being designed.

2. LMFBR Safety Studies

2.1 Program Coordination

A detailed experimental program for Test Series I, which includes the baseline tests and the partial blockage experiments in the fuel failure mockup (FFM) facility, was completed and sent to AEC, ANL, and HEDL for review. Systems acceptance procedures, operating and maintenance procedures, and the final system design description are nearly complete. Coordination has been maintained with AEC and HEDL and has been initiated with AI.

2.2 Analytical Studies

Calculations of the temperature distribution within electric heater rods with partial surface blockage were continued. Calculations of UO_2 fuel rods with similar boundary conditions were performed for comparison. Estimates were made on the effect of using stainless steel as a blockage material compared with UO_2. Data-handling programs were initiated by the PDP-8-Dextir system, and data-treatment and plotting programs were initiated for use on the IBM 360 model 91 with FFM data tapes.

2.3 Water-System Mockup of FFM Facility

Tests were performed on the dynamically cooled water mockup of the FFM inlet piping to determine the need for turning vanes or flow straighteners. It was found that the flow profile at the inlet of the test bundle is adequately flat, and turning vanes are not needed.

2.4 FFM Noise Analysis

Most of the effort this month was on evaluating diagrammatic techniques on HFIR. Final arrangements were made for installing noise monitoring and analyzing equipment in the FFM.

2.5 FFM Facility Activities

Construction work was essentially completed, except for the installation of the oxide control and indication (OCI) package, and electrical shakedown in under way. An analysis of stresses due thermal transients

in the FFM that might be caused by loss of power at full flow showed that the FFM could be expected to survive at least 100 such cycles.

3. Spray and Pressure-Suppression Technology

3.1 Program Coordination

Two program reports were issued and three others are being edited. The reports cover protective coating tests, BWR coolant radiolysis, elemental iodine removal by sprays, and a methyl iodide bibliography.

3.2 Search for Additives to Increase Absorption of CH_3I

The effects of additive concentration and temperature on the rate of reaction of CH_3I with a base-borate solution containing a small quantity of a rare-earth complex (10^{-4} to 10^{-5} *M*) are given. Rates comparable to those for the base borate-thiosulfate system have been measured.

3.3 Nuclear Safety Pilot Plant

Reports detailing the completed spray program experiments and a methyl iodide bibliography were completed.

3.4 Radiation and Thermal Stability of Spray Solutions

Dynamic loop tests are being run to confirm the use of $NaVO_3$ as a hydrogen recombiner. Preliminary results confirm earlier capsule tests.

Zinc-loaded primer paints were tested for evaluation of hydrogen production when exposed to high temperatures and to spray solutions. Initial results indicate that a large fraction of the zinc is reacted to form hydrogen.

3.5 Corrosion Studies in Spray Solutions

Low-pH (4.5, 7.5) loop tests are in progress. Preliminary results are expected soon.

4. HTGR Safety Program

4.1 Studies of Reactions of Graphite with Steam

Samples of H-327 graphite received from different sources and manufactured at different times were found to differ in impurity content. It is suggested, on the basis of previous observations on catalysis of the steam-carbon reaction, that these differences may be responsible for the observed differences in oxidation rate. There is reason to believe that the H-327 graphite obtained from the vendors in 1968 (that having the lower oxidation rate) is not typical of material being used in the Fort St. Vrain Reactor.

The first model fuel element has been exposed to steam in-pile. After 25% of the total carbon had been removed the average radial thermal conductivity of the fuel element was observed to have been halved. Corrosion was by a pitting mechanism, as in the laboratory, and radiolytic reactions were unimportant at those temperatures where the corrosion rate was significant. While some fuel coatings failed, little fission-product loss occurred.

4.2 Fuel Integrity and Fission-Product Release

An irradiated bonded bed of BISO-coated UO_2 particles was annealed at 1250°C. The cesium release at the end of a 2500-hr anneal was 25%. The postannealing examination revealed no failure of outer pyrolytic-carbon coatings of the coated UO_2 particles. Individual BISO-coated UO_2 particles were annealed at 1400°C. Diffusion coefficients calculated for cesium in the pyrolytic-carbon coating ranged from 2.6×10^{-11} to 1.3×10^{-10} cm^2/sec. The cesium release ranged from 0.5 to 17%.

SiC layers in TRISO-coated fuel particles broke down at temperatures above 1800°C and released solid fission products. The failure of the SiC may be due to cracking or possibly to porosity. The Walther Stress 2 computer code was used to analyze the mode of failure. This study showed a high probability of SiC coating failure without simultaneous pyrolytic-carbon coating failure in the TRISO-coated particles and indicated a relation between internal fission-gas pressure and failure of the SiC. The calculations compared favorably with experimental results.

4.3 Fission Products in an HTGR Coolant Circuit

Exploratory aerosol generation tests and equipment acquisition are under way in preparation for construction of the dust deposition facility (DDF). Comparative wall shear stresses in the DDF flow channel and a commercial HTGR coolant duct were estimated to determine corresponding reentrainment conditions.

Equipment for fission-product surveillance at Peach Bottom HTGR continues to be evaluated. Some additional observations on Peach Bottom diffusion-probe and filter samples were made. The conclusions remain unaltered.

5. Pressure-Vessel and Piping Technology

5.1 Heavy-Section Steel Technology Program

Three reports were issued under the HSST program, and six are under review or in the reproduction process. Fabrication of the intermediate test vessels is proceeding; however, unexpectedly high tensile properties in the cylindrical test sections have delayed final assembly of the vessels.

Work is continuing in the variability and fracture mechanics investigations. A new activity to investigate further the behavior of thick sections in the transition and tough regimes was initiated. Both experimental and analytical tasks are involved.

Recent results from the irradiation of Charpy V-notch and dynamic-tear specimens became available. Postirradiation shelf values of Charpy V-notch and dynamic-tear specimens show a linear correlation. Irradiations of submerged-arc welds showed a transition shift of some 200°F for a fluence of 1×10^{19} neutrons/cm^2 ($E > 1$ Mev) at 550°F. The shelf was also lowered significantly. A similar study on an electroslag weld showed that irradiation produced much less degradation. A feasibility study for irradiating 4T compact-tension specimens continues.

A procedure for locally fatiguing machined flaws by internal pressure was developed. The method was successfully applied to two large flawed (6-in.-thick) tensile specimens.

Three large flawed tensile specimens (18 in. long and 6 in. thick) were tested, one at 75°F and two at 100°F. This completed the tests of the first series of six specimens. Flat fracture was obtained at 50, 75, and 100°F. Ductile fracture was also obtained at 100°F and at 215°F. The anomalous behavior at 100°F is being investigated further. The fracture behavior of five of the six specimens was successfully predicted; the tough behavior specimen at 100°F was the exception.

Drafts of final reports on both the thermal-shock investigation and the correlation of Charpy V-notch energy and fracture toughness were received.

5.2 Experimental and Analytical Investigations of Nozzles

Experimental and analytical studies of nozzles attached to shells, as well as studies of perforated models of pressure vessels, are continuing. Reports are currently being prepared on the results of many of the studies, including (1) an analysis of a radial nozzle attached to a cylindrical shell compared with photoelastic results, (2) analyses of perforated flat plates and plates with nozzle clusters, (3) analysis of stepped cylindrical shells, (4) analysis of radial nozzle reinforcement, (5) pressure test of a spherical vessel containing clusters of holes, (6) plastic collapse test of a large thin-walled tee under internal pressure, (7) tests of two 7.002-in.-OD radial nozzles subject to thrust and moment loadings, (8) analyses of single nonradial nozzles, and (9) computer data plots from tests of a 22 1/2° nonradial nozzle. Also a report describing a method for computerized plotting of stress versus profile drawings developed at the University of Tennessee is being revised prior to release.

At the University of Tennessee, testing of the 2.625-in.-OD, 22 1/2° nonradial nozzle, which was bored to 0.0625-in. wall thickness, is under way.

At Auburn University tests will begin soon on a one-nozzle flat-plate model, and a two-nozzle hemispherical-shell model is being modified to include two additional nozzles.

5.3 Design Criteria for Piping, Pumps, and Valves

Both analytical and experimental tasks are in progress under the ORNL portion of the joint AEC(ORNL)-Industry(PVRC) program to develop stress indices and flexibility factors for nuclear-service piping, pumps, and valves. Projects under the ORNL piping program are currently under way both at ORNL and at various facilities under subcontract to ORNL. Subcontract work is being done at Auburn University, the University of California, Battelle Memorial Institute, Combustion Engineering, Inc., Southwest Research Institute, and Westinghouse Research Laboratories.

Three of the five 12-in. ASA B16.9 tees being tested for elastic response and low-cycle fatigue failure at SwRI had indicated apparent nonlinear strain-gage response for several of the loadings. This apparent anomaly was corrected, and one of the tees (T-8) was retested. T-6 and T-15 will be retested before the fatigue tests are conducted. Currently, T-7 and T-8 are being fatigue tested with target failure points of 7000 cycles.

Elastic-response tests of T-10, a 24 × 24 × 24-in. carbon steel ASA B16.9 tee being tested at CE, were completed. The tee is currently being fatigue tested with an in-plane bending moment on the branch pipe. The target failure point is 7000 cycles.

Surface stresses were determined for two of the four photoelastic models of 12-in. ASA B16.9 tees being analyzed at Westinghouse Research Laboratories. The two remaining models are being analyzed.

Finite-element stress calculations, being developed at the University of California, were made for T-8 and compared with the strain-gage data obtained at SwRI. Excellent agreement was found for the out-of-plane bending load on the branch pipe. Results from the other loadings are currently being plotted for comparison.

A series of fourteen 6-in.-elbow limit load tests was completed at ORNL, and previously unreported plastic limit load data obtained from Tube Turns, Inc., were analyzed. Both sets of data will be used to establish primary load stress indices (B indices) for code use.

6. RDT Standards Program

6.1 Program Objectives and Activities

The prime responsibility for organizing, developing, preparing, and distributing engineering standards was assigned to the Oak Ridge National Laboratory by the AEC Division of Reactor Development and Technology. The RDT Standards Group at ORNL prepares standards applicable to water-cooled reactor systems and liquid-metal-cooled systems. The standards for the liquid-metal-cooled systems are prepared in cooperation with the Liquid Metal Engineering Center (LMEC), which has the prime responsibility.

Typical program activities include (1) analyzing RDT project needs for standards; (2) providing assistance in application of standards to reactor projects under the direction of RDT; (3) preparing and distributing new standards and revising and updating existing standards; and (4) directing and reviewing the participation of subcontractors and engineering consultants in the standards program.

During this period, two standards were issued as tentative RDT standards; 11 drafts were submitted to RDT for approval; four standards prepared by LMEC were reviewed, and comments received on eight drafts prepared by ORNL are being evaluated. RDT numbers were assigned for 19 new standards. In total, 91 tentative standards are available for use and 93 draft standards are awaiting approval by RDT.

6.2 Reactor Coolant Systems and Equipment Standards

Work continued in preparing and revising drafts and in reviewing and evaluating comments received on piping, valve, pump, static seal, heat exchanger, and pressurizer standards. Included in this are a number of standards prepared for use by LOFT, and additional standards were requested. Planning was initiated on standards for radioactive waste systems and containment spray systems.

6.3 Instrumentation, Controls, and Electrical Equipment

Activities included ORNL review of drafts prepared by LMEC, correlation of comments, transmittal of two tentative standards approved by RDT, and preparation of draft standards.

6.4 Programmatic and Procedural Standards

Work continued in preparation of drafts, review and evaluation of comments, and revision of quality-assurance, cleaning, and air-cleaning standards. A revised proposal for the seismic standards program is being prepared and will be resubmitted to RDT.

6.5 Materials and Fabrication

Comments received on materials standards are being reviewed and evaluated.

7. General Nuclear Safety Studies

7.1 HTGR Safety Program Office

The HTGR Safety Program Office undertakes continuous evaluation of the needs and accomplishments of the HTGR safety research and development program. Principal activity during the past month has been concerned with the participation in safety evaluation of the Fort St. Vrain reactor for an operating license.

7.2 LOFT Assistance Program

The investigation of the natural deposition behavior and the accompanying changes in chemical form of radioiodine released in the CRI Amercoat-lined containment vessel has confirmed an expectation of a highly irreversible sorption process. Change in chemical form is apparently sensitive to iodine mass concentration and is shown by a hundredfold decrease in the total amount of persistent iodine (CH_3I) produced over the range from 0.03% to greater than 3% of the total iodine inventory.

7.3 Reactor Air-Cleaning Systems

In one investigation the contribution of iodine produced as tellurium daughters on the possible ignition of a charcoal adsorber was examined. It was concluded that the tellurium will react in such a manner as to preclude that iodine from reaching the bed and that it represents a significant fraction of the decay heat. In another investigation the

efficiencies of commercial absolute filter media as a function of velocity are being determined by using an electric arc-generated stainless steel oxide-UO_2 aerosol. This oxide aerosol is a good facsimile of anticipated reactor accident aerosols. Some preliminary data are reported that show maximum penetration in the velocity range 10 to 20 ft/min.

7.4 Seismicity and the Seismic Resistance of Nuclear Power Plants

A preliminary draft was received on the report being prepared by UCLA on the explosive response test work conducted during July and August 1970 at the EGCR. Analysis of the data obtained is continuing. ORNL met in Washington with AEC representatives and ORNL soil and seismic consultants to review the recently submitted SW-AJA Program Definition report. SW-AJA is preparing a state-of-the-art report on soils properties and behavior. A proposal to develop seismic design input criteria for siting nuclear reactors is being reviewed.

8. Nuclear Safety Information

8.1 Nuclear Safety Information Center

The Nuclear Safety Information Center was established by the USAEC to collect, evaluate, and disseminate nuclear safety information to governmental agencies, research and educational institutions, and the nuclear industry. Two new cathode-ray-tube terminals for communication with the central computer were installed and placed in service during September, bringing the total number of scopes at NSIC to four. Three state-of-the-art reports were recently completed and are currently undergoing review. Two reports were published, and NSIC responded to 308 inquiries, of which 143 were technical.

8.2 Technical Progress Review *Nuclear Safety*

The September–October 1970 issue of *Nuclear Safety*, a bimonthly Technical Progress Review sponsored by AEC's Division of Technical Information, was distributed in mid-September. It contained a lead article entitled "The AEC Goes Public — A Case History," by Howard C. Brown, Jr.,

AEC Assistant General Manager. Other articles were written by four non-ORNL and six ORNL authors, including four journal staff members. Subsequent issues of *Nuclear Safety* through the November–December 1971 issue are in various stages of development.

1. FAILURE MODES OF ZIRCALOY-CLAD FUEL RODS

P. L. Rittenhouse, Program Coordinator

1.1 PROGRAM OBJECTIVES AND COORDINATION

(AEC Activity 04 60 01 10 1)

P. L. Rittenhouse

One of the accidents considered "credible" for light-water reactors is the loss-of-coolant accident. In this accident a rupture in some portion of the reactor primary system results in loss of coolant and pressure. The heat stored in the fuel then quickly redistributes and causes a rapid increase in the temperature of the fuel cladding. Decay heat contributes to this initial rapid temperature increase and also causes a continued, but less rapid, increase after the stored heat redistribution period. A third contribution to increase in cladding temperature, substantial only above 2000°F, is the heat of the exothermic reaction between the Zircaloy cladding and steam. Emergency core-cooling systems are provided in light-water reactors to arrest the temperature transient prior to the attainment of any condition compromising an acceptable termination of the accident. Even with the emergency core-cooling system operating at full efficiency, portions of the reactor core will reach temperatures sufficient to cause deformation and rupture of the fuel rods. The deformation (swelling) of the rods prior to rupture can be considerable and could restrict passage or cause bypass of emergency coolant to such an extent that the deformed sections would be inefficiently cooled. This, in turn, might result in embrittlement, disintegration, or melting of the rods. Because of these possibilities, efforts are under way to assess the modes of failure of the fuel cladding in terms of accident conditions and reactor operating history and to determine the effect of the failures on emergency cooling performance. It is also necessary to determine the margins of safety relative to the above.

Discussions were held recently in Idaho with members of Idaho Nuclear Corporation on several of their projects related to fuel rod failure. These included the Power Burst Facility, LOFT, and FLECHT programs. Several avenues of action related to experimental information needed to analyze LOFT core reusability are currently being investigated. The results of BWR-FLECHT, especially in relation to the metallurgical behavior of the Zircaloy-clad heater rods, were discussed with General Electric

personnel at San Jose. Heaters incorporating ZrO_2 or other material more compatible with zirconium than Al_2O_3 were considered.

Discussions were also held with the AEC regarding program priorities and the allocation of available funds. The strike at the Union Carbide Corporation operations in Oak Ridge last spring caused deferment of significant facility modifications and costs into FY-1971, with the result that planned testing must be curtailed. This will reduce the work on "High-Temperature Properties and Metallurgical Evaluation of Zircaloy Cladding," Section 1.2, by 25% or more; the blowdown tests in "Cladding Behavior in Loss-of-Coolant Accident Experiments," Section 1.3, to two (50% reduction); and eliminate any further work on the TREAT test (Sect. 1.4) this year. However, it is proposed to compensate for the loss of the TREAT tests by using irradiated rods scheduled for use in that test in a hot cell transient burst test (Sect. 1.5).

1.2 HIGH-TEMPERATURE PROPERTIES AND METALLURGICAL EVALUATION OF ZIRCALOY CLADDING

(AEC Activity 04 60 01 10 1)

R. D. Waddell, Jr. D. O. Hobson
W. R. Gambill P. L. Rittenhouse

Studies of the transient burst behavior and embrittlement of Zircaloy cladding were continued. The information being obtained is needed to assess the degree, type, and extent of core damage and blockage under a wide range of accident conditions.

Transient Burst Tests

Specimens of annealed, BWR-size tubing are being prepared for single-rod burst testing. The data generated in these tests will be compared with that obtained previously in single-rod tests of as-received (stress-relieved) tubing. Test parameters, heating rates, and internal pressures will cover the range of conditions that produced high expansions (50, 100, and 700 psig at 10 and 100°F/sec) and low expansions (400 psig at 10 and 100°F/sec) in the earlier tests.

The first transient burst test of a 32-rod bundle was successfully accomplished on October 23. The bundle was of PWR-configuration (tubing size and spacing), with an Inconel grid spacer at mid-elevation. All rods were pressurized to 210 psig at 600°F and then heated at 10°F/sec to failure. The bundle has not yet been sectioned; therefore, neither values of individual tube expansion nor coolant channel blockage are available. However, it appears that the degree of individual tube expansion is consistent with that in single-rod transient tests under the same test conditions (i.e., less than 50% circumferential expansion). It was significant that the "home-made" internal heaters, as well as the power supply and programmer, appeared to work perfectly. These heaters are the type designed for use in all subsequent PWR bundles.

The 16-rod bundle received from Combustion Engineering was fitted with heaters, and both ends of all tubes were welded. After each tube is fitted with pressurizing lines and the heater leads are insulated, the bundle will be placed in the sleeve provided by Combustion Engineering and

assembled in the ORNL test facility. This test is scheduled for November 3. Combustion Engineering has requested test parameters of 200 psig and 90°F/sec.

Pressure Drop in Deformed Rod Bundles

Axial static-pressure distributions will be measured for 32-rod, grid-spaced bundles before and after rod deformation by radial swelling (modeling of cladding distortion in loss-of-coolant accidents). It is anticipated that observed pressure-drop changes can be related to the particular deformation patterns in the test bundle.

Two undeformed bundles, each containing thirty-two 0.420-in.-OD 2-ft-long rods on a square pitch, were received; these were used for baseline measurements of the static-pressure gradient. The system piping was completed, and nine pressure-tap tubes were welded in place. O-rings were placed under the six set screws bearing on the cage-type spacers, and hexagonal rubber gaskets were cut for the flanged connections. All rods in the upstream flow-development bundle were tight, but several rods in the downstream test bundle were loose. This was corrected by slightly expanding the holes behind the spacer dimples.

The first test series consisted of nine runs with water at about 30°C and flow rates from 205 to 575 gpm. The mean line of pressure drop versus flow was in good agreement with calculated values, but the average data scatter (6.2%) was considered somewhat high. Posttest examination showed that each bundle had shifted in the downstream direction, and the spacers were therefore modified by penetrating the edge straps with the set screws to prevent axial bundle shifting.

The second test series, consisting of 12 runs with water at about 30°C, produced pressure drops ranging from 0.27 psi at a minimum flow rate of 73 gpm to 4.88 psi at a maximum flow rate of 376 gpm. No bundle shifting occurred, and the average data scatter was 3.6%. All results noted relate to pressure taps 15 in. apart in the downstream bundle. For all 21 tests taken together, the Reynolds number (based on equivalent diameter) varied from 1.7×10^4 to 1.33×10^5.

The swollen bundle described in the preceding section will be tested next.

Evaluation of Fuel Rod Embrittlement Due to a Loss-of-Coolant Accident

In the preceding report of this series the metallographic examination of a number of PWR-size Zircaloy tubes that had been heated to temperatures between 2200 to 2500°F in steam and then quenched in cold water was discussed. Since then specimens were received with which to extend the temperature range down to 1800°F and to give a range of times at 2200°F of from 4 to 16 min. The specimens exposed at 1800°F were held at temperature for up to 1 hr. Metallographic and hardness examinations are in progress on these specimens.

As mentioned previously, ring specimens from these tubes are to be tested at elevated temperatures to determine the ductile-to-brittle transition temperature. These rings will be diametrally flattened (impact-compression along a diameter) predetermined amounts at various temperatures. The amounts of flattening required to produce tensile strains in the outer fibers of the rings equal to the longitudinal strains that would occur in the outer fibers of PWR fuel tubes horizontally deflected various amounts have been calculated. It was assumed that these tubes would be supported in a vertical position between grids spaced 18 in. apart and that the tubes would deflect into a circular arc. Calculations based on radius of curvature, changes with ring compression, neutral axis position, and outer circumference expansion gave strain data for the ring specimens. The two sets of data were combined to give the graph shown in Fig. 1.1, which is applicable to PWR tubing. From this graph it is possible to read the amount the outside diameter of a ring must be compressed to give an outer fiber strain equal to that strain in the outer fiber of a tube that has been deflected a given amount between grids. Similar data are available for BWR-size tubing. Strains were also calculated for layers inside the outer surface in rings of both sizes. The latter data are useful for calculating strains beneath the oxide layer.

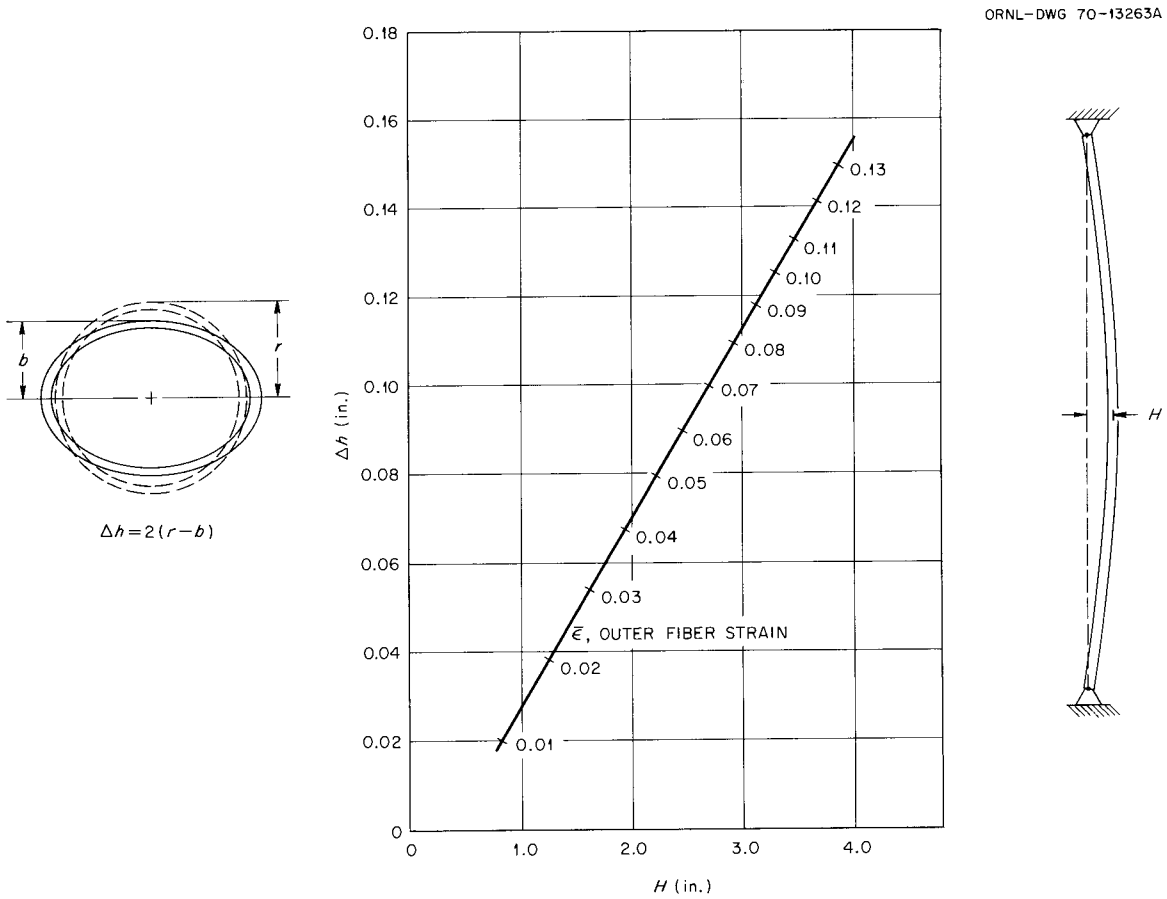

Fig. 1.1. Curve Correlating Diametral Compression with Postulated Fuel Tube Deflection to Give Equivalent Outer Fiber Strains.

A testing device capable of producing diametral strains in ring specimens to an accuracy of ±0.001 in. of compressive height change was designed and built. This device is inside a furnace capable of temperatures up to 1800°F. Ring specimens were cut from all specimen tubes, and testing was started.

1.3 CLADDING BEHAVIOR IN LOSS-OF-COOLANT ACCIDENT ENVIRONMENT (AEC Activity 04 60 01 10 1)

C. G. Lawson T. H. Mauney

The response of heated rods constructed to simulate fuel rods and subjected to simultaneous loss of system coolant and pressure is being studied in an experimental facility that consists of a closed-cycle high-pressure water-cooled loop that can be emptied and depressurized through a pipeline containing a dual rupture-disk assembly and a sharp-edged discharge orifice. A spray tank absorbs the thermal energy of the discharged water. Selection of an appropriate discharge orifice controls the depressurization and coolant-loss time to simulate a postulated loss-of-coolant accident for either a PWR or BWR. A preset program controls the test section power to simulate a change from full reactor power to appropriate decay heat levels at any chosen time after the rupture disks fail for a bundle of seven 2-ft-long rods.

All construction associated with the current phase of the tests was completed, and all systems were checked out for circuit logic and construction according to design. The only remaining operating checkouts require a heated seven-rod cluster. The loop, including all construction, control system, and material changes, was operated satisfactorily for a period of 24 continuous hours. About 80% of this time was at full pressure and temperature on automatic control. This operation was performed with an unheated dummy assembly in the place of the seven-rod cluster.

A cluster of seven heater rods is now being assembled within the test section. The assembly is shown in cross section in Fig. 1.2. The parameters of the seven-rod cluster are compared with those of a typical PWR fuel bundle in Table 1.1. For the fuel rod failure program, these parameters are close enough to permit comparison of cladding growth under transient conditions.

Assembly of the cluster within the test section was slowed as a result of budget difficulties. The test section housing was in use during the loop preliminary testing. To conserve funds no spares were fabricated. Costs carried over from FY-1970 as a result of the craft strike in Oak Ridge plants resulted in a reduction of approximately one-half the FY-1971

Table 1.1. Comparison of Parameters of PWR Fuel Bundle and Test Bundle

Parameters	Test Bundle	Typical BWR Bundle
Array	Seven rod hexagonal pattern	15 × 15 square pattern
Fuel rod length, ft	2	15
Fuel rod diameter, in.	0.5	0.422
Lattice open area, %	37	45
Coolant mass velocity, $lb_m/ft^2 \cdot hr$	$\sim 1 \times 10^6$	$\sim 2 \times 10^6$
Coolant inlet temperature, °F	500	545
Coolant outlet temperature, °F (av)	585	600
Axial coolant temperature drop, °F	85	55 av, 85 max
Coolant pressure, psia	1500	2200
Axial power rating, kw/ft	19 (uniform)	19 peak
Surface heat flux, $Btu/hr \cdot ft^2$	495,000	600,000
Average internal rod temperature, °F	1900	2500
Estimated DNB flux, $Btu/hr \cdot ft^2$	$\sim 800 \times 10^3$	
Cladding material	Zircaloy	Zircaloy
Cladding thickness, in.	0.035	0.026
Filler material	MgO and Kanthal A-1 wire	UO_2
Gas gap at full power	None	None
Coefficient of thermal expansion, $°C^{-1}$		
Cladding	5×10^{-6}	5×10^{-6}
Filler	10×10^{-6}	11×10^{-6}
Ratio of cladding thickness to tube inside diameter	0.74	0.703
Heater or fuel time constant, sec		
With no gas gap	~ 7	~ 6
With gap	~ 15	Unknown

ORNL-DWG 70-5280

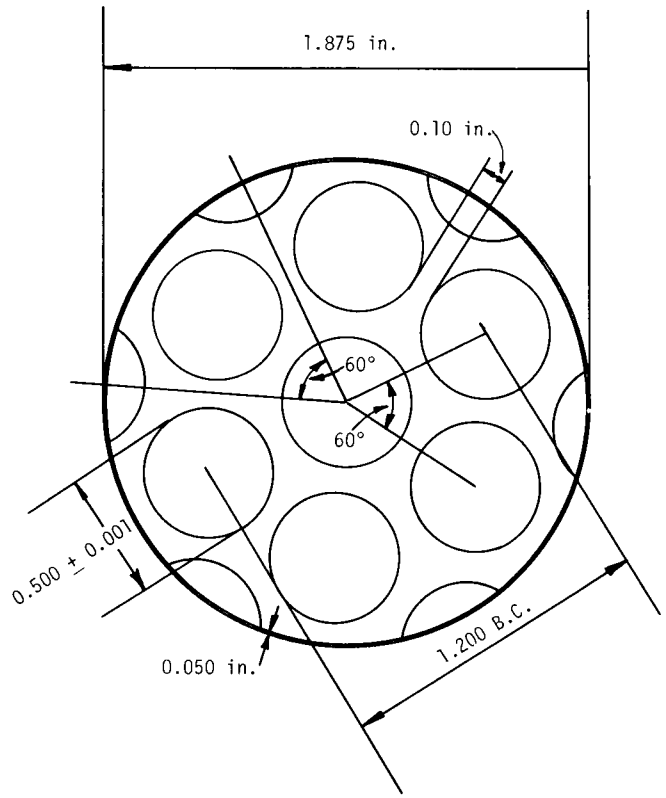

Fig. 1.2. Plan View of Zircaloy-Clad Seven-Rod Heater Cluster.

operating budget. Consequently, only two blowdown tests in this facility are now contemplated in FY-1971.

The test now being prepared will be performed with the load orifices in the loop distributed to force the major portion of the blowdown coolant to bypass the heated rods in the test section. This should force the heater rods into a critical heat flux condition during the early portion of the saturated blowdown. The initial testing with the first seven-rod bundle will involve a reduction in heat to the rods to simulate reactor scram and decay heat generation when saturation conditions are reached. Under these conditions, which simulate a design reactor blowdown, the transient, transitional heat-transfer rates will probably recover the cladding temperature and prevent heating beyond 2000°F. If this proves to be the case, subsequent experiments will be conducted on the same bundle with longer scram delay times.

1.4 TRANSIENT TESTS OF ZIRCALOY-CLAD FUEL ROD CLUSTERS IN TREAT

(AEC Activity 04 60 01 10 1)

R. A. Lorenz G. W. Parker

Fuel rod failure under water reactor loss-of-coolant conditions is being investigated in TREAT with seven-rod clusters of Zircaloy-clad UO_2 fuel rods. In a reactor, emergency cooling systems are designed to prevent excessive fuel rod temperatures in spite of many ruptured rods, and the TREAT experiments are being conducted to determine under realistic in-reactor conditions whether swelling and rupture of fuel rods will interfere with emergency cooling effectiveness. In TREAT, fissioning in the UO_2 pellets provides duplication of the stored energy and decay heat that would be expected if a loss-of-coolant accident occurred.

Analyses of the first two TREAT tests (designated FRF-1 and FRF-2) are reported here, although work toward further TREAT tests has been terminated. In both the first two tests, the test assembly consisted of a seven-rod cluster of 27-in.-long Zircaloy-clad UO_2 fuel rods. The center rod contained fission products from irradiation in either the MTR or ETR in order to test the effect of irradiation on rupture characteristics, as well as to measure fission-product release. The rods were pressurized with helium to simulate fission-gas accumulation after high burnup. The tests were performed by operating the reactor at steady power so that fission heat in the UO_2 pellets raised the cladding temperature sufficiently to duplicate temperature behavior that would occur immediately following blowdown caused by a loss-of-coolant accident. A flowing steam atmosphere simulated residual steam boil-off from the reactor vessel. Preliminary information from these experiments was reported previously, and additional calculations relating to swelling of the cladding are reported here.

Correlation of Maximum Circumferential Expansion

Waddell, Hobson, and Rittenhouse found a ductility minimum from tube-burst tests with Zircaloy-4 tubing in an argon atmosphere.[1] The minimum occurs around 1700°F, where Zircaloy is in the $\alpha + \beta$ two-phase region.

For tube-burst tests with typical BWR tubing at heating rates between 10 and 50°F/sec, this condition corresponds to a maximum measured pressure differential of 450 psi. The envelope of data for these tube-burst tests is shown in Fig. 1.3, where maximum circumferential expansion is plotted as a function of maximum pressure differential. Data from rods in the TREAT experiments are also plotted. Maximum pressure was calculated for most TREAT rods, since only two were pressure-monitored in each experiment. The letter C designates the center irradiated rods. Agreement with baseline tube-burst data is favorable in spite of irradiation of two rods and major experimental differences, such as atmosphere, heat source, rod and plenum length, and radial temperature gradient (experiment FRF-1).

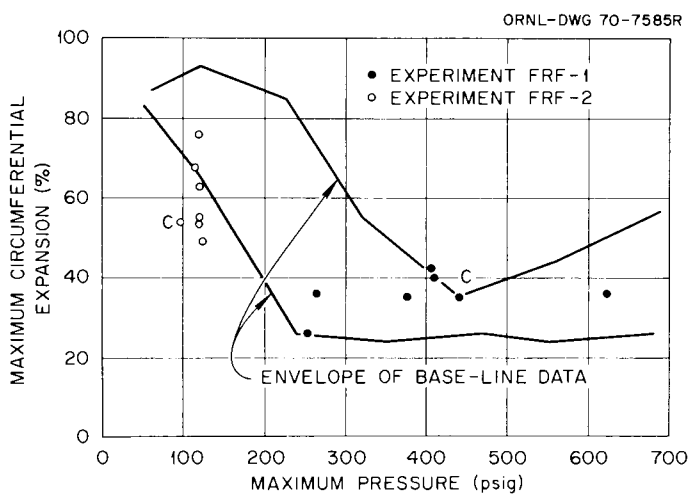

Fig. 1.3. Fit of FRF-1 and FRF-2 Cladding Expansion Data to Baseline Data.

Coolant Channel Blockage

The average diameters were measured along the length of each rod with micrometers on the outer rods and photographs of the center irradiated rods. Individual coolant channel size could not be measured directly, so the average rod cross-section was subtracted from the total area. In experiment FRF-2 the total area was greater than that occupied by seven rods

in a typical BWR spacing, so this calculation was performed with actual experiment total area and also with typical BWR total area.

The results are shown in Fig. 1.4. The maximum coolant channel blockage was 48% in experiment FRF-1. Maximum blockage in experiment FRF-2 was between 85 and 106%, depending on the reference total area. The greater cladding expansion and coolant channel blockage in experiment FRF-2 may be attributed to the more uniform radial temperature provided by the reflective heat shield and a lower gas pressure. The lower pressure allowed expansion to occur at a higher temperature, where the Zircaloy is more ductile.

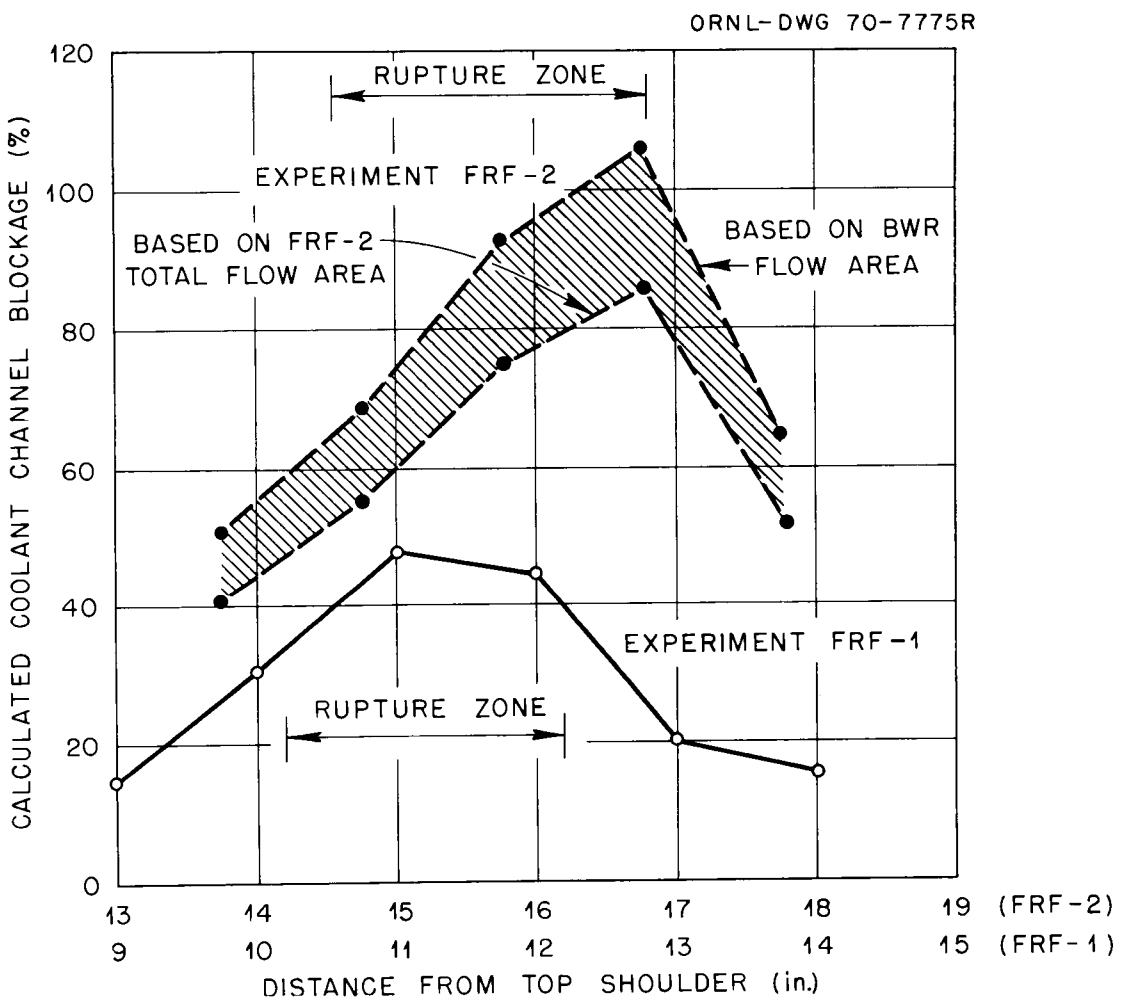

Fig. 1.4. Coolant Channel Blockage for BWR Rod Spacing.

Fuel Rod Failure Propagation in Experiment FRF-1

The fuel pellets were removed from the outer rods of experiment FRF-1, and the cladding was examined for evidence of rod-to-rod contact that was not detectable from photographs previously used for this purpose. Figure 1.5 is a diagram showing the direction of rupture and the points of contact where pressure was sufficient to cause cladding deformation. The close examination permitted accurate reconstruction of the orientation of the rods at the time of swelling and rupture.

The center rod contacted every other rod at some point with sufficient pressure to cause metal deformation. Most points of contact can be seen in Figs. 1.6 and 1.7. The center rod contacted rod 4-1 at 10.7 in. from the top shoulder, rod R at 11.6 in., rod 4-2 at 11.0 in., rod L at 11.6 in., rod I at 10.2 in., and rod H at 120.0 in. Other rod contacts that caused deformation occurred between rods 4-1 and H at 10.7 in., rods 4-2 and L at 10.9 in., and rods 4-2 and R at 11.6 in. The median location for rod-to-rod contact is 11.0 in. from the top shoulder, which is precisely the location found for maximum coolant channel blockage.

The contact between the center rod and rod H occurred almost directly at the points of rupture. The metal on the right side of the rod H rupture was, as may be seen in Fig. 1.6, depressed more than 1/16 in. by a piece of material approximately 1/16 in. square. It is believed that a chip of UO_2 from the ruptured center rod caused the depression. Calculations based on

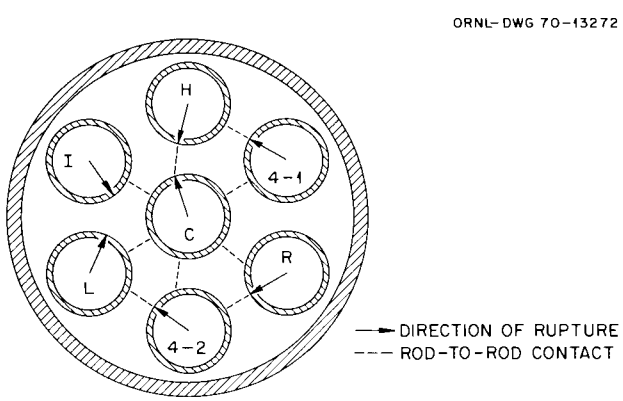

Fig. 1.5. Direction of Rupture and Fuel Rod Contact in TREAT Experiment FRF-1.

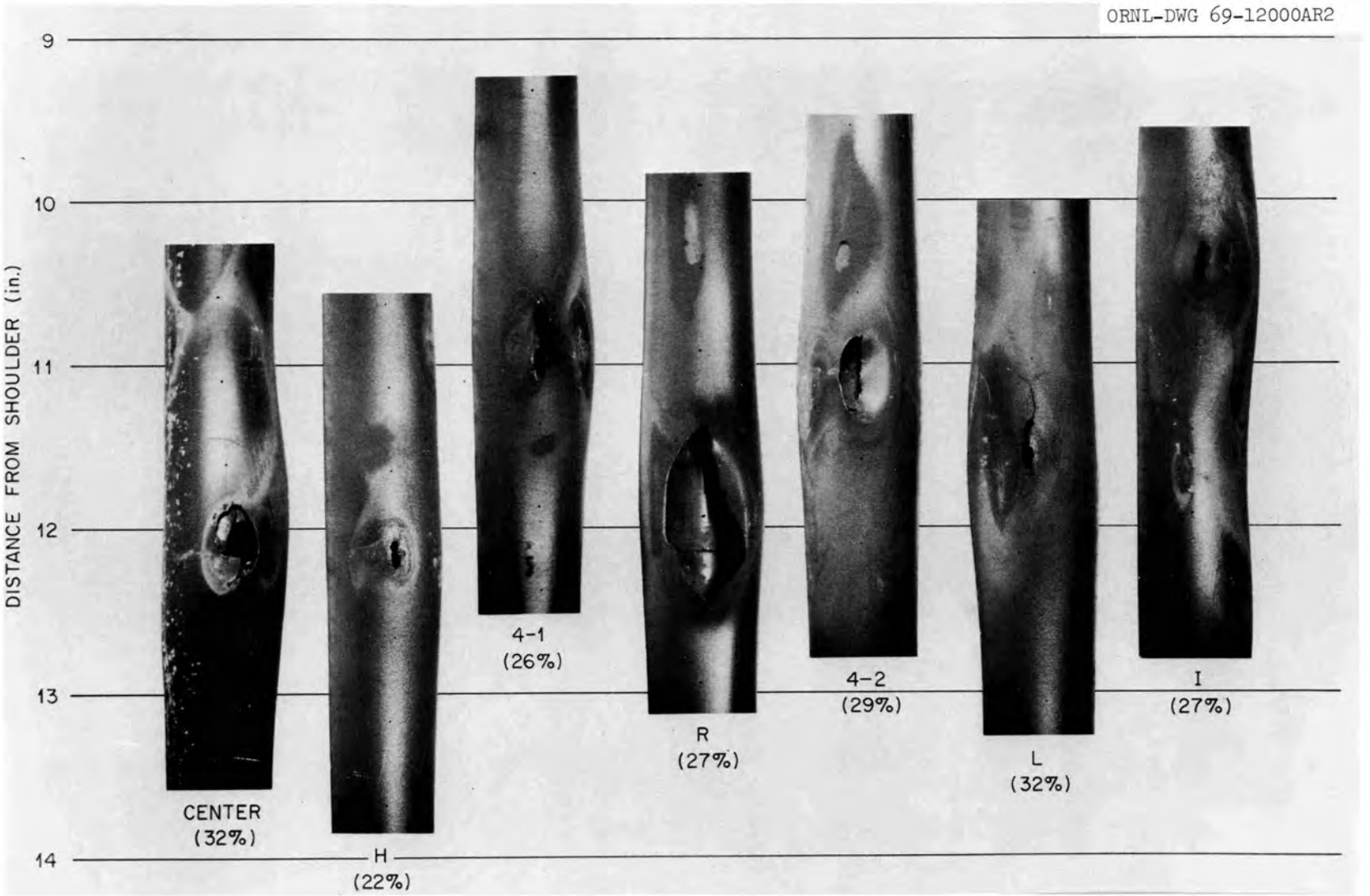

Fig. 1.6. Head-On View of Ruptures in TREAT Experiment FRF-1.

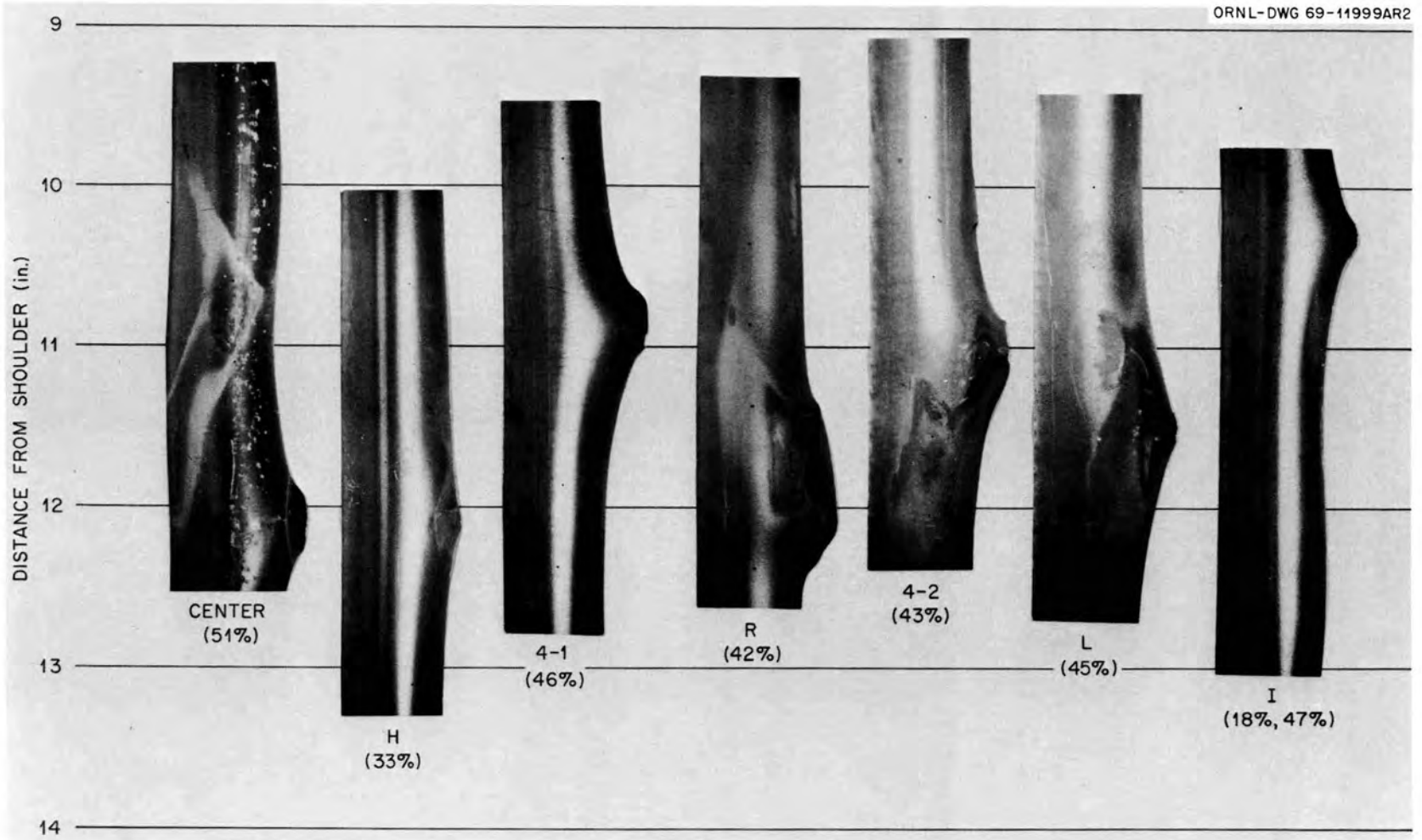

Fig. 1.7. Side View of Ruptures in TREAT Experiment FRF-1.

hoop stress show that the center rod should have ruptured several seconds before rod H. The pellets in the center irradiated rod were cracked into small pieces, and the pieces may have settled inside the rod as the cladding swelled, thus making a somewhat concentrated heat source. The direct effect on rod H was probably the spilling out of UO_2 chips that heated and caused local stress concentrations where the expanding cladding of rod H pressed against the UO_2 pieces. In experiment FRF-2 the UO_2 pellets in the center irradiated rod were also fragmented, but the small rupture opening prevented the UO_2 chips from coming out.

This form of fuel rod failure propagation would not occur in out-of-reactor fuel rod failure tests and apparently could not occur in TREAT experiments with unirradiated rods, since unirradiated pellets remain intact. The ideal test of this fuel rod failure propagation mechanism will be with a bundle of all-irradiated rods, such as the 13-rod bundle of 30,000-Mwd/ton-burnup rods planned for experiment FRF-3. No other irradiation effect on fuel rod failure was observed in the two TREAT tests with 650- and 2800-Mwd/ton-burnup center rods.

Plans for Experiment FRF-3 (PWR Bundle)

Prior to the termination of this work the in-reactor experimental apparatus had been redesigned to accommodate a larger bundle of longer fuel rods. The new design provides space for a 13-rod bundle of PWR-size rods. Construction had been initiated.

A group of rods originally irradiated in the VBWR and later irradiated to a total burnup of 30,000 Mwd/ton in the SA-1 bundle in Dresden-I were acquired for use in the FRF-3 TREAT test. These rods are 40 in. long, 0.424 in. in diameter, and clad with Zircaloy-2. It is now planned to use these rods to perform a hot cell test (see Sect. 1.5).

Reference

1. R. D. Waddell, Jr., D. O. Hobson, and P. L. Rittenhouse, High-Temperature Properties and Metallurgical Evaluation of Zircaloy Cladding, pp. 8–15, ORNL Nuclear Safety Research and Development Program Bimonthly Report for March–April 1970, USAEC Report ORNL-TM-2984, Oak Ridge National Laboratory.

1.5 RUPTURE TESTS OF IRRADIATED FUEL RODS

(AEC Activity 04 60 01 10 1)

M. F. Osborne G. W. Parker

Irradiation in a power reactor could conceivably, over a period of time, influence cladding properties such as strength and ductility and thereby alter the swelling and rupture characteristics predicted from studies of unirradiated material. Consequently irradiated fuel rods are being rupture-tested in a hot cell facility under conditions simulating a loss-of-coolant accident.

Seven rods, all BWR diameter (0.564 in.), irradiated in the VBWR to 3000-Mwd/MT burnup were tested during this reporting period. These experiments covered the internal pressure range of 100 to 700 psig and nominal heating rates of 10, 25, and 50°F/sec. The results of one test were invalid because of a malfunction of the RF generator during the test; the conditions and results of the other six tests are summarized in Table 1.2. The rupture areas of two rods are shown in Figs. 1.8 and 1.9. These photographs illustrate typical appearances of ruptures in the high-ductility β-phase region (>1780°F) in contrast to the lower ductility $\alpha + \beta$ phase region (1500 to 1780°F). Greater expansion, more oxidation, and more cracking of the surface oxide layer occurred in the higher temperature rupture, as shown in Fig. 1.8.

Table 1.2. Results of Fuel Rod Rupture Tests of BWR Diameter (0.564 in.) Rods Irradiated to 3000-Mwd/MT Burnup

Test No.	Maximum Pressure (psig)	Heating Rate (°F/sec)	Rupture Temperature (°F)	Circumferential Strain (%)
R-105	402	10	1590	36
R-106	403	23	1620	15
R-107	112	10	2005	51
R-108	720	13	1520	35
R-109	101	47	2200	35
R-110	402	53	1760	16

R-53046

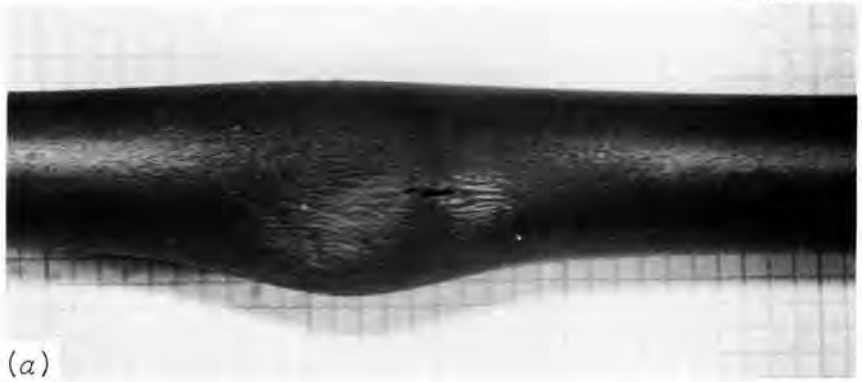

(*a*)

R-53049

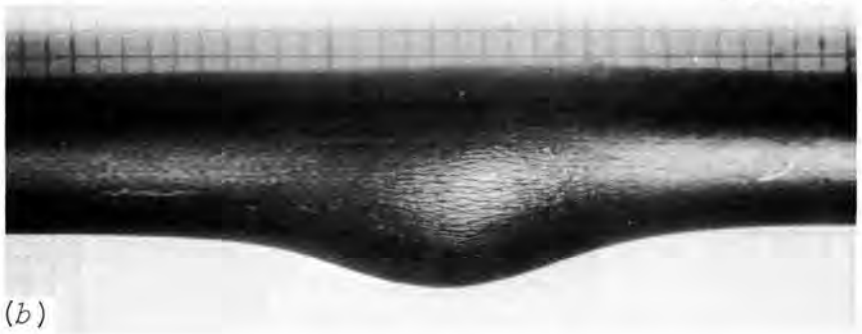

(*b*)

Fig. 1.8. Rupture Area of Rod in Test R-107, as Viewed (a) 0° and (b) 90° from the Rupture. The rupture occurred at 2005°F and 112 psig. 1.35×

Maximum internal pressures (which occur somewhat before rupture) and maximum circumferential expansions for all tests of irradiated rods are plotted as a function of rupture temperature in Figs. 1.10 and 1.11. The curve in each figure is a visual fit of baseline data discussed previously.[1] As shown in Fig. 1.10, these tests of irradiated rods seem to indicate lower rupture temperatures compared with the baseline data. However, since similar results were obtained from tests of unirradiated fuel rods, this difference is thought to be attributable to the differences in heating methods. In the baseline tests, unfueled tubes were heated by 10-in.-long internal lamps, and the maximum temperature zone was always at the center of this heated length and near the thermocouple location. Conversely, in the hot cell tests, the fuel rods were heated by a 20-in.-long induction coil. Although at least two thermocouples were attached to the rod for

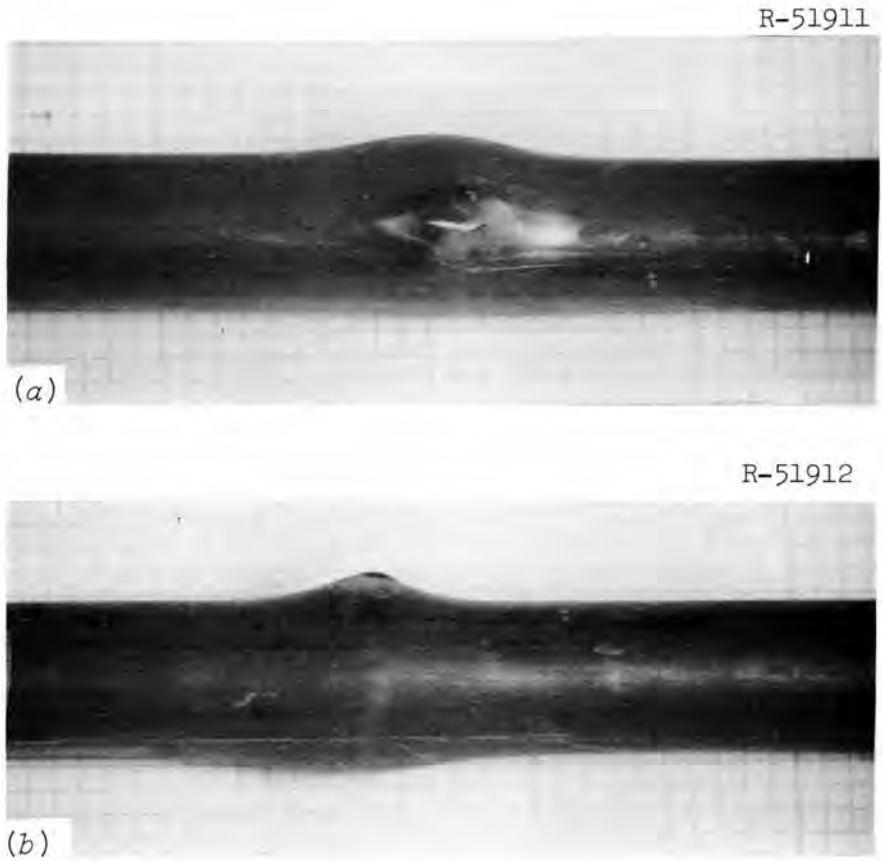

Fig. 1.9. Rupture Area of Rod in Test R-105 as Viewed (a) 0° and (b) 90° from Rupture. The rupture occurred at 1590°F and 402 psig. 1.38×

each test, the location of the maximum temperature zone (where rupture occurred) was less predictable; the rupture locations varied over the central 12 in. of the heated length. Presumably, this is an effect of variations in cladding wall thickness and in fuel-to-cladding clearance. Posttest examinations frequently disclosed that the nearest thermocouple was located several inches from the rupture. Comparisons of measured temperatures with rupture locations indicate that temperature variations of approximately 100°F over 2 or 3 in. could be expected within the heated zone. This observation agrees with the data in Fig. 1.10, where most of the data points lie within about 100°F of the baseline curve.

Cladding strain, or swelling, is plotted as a function of rupture temperature in Fig. 1.11. With one exception, all the data for the irradiated rods fall below the baseline curve. On the basis of thermocouple

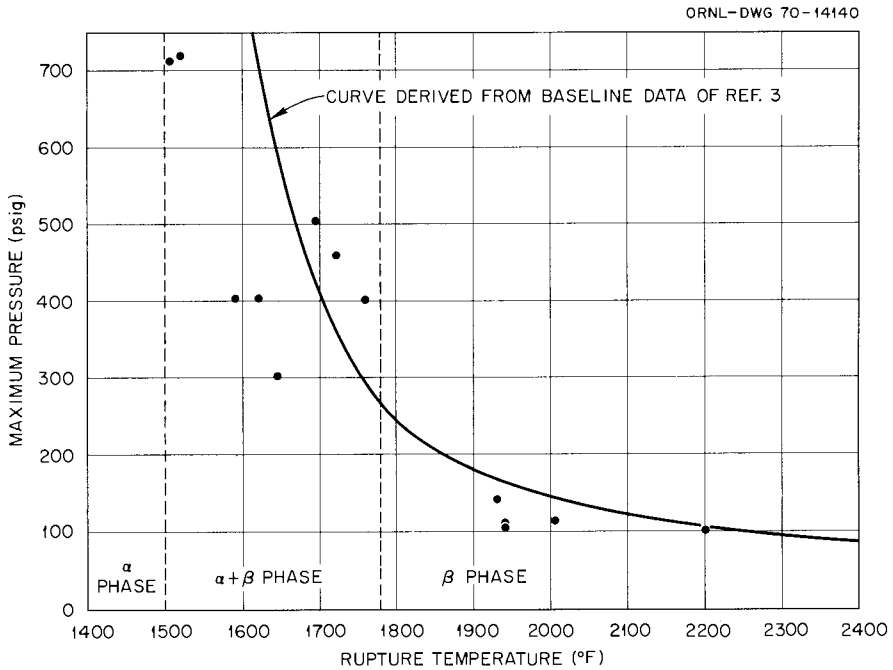

Fig. 1.10. Maximum Internal Pressure Versus Rupture Temperature of Irradiated Zircaloy-2 Clad UO_2 Fuel Rods.

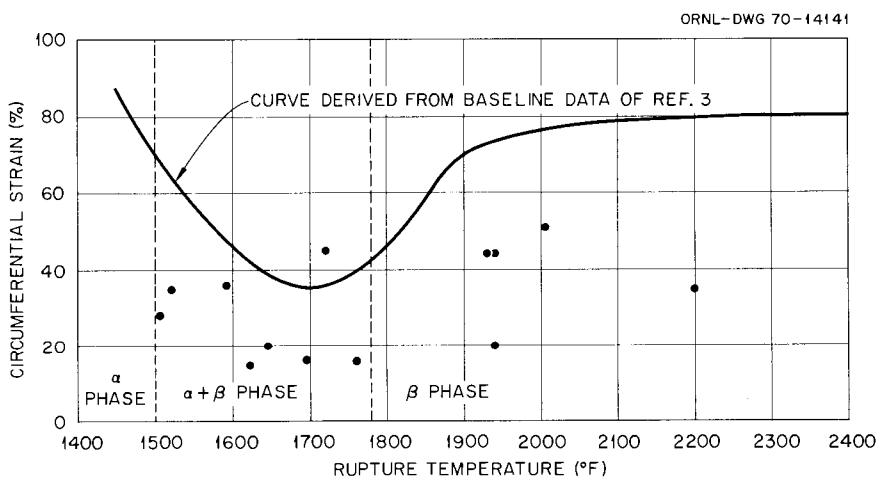

Fig. 1.11. Maximum Circumferential Strain Versus Rupture Temperature of Irradiated Zircaloy-2 Clad UO_2 Fuel Rods.

location and the extent of cladding oxidation for the exception (test R-102), the temperature at the rupture point is estimated to have been about 100°F higher than the nearest measured temperature. Such a 100°F shift would place this point slightly below the curve. While tests of

unirradiated rods in the hot cell equipment yielded somewhat lower circumferential strains than the baseline tests, probably because of the aforementioned differences in heating method, the strains obtained in unirradiated rod tests were generally higher by 25 to 50% than those shown for irradiated rods. The distinctly lower ductility in the $\alpha + \beta$ phase region, which was reported by Hobson and is illustrated by the curve in Fig. 1.11, is less obvious, but is observable, in these data. Thus it appears that irradiation effects reduce cladding ductility to a small though measurable extent. However, this reduction in ductility is probably caused by a combination of chemical (oxidation and hydriding) and radiation (fast-neutron damage) effects, rather than by radiation alone. In addition, these tests have included only low-burnup fuel rods (3000 to 7000 Mwd/MT); future testing will extend to core lifetime burnups (20,000 to 30,000 Mwd/MT).

After completion of this series of single-rod tests, a multirod test of irradiated fuel cladding will be conducted in the hot cell. The equipment needed to remove the UO_2 fuel and fission products from irradiated rods and to assemble and conduct such a test is being designed. This test will involve a 13-rod assembly of PWR diameter tubes heated by internal lamps. It is being designed to correlate with the results of Waddell's multirod tests[2] of unirradiated material and also with the TREAT tests conducted by Lorenz.[3] This test is scheduled for the third quarter of FY-1971.

References

1. D. O. Hobson, M. F. Osborne, and G. W. Parker, Comparison of Rupture Data from Irradiated Fuel Rods and Unirradiated Cladding, *Trans. Amer. Nucl. Soc.*, 13(1): 150 (1970).

2. R. D. Waddell, Measurement of LWR Coolant Channel Reduction Arising from Cladding Deformation During a Loss-of-Coolant Accident, *Trans. Amer. Nucl. Soc.*, 13(1): 150–151 (1970).

3. R. A. Lorenz, D. O. Hobson, and G. W. Parker, Fuel Rod Failure Under Loss-of-Coolant Conditions in TREAT, *Trans. Amer. Nucl. Soc.*, 13(1): 152 (1970).

2. LMFBR SAFETY STUDIES

2.1 PROGRAM COORDINATION

(AEC Activity 04 60 01 09 1)

M. H. Fontana R. E. MacPherson

The fuel-failure mockup (FFM) is a large high-temperature sodium-cooled facility in which simulated LMFBR core segments (19-pin bundles) may be subjected to thermal and hydraulic testing at typical operating conditions. The core segments are simulated by cartridge electric heaters fabricated to duplicate a fuel-pin geometry and assembled with spirally wrapped wire-like spacers containing internal thermocouple junctions.

Coordination

A detailed experimental program for test series I in the FFM was completed and sent to the AEC, ANL, and the Hanford Engineering Development Laboratory (HEDL) for review. Test series I will include baseline tests of the unblocked heater bundles and experiments with partial inlet blockage. System acceptance procedures were completed and reported to the AEC. Operating and maintenance procedures and the Final System Design Description are nearing completion. A worst-case analysis of thermal stresses resulting from loss of power was performed, and it was found that the FFM could withstand over 100 such cycles. An experiment to determine the need for a flow straightener on the inlet section of the FFM was performed in the water rig, and it was found that no straightener was needed. The results of these last two tasks were forwarded to the AEC as requested.

Coordination has been maintained with HEDL to assure that the FFM will provide the required features and that the ORNL-designed Watlow-built heater can be made available to other installations if needed. A meeting was held with HEDL personnel on exchange of technical information on the construction of high-temperature liquid-metal facilities. Also a two-day meeting was held with Atomics International management to familiarize ORNL with AI's demonstration plant and to present ORNL's LMFBR activities.

FFM Test Program — Test Series I

The test program for the FFM is designed for investigation of the effect of various types of flow blockage on temperature profiles in the core downstream of the blocked area. The core parameters and operating conditions of the FFTF reactor are being emphasized in all current test program plans. The detailed test program for the first test series was developed and is summarized below. This test series is concerned with the thermal and hydraulic effects of a blockage of contiguous coolant channels by an obstruction at the coolant inlet end of a fuel pin bundle. The heated zone of the fuel pins will be separated from this blockage region by 6 in. of blanket region so that cross flow from adjacent unblocked channels will tend to ameliorate the effect of the blockage. This geometric consideration is mocked up in the test piece to be operated in the FFM.

The following seven tests were identified as desirable during the course of test series I:

Test 1. *Determine the relationship between flow and pressure drop across the test section over the operating temperature range without the test piece installed.* This will permit later correction of pressure-drop measurements to eliminate miscellaneous pressure losses not associated with the test piece itself.

Test 2. *By heating a single rod in the 19-rod bundle, determine the effect of heat flux on the temperature measurements from thermocouples installed in the wire-wrapped spacers used to separate the heaters.* The spacer is a stainless steel-sheathed magnesium-oxide-filled unit with the thermocouple junctions embedded in the central MgO core. If significant heat flux passes through the thermocouple, errors might be introduced into the thermocouple reading of the bulk sodium temperature. The results of this test, in conjunction with a dynamically scaled water test, will partially define the flow field and heat transport mechanisms within the unblocked rod bundle.

Test 3. *While operating all heater rods at equal power levels, obtain baseline data over the normal operating range on temperature distribution within the test piece and the pressure drop across the test*

piece without *the flow obstruction installed at the coolant inlet end of the simulated fuel pin assembly.*

Test 4. *While operating all heater rods at equal power levels, obtain data over the normal operating range on the temperature distribution within the test piece and the pressure drop across the test piece* with *the flow obstruction installed at the coolant inlet end of the simulated fuel pin assembly.*

Test 5. *Obtain data that will allow the inference of flow fields and heat transport mechanisms within the rod bundle with the inlet blockage in place.* This will be done by heating the central rod only and measuring the resultant temperature field. This experiment repeats a similar experiment in the dynamically scaled water-cooled facility.

Tests 6 and 7 (Optional). *Obtain data on bundle exit temperature profiles resulting from two- and four-channel inlet blockages to determine the ability of thermocouple "rakes" in the exit of an FFTF fuel subassembly to detect partial blockages.*

2.2 ANALYTICAL STUDIES

(AEC Activity 04 60 01 09 1)

M. H. Fontana P. A. Gnadt
A. Fukuda L. F. Parsly
J. L. Wantland

Analytical studies in support of the FFM program are being performed to aid planning of the experimental program and to insure that maximum information will be obtained from the experiment. At present the studies involve the adaptation of computer programs to calculate flow and temperature profiles in rod bundles with partial blockages, the development of simple programs to treat experimental data, studies to determine optimum thermocouple placements, and calculation of the three-dimensional temperature distributions within a heater or fuel rod for various degrees of surface blockage. Preliminary work on the latter is reported here.

Temperature Distribution in Heater Pins

The computer program for calculating steady-state temperature distribution in electrically heated simulated fuel pins described in the last report was used to calculate the effect of blockages of different lengths on the internal temperature distribution within the heater. This was done to determine the minimum length of blockage (over a 120° sector of the fuel rod) that would cause the same internal temperature as would be obtained with an infinite-length blockage. Calculations were also performed for two different heat transfer coefficients in the "insulated" patch to compare the effects of a blockage of UO_2 (as might exist in a reactor) with that of stainless steel (which will be used in the FFM experiment).

The variation of the outer cladding temperature with patch axial length is shown in Fig. 2.1. It can be seen that for the case of very low patch conductance (50 Btu/hr·ft^2·°F) the effect of length becomes negligible at lengths exceeding about 0.03 ft (∿0.36 in.) and is completely wiped out at approximately 0.05 ft (0.60 in.).

The internal temperatures of the electric heater are shown in Fig. 2.2 for the case of a patch heat transfer coefficient of 1000 Btu/hr·ft^2·°F, which simulates a plug of UO_2. Figure 2.3 shows the temperature for a

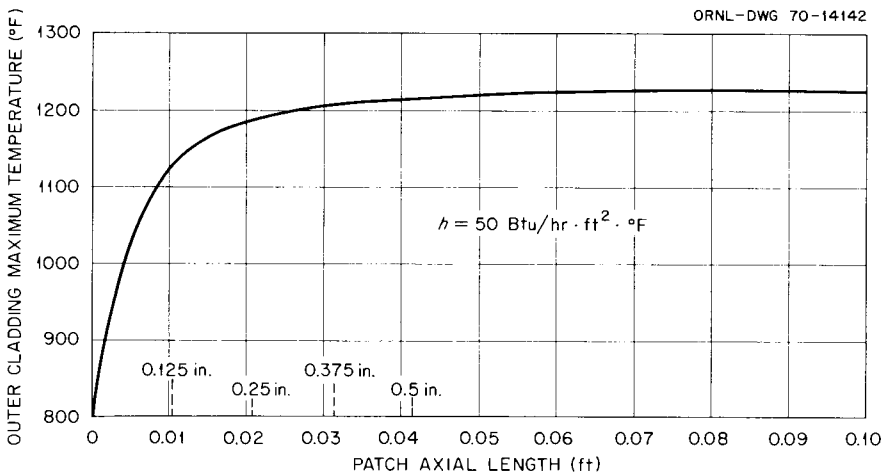

Fig. 2.1. Effect of Blockage Length on Maximum Outside Cladding Temperature.

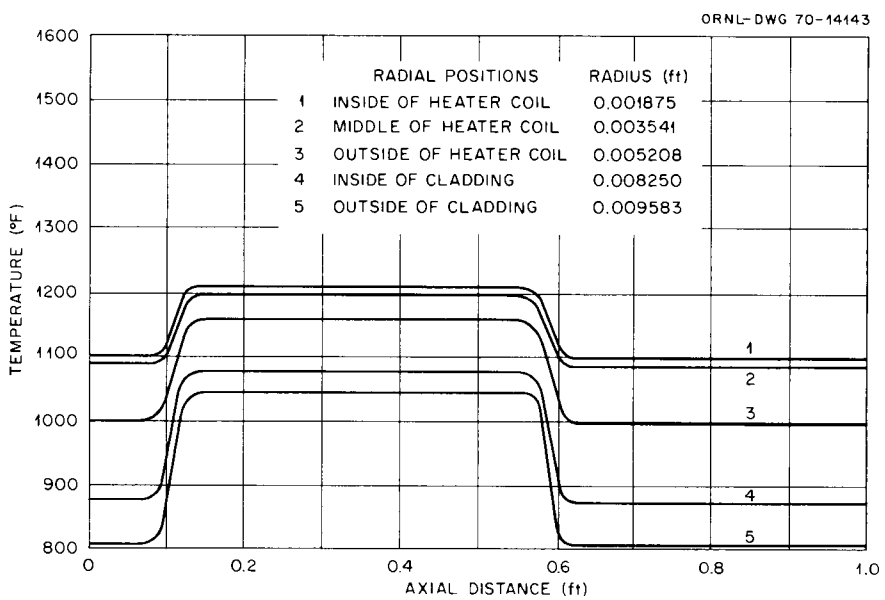

Fig. 2.2. Temperature Versus Axial Position at $\theta = 110.0°$. Rod electrically heated at 10 kw/ft with simulated UO_2 blockage.

UO_2-fueled pin with the same surface blockage. The UO_2-fueled pin has an outer cladding surface temperature about 200°F hotter than that of the heater pin. This is due to the poorer lateral heat conductance of the UO_2.

The effect of a higher conductivity blockage material may be seen by comparing Fig. 2.4 with Fig. 2.2. The maximum outside temperature reaches 880°F for the stainless steel blockage case compared with 1050°F for the

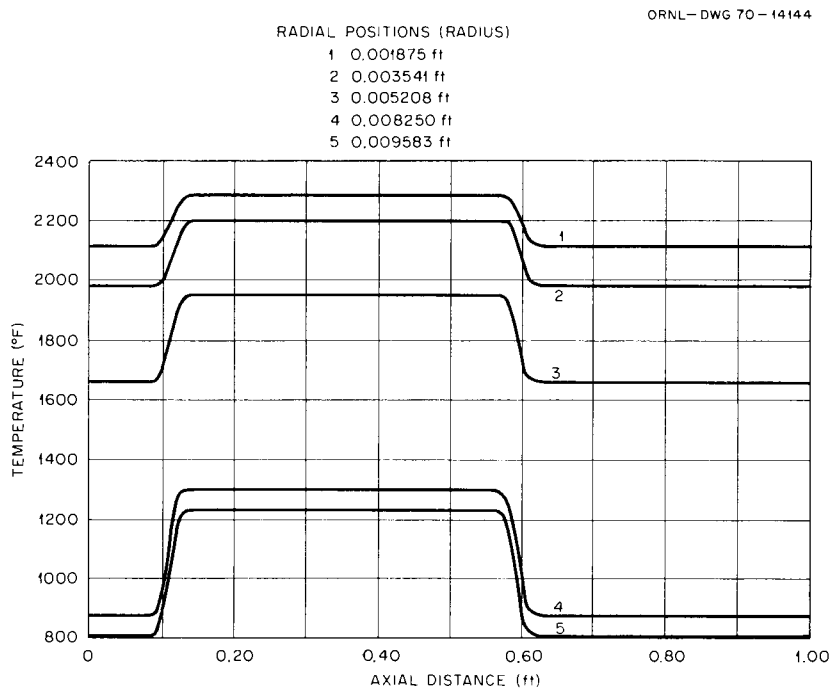

Fig. 2.3. Temperature Versus Axial Position at $\theta = 110.0°$. UO_2-fueled rod heated electrically at 10 kw/ft.

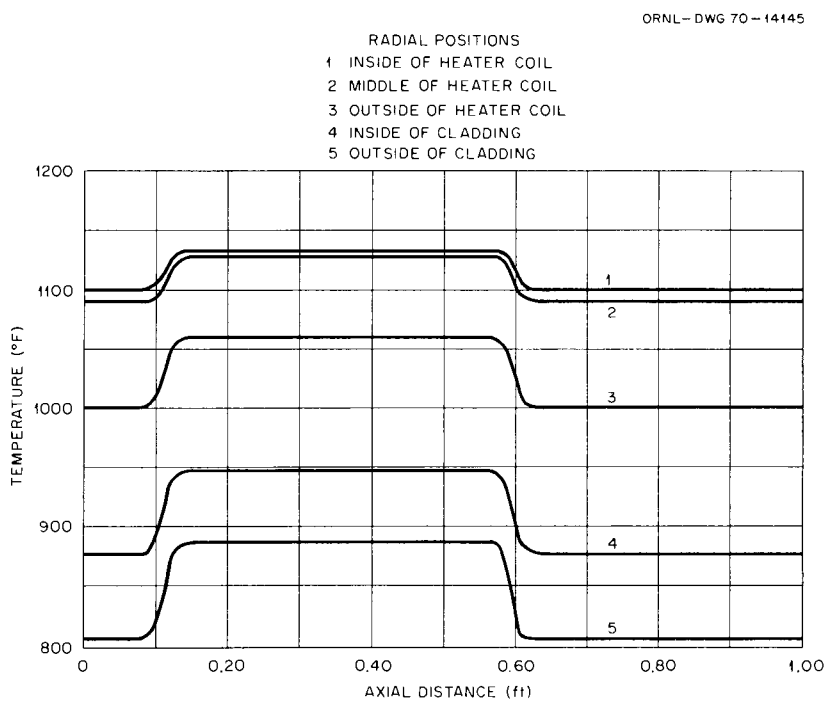

Fig. 2.4. Temperature Versus Axial Position at $\theta = 110.0°$. Rod electrically heated at 10 kw/ft with simulated stainless steel blockage.

UO_2 blockage case. This effect must be accounted for in evaluating the pertinent out-of-pile experiment.

FFM Data Handling

The FFM has five levels of instrumentation and data handling:

1. Annunciator-alarm system with provisions for automatic shutdown.
2. On-site display of operational variables by the usual indicators and recorders. In particular, provision is made for any combination of 16 major parameters to be recorded on two eight-channel Sanborn recorders.
3. On-line reduction and tabular presentation of all variables by the PDP-8 computer on demand of the operator for operational purposes. Provision is made for automatic distinguishing between data needed for operational purposes and those to be used in further engineering analyses.
4. Day-by-day computer printouts of reduced data gathered by the DEXTIR system.
5. Further processing and plotting of data on the DEXTIR tapes by special computer programs written for this purpose.

All work is on schedule. Segments of the softwear should be completed as needed by the FFM test program.

2.3 WATER-SYSTEM MOCKUP OF FFM FACILITY
(AEC Activity 04 60 01 09 1)

W. R. Gambill

Tests were conducted to determine whether turning vanes are needed in the tee 20 in. below the entrance to the FFM rod bundle. A full-scale subloop was installed between two existing vertical pipe runs in the FFM mockup system. Measurements were made of the static-pressure drop across the tee and of the velocity distribution at stations 20 and 46.5 in. downstream of the tee, with and without the turning-vane insert in place. For dynamic similitude (a Reynolds number of $\sim 3 \times 10^5$), a water flow rate of 200 gpm was required.

As indicated on Fig. 2.5, the static pressure drop was obtained by measuring the upstream and downstream static pressures separately, applying a static-head correction to each, and taking the difference. Pressure indications were taken from a calibrated 0- to 25-psig Heise gage. Velocity distributions were obtained by making a five-point diametral traverse, with a 0.095-in.-OD pitot probe, and another five-point traverse, at the same station but at right angles, with a 0.072-in.-OD probe. The velocity head sensed by the pitot probes was impressed on a differential-pressure cell, which converted an input of 0 to 80 in. H_2O to an output of 3 to 15 psig (pneumatic). The same Heise gage was employed to indicate the differential-pressure cell output signal.

The pressure-drop results are summarized in Table 2.1, and the velocity-distribution data are given in Table 2.2. In Table 2.2, probe A refers to the 95-mil probe with its axis parallel to the inlet piping upstream of the tee, and probe B to the 72-mil probe at a right angle. The numbers 1 through 5 associated with each probe in Table 2.2 refer to the five equally spaced points at which readings were recorded (1 to the point nearest the opposite wall, 3 to the center line, and 5 to the point farthest from the wall opposite the probe). From the above it was concluded that the velocity distribution at the inlet of the FFM rod bundle will be adequately flat without the use of turning vanes or other inserts in the tee below the bundle.

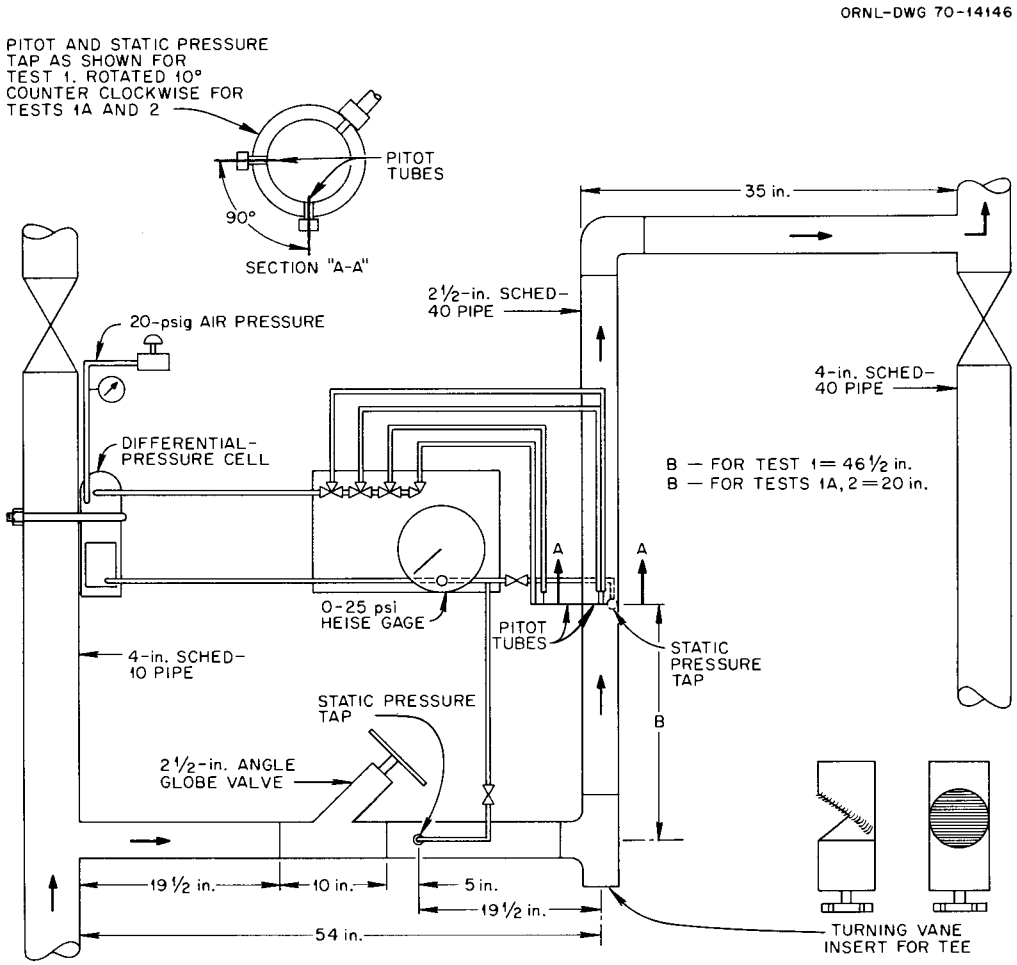

Fig. 2.5. Schematic Diagram of Water-Loop Mockup of FFM Inlet Piping.

Table 2.1. Pressure-Drop Results Obtained in Water-System Mockup of FFM Facility

Test No.	Condition	N_{Re}	Pressure Drop (psi)	
			Calculated	Experimental[a]
		$\times 10^5$		
1	Without turning vanes; downstream tap 46 1/2 in. above tee	3.20	2.28	2.77
1-a	Without turning vanes; downstream tap 20 in. above tee	3.15	2.02	1.53
2	With turning vanes; downstream tap 20 in. above tee	2.97		5.45

[a]Corrected for hydrostatic heads between static taps and pressure gage.

Table 2.2. Velocity Distribution Results Obtained with Water-System Mockup of FFM Facility

Test No.	Condition	Mean N_{Re}	Velocity (fps)										V_{max}/V_{min} (overall)
			Probe A					Probe B					
			1	2	3	4	5	1	2	3	4	5	
		$\times 10^5$											
1	No turning vanes; probes 46 1/2 in. above tee	3.34	14.17	14.50	14.55	14.38	13.90	13.80	14.04	14.01	13.98	13.59	1.071
1-a	No turning vanes; probes 20 in. above tee	3.19	15.13	14.91	14.89	14.99	14.87	14.77	14.65	14.62	14.41	14.29	1.060
2	With turning vanes; probes 20 in. above tee	3.21	13.71	13.43	14.29	15.51	16.80	15.49	14.31	13.32	13.71	14.90	1.261

2.4 FFM NOISE ANALYSIS

(AEC Activity 04 60 01 09 1)

D. N. Fry R. Saxe
J. C. Robinson*

Most of the effort this past two months has been spent in evaluating techniques used on the HFIR. As a result final arrangements were made to install noise detection and analyzing equipment on the FFM. Six noise monitor probes were attached to the test section. Measurements from these probes and other available signals (thermocouples, EM flowmeters, and pressure transmitters) will be evaluated for possible use in the noise diagnostics program.

---

*Consultant from the University of Tennessee, Knoxville, Tennessee.

2.5 FFM FACILITY ACTIVITIES

(AEC Activity 04 60 01 09 1)

P. A. Gnadt A. G. Grindell
R. E. MacPherson

Construction and Procurement

Construction work, except for the installation of the oxide control and indication (OCI) package, was essentially completed, and instrument and electrical shakedown operations are under way. The completed status of the facility just prior to installation of the insulation is shown in the following series of construction photographs. Figure 2.6 is a photograph of the facility cubicle. The lubrication package for the PKA pump is shown at the far right. Figure 2.7 shows some of the main system piping. The radiator enclosure is at the upper left, the pump is at the upper right, and the drain tank is at the bottom. The main operating controls for the facility are directly west of the loop.

The oxide control and indication package has been shipped. Review of all materials and fabrication records was completed by the ORNL Inspection Engineering Department.

A spacer wire (contining two separate thermocouple junctions) was attached to each of the 19 heaters, and the assembly of the heaters into the bundle was started.

Analysis of Stress Due to Thermal Transients in Test Series I, Core Inlet Blockage

The thermal transients and thermal shocks to be imposed on the fuel failure mockup (FFM) during performance of the presently approved test program were examined, and it was determined that even with very conservative assumptions, there is no probability of thermal-stress-induced failures in the facility.

The normally slow thermal transients of the type imposed by initial startup or a complete shutdown and restart of the test facility can be characterized by temperature changes as large as 1100 to 1200°F. However, normal operating procedures will specify a low-temperature isothermal

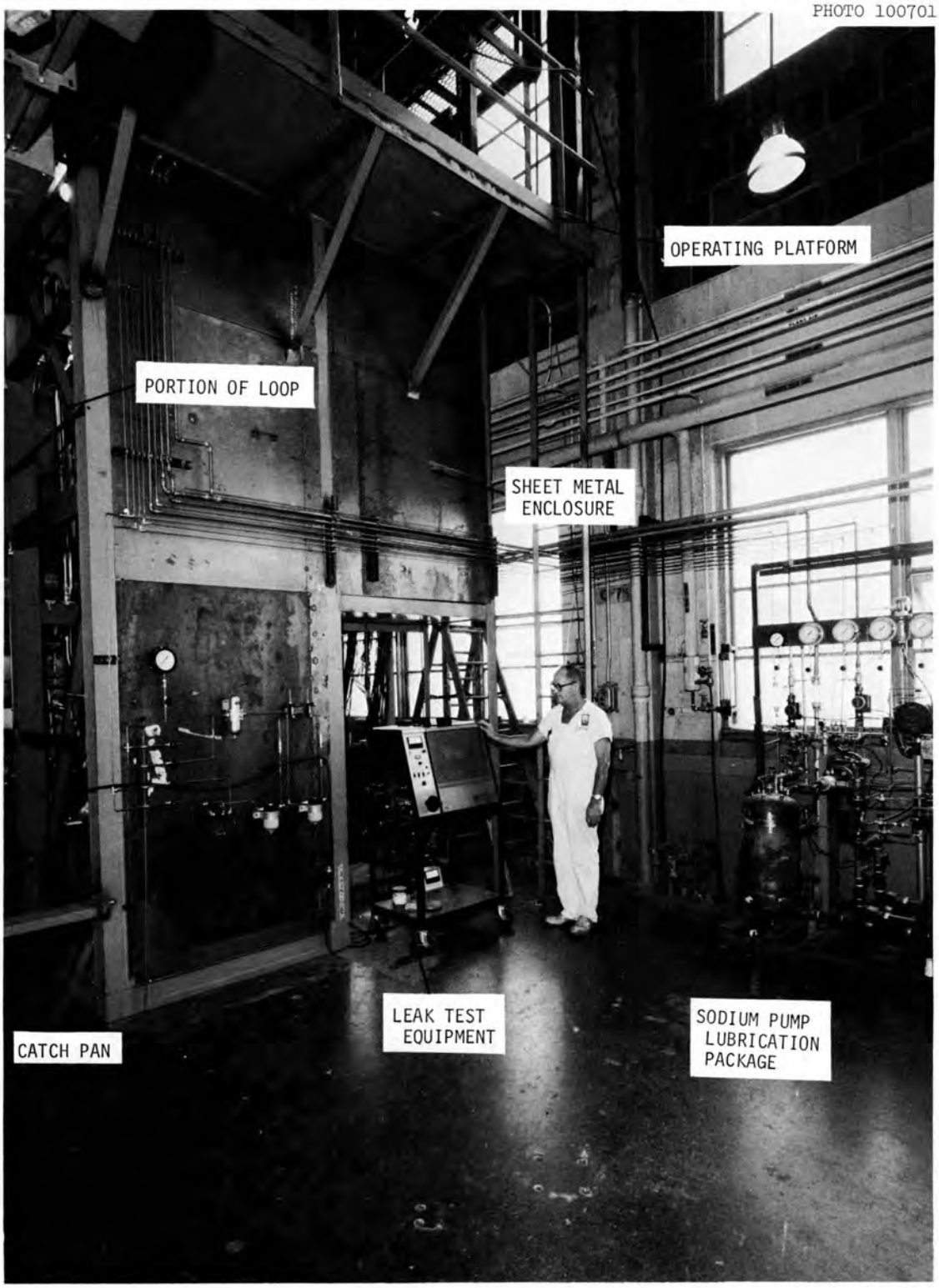

Fig. 2.6. West Elevation of FFM Facility.

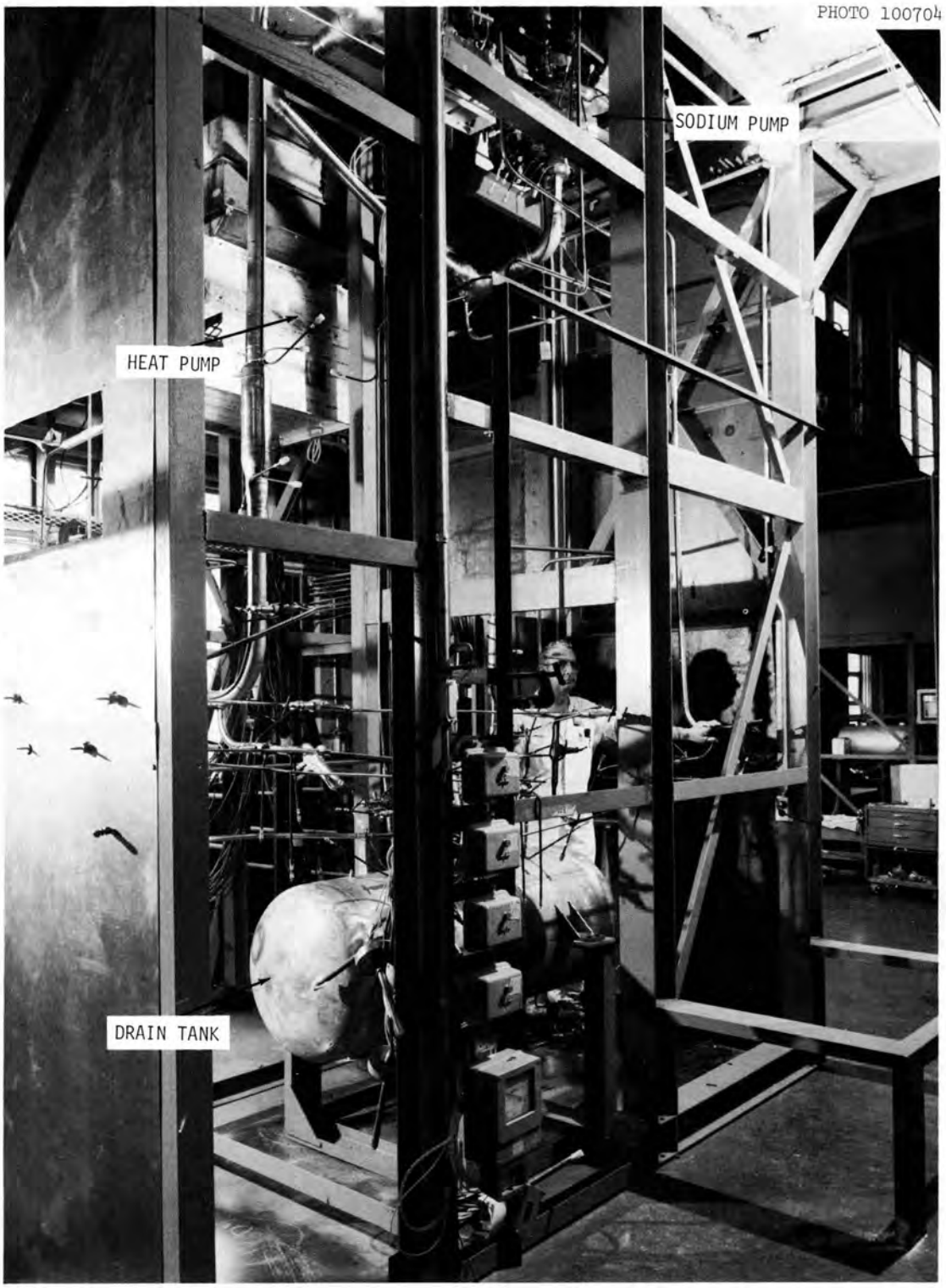

Fig. 2.7. South Elevation of FFM Facility.

operating condition for the sodium loop between test runs, and a more typical slow thermal transient will be from an isothermal condition at approximately 700°F to test operation conditions and return.

The imposition of these types of thermal transients on the loop geometry was investigated as a routine step in loop design by using the piping flexibility analytical technique developed by the Mare Island Naval Shipyard, MEL-21P. The system layout was modified as necessary to meet the criterion imposed by this design procedure that all stresses be within the elastic range at room temperature following elevated temperature operation of the system. It should also be noted that the Power Piping Code, USAS B31.1-1967, Section 119.7, Analysis, states that a system which experiences less than 7000 total cycles of this type is in essentially noncyclic service. It is considered that the above analysis of the normally slow thermal-transient-induced stresses gives adequate assurance against failure from this cause.

Thermal-shock stresses can be quite severe in a sodium system, and a reaslistic analysis of the situation in the FFM could be quite difficult. In order to provide a satisfactory "worst case" analysis, the FFM thermal-shock stresses were examined in an area of the test section just downstream from the 3-ft section of the test piece that simulates the 6-in. inlet blanket, a 2-ft heated zone, and a 6-in. outlet blanket. This area of the test section is the primary sodium containment vessel, and during a test it is normally at the test-piece outlet temperature. Loss of power to the bundle heaters will impose a steep temperature ramp from outlet to inlet temperature in a fraction of a second. The potential for thermal shock is greater at this point than at any other point in the system.

For analysis, the temperature profile in this section of the primary containment vessel was calculated from time zero based on the assumption that the wall at the maximum outlet temperature of 1200°F was exposed to sodium at a temperature of 950°F (maximum proposed temperature drop of 250°F) at time zero. Temperature profiles generated by computer code analysis of heat transfer during the 2 sec following time zero indicated that a maximum wall temperature difference of 135°F occurred at 0.7 sec

after the step change occurred. From the equation for thermal-shock stress,

$$S = \frac{E\alpha\ \Delta T}{1 - V},$$

where

E = modulus of elasticity (22.3×10^6 psi),

α = coefficient of thermal expansion ($10.3 \times 10^{-6}/°F$),

F = modified Poission's ratio (0.444),

and Fig. 2 of Code Case 1331-4 for high-temperature nuclear vessels, the calculated peak thermal stress of 55,770 psi can be shown to be allowable for 100 such thermal-shock events.

This analysis of thermal shock is conservative for the following reasons:

1. Adiabatic conditions are assumed at the test section wall, whereas the current intention is to operate at wall preheat conditions corresponding to the average test section temperatures. This means that the downstream (hotter) section of the test piece will be losing heat and the outer surface of the test section will be at a temperature somewhat below that assumed in the calculation.

2. The thermal stress was evaluated by using the equation for thermal shock that applies to steep temperature gradients in a portion of a wall thickness. The equation for a linear thermal gradient imposed across the thickness of a slab gives a stress level a factor of 2 lower, since one surface would be in tension and the other surface would be in compression.

3. The imposition of a 250°F step temperature change at time zero is more severe than the actual case of a ramp change of the same magnitude over a time period $0.1 < t < 1.0$. If it becomes necessary at a later date, a more refined analysis can be done, and a higher number of thermal-shock cycles can readily be justified.

3. SPRAY AND PRESSURE-SUPPRESSION TECHNOLOGY

T. H. Row, Coordinator

3.1 PROGRAM COORDINATION
(AEC Activity 04 60 80 01 1)

T. H. Row

The spray and pool absorption technology program was started in FY-1968, and a detailed experimental program for establishing the technology of reactor containment spray systems has since been completed. With the end of FY-1970 the major large-scale experiments were completed, and the staff was curtailed accordingly. Fiscal year 1971 will involve work on completion of spray system modeling, further development of spray-solution additives for both CH_3I gettering and radiolytic hydrogen reduction, and various design aspects of interest. Because of the greatly reduced program the informal information meetings will also be confined to those normally held in conjunction with the nuclear safety program annual information meeting.

Approximately one-half the papers presented at the Los Angeles symposium on Reactor Containment Spray System Technology have been reviewed and accepted for publication in *Nuclear Applications and Technology*. The remaining papers are in various stages of review and rewrite. The single issue on the symposium will be published in early 1971.

Two program reports were issued during this period. The testing of protective coatings (paints) is reported in "Design Considerations of Reactor Containment Spray Systems — Part V. Protective Coatings Test," by J. C. Griess, T. H. Row, C. D. Watson, and G. A. West, ORNL-TM-2412, Part V. Loop tests under simulated design-basis accident conditions with base-borate and base-borate-thiosulfate solutions are described, and photographs of all samples exposed are presented. Also included are the results of blowdown tests at the CVTR in conjunction with the research program conducted by Phillips Petroleum Company for the AEC.[1]

The second document details the results of water radiolysis studies conducted for General Electric Company, San Jose. The report is "Design Considerations of Reactor Containment Spray Systems — Part VIII. Boiling Water Reactor Analysis Radiolysis Studies," H. E. Zittel, ORNL-TM-2412, Part VIII.

Three reports are currently being edited and will be issued soon:

1. T. H. Row and J. C. Griess, Evaluation of Protective Coatings for Nuclear Plant Application — Burgess Fobes Paint Company, Inc., Test, ORNL-TM-3104.
2. L. F. Parsly, Removal of Elemental Iodine from Containment Atmospheres by Sprays, ORNL-4623.
3. L. F. Parsly, An Annotated Bibliography on the Chemical and Physical Properties of Methyl Iodide and Its Occurrence Under Reactor Accident Conditions, ORNL-NSIC-82.

The spray program was reviewed in a recent article in *Nuclear Safety:* Research on the Use of Containment Building Spray Systems in Pressurized Water Reactors, Thomas H. Row, Vol. 11, No. 3, pp. 223—234, May—June 1970.

Reference

1. J. A. Norberg et al., Simulated Design Basis Accident Tests of the Carolinas Virginia Tube Reactor Containment — Preliminary Results, USAEC Report IN-1325, Idaho Nuclear Corporation, October 1969.

3.2 SEARCH FOR ADDITIVES TO INCREASE ABSORPTION OF CH_3I

(AEC Activity 04 60 80 01 1)

B. A. Soldano

It was suggested that if the rate of reaction of CH_3I with $Na_2S_2O_3$ could be increased by a factor of at least 2, the removal half-time for this troublesome fission-release product would be so reduced that removal credit of magnitude useful to plant siting would become a possibility. Solution kinetic techniques led to the discovery that the addition of trace amounts of $NiSO_4(NH_4)_2SO_4$, as well as $CoSO_4(NH_4)_2SO_4$, resulted in a significant increase in the reaction rate of CH_3I with $Na_2S_2O_3$. More recently, preliminary results at room temperature (see preceding report in this series) suggested that trace concentrations of a rare-earth complex would give rise to reaction rates of CH_3I in base-borate solution comparable in magnitude to those found for the reaction of CH_3I with 0.13 *N* $Na_2S_2O_3$ in the base-borate. However, since nothing was known of the effects of pH, concentration, and temperature on the additive, these variables were studied.

It was found that the rate of disappearance of CH_3I introduced at an initial concentration of 4×10^{-8} *M* into the reaction vessel obeyed first-order kinetics. Part of this disappearance of CH_3I could be attributed to the sweeping action of the N_2 gas, with the latter's zero flow intercept constituting a measure of the chemical reaction rate of about 10^{-5} *M* rare-earth complex with CH_3I. As shown in Fig. 3.1, for two different concentrations of the additive (2.75×10^{-5} *M* and 1.93×10^{-4} *M*) an elevation of temperature initially suppresses the rates of reaction. This tendency peaks at about 40°C for the lower concentration of additive. Higher temperatures then lead to the reaction rates that increase in a manner similar to that found for $Na_2S_2O_3$ (Fig. 3.2).

It is apparent that two opposing effects are involved. One explanation lies in the behavior of most surface-active agents such as the rare-earth complex. The latter has both hydrophobic and hydrophilic substituents. The initial rise in temperature, with its accompanying reduction in dielectric constant, gives rise to more intramolecular association of the complex (micelle formation). At the higher temperatures, the increased solubility of the surface active agent into water counteracts the adverse

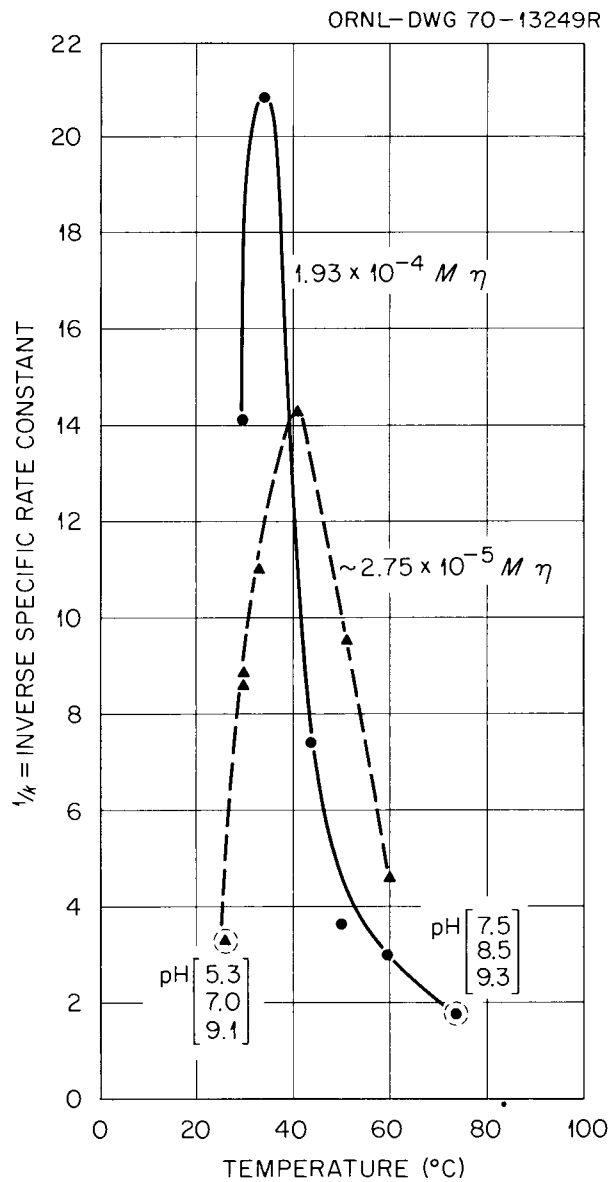

Fig. 3.1. Effect of Additive Concentration and Temperature on the Rate of Reaction of η with CH_3I in pH 9.1 Standard Borated Water.

effects of association. Equivalently, this behavior can be described in the language of an interfacial tension between the rare-earth complex and H_2O.

Concerning the effect of variations in the concentration of the additive, two points sould be made. First of all, it is clear (Fig. 3.1) that raising the concentration of additive increases the rate of reaction

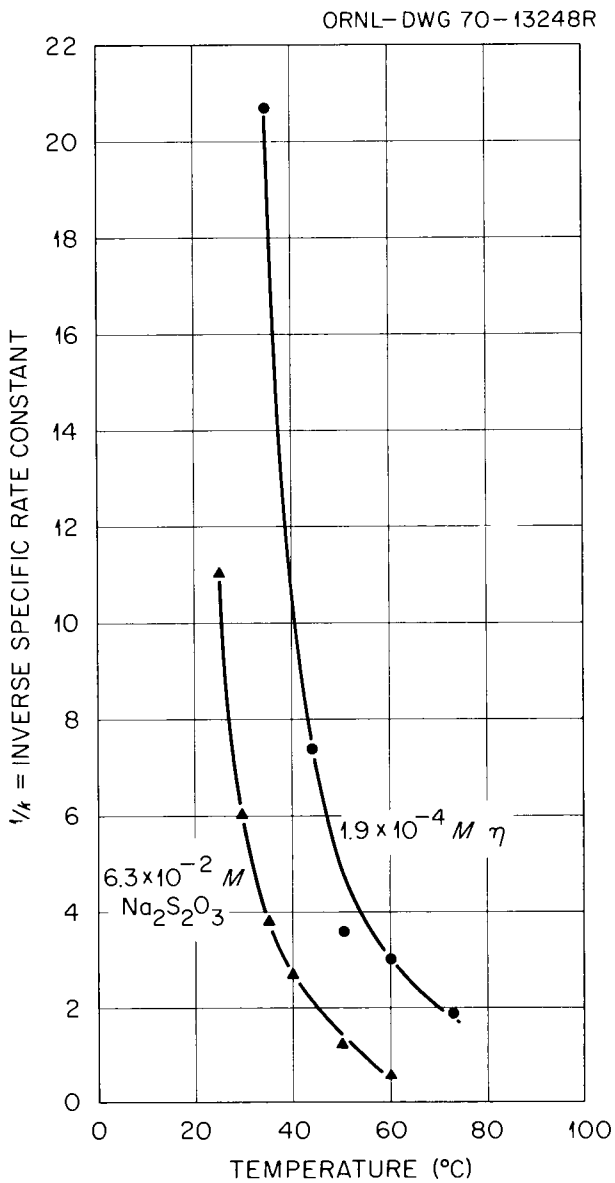

Fig. 3.2. Comparison of Rate of Reaction of CH_3I (in pH 9.1 Standard Borated Solution) with 6.3×10^{-2} *M* $Na_2S_2O_3$ and 1.9×10^{-4} *M* η.

with CH_3I. As a matter of expediency the concentration of additive was kept low ($\sim 10^{-4}$ *M*) but far in excess of the concentration of CH_3I ($\sim 10^{-7}$ to 10^{-8} *M*) expected in an actual incident. Secondly, it would be expected that there would be less reluctance to using an additive for CH_3I removal if so little additive was required that complications would not be introduced into the proposed overall spray solution composition. To be sure,

the solubility of the rare-earth complex is relatively low ($\sim 4.4 \times 10^{-3}$ moles/liter), but this poses no problem because, as recently found, the lithium salt form of the identical compound has a solubility of 2.7×10^{-2} moles/liter at 25°C. It is clear from these results that the concentration of additive could be considerably increased over the values used in this study.

A more pressing problem, however, with any additive containing a multivalent ion is related to the latter's stability against hydrolysis at elevated temperatures. One way to check this point would be to examine the reaction rates of the additive with CH_3I at 76°C as a function of pH. For all practical purposes, there was no pH effect at an additive concentration (1.9×10^{-4} *M*) for the three pH's studied (Fig. 3.1). This behavior suggests that there is little evidence of hydrolysis, at least at these temperatures. In a related vein, indirect evidence also exists that the additive is thermally stable at least at the highest temperatures studied, 80°C. This conclusion is suggested by the reproducibility in all the reaction rates for an additive sample cycled repeatedly between 25 and 80°C and retested from a reaction rate standpoint.

A kinetic variable it would have been desirable to examine is the effect of I_2 concentration on the reaction of the rare-earth complex with CH_3I, but the limited support for this work will not permit this. Not only is this effect a practical question but there is reason to believe that the micelle system represented by this additive is strongly affected by the presence of I_2. This latter factor could prove to be highly beneficial. Finally, measurements of the complexing ability of the rare-earth reflected in the steady-state distribution coefficient K_d would have proven highly useful, since it is the combination of this latter factor and the kinetic rate of reaction that controls the efficiency of the additive in promoting the absorption of CH_3I.

A detailed discussion of these two important variables will constitute the essence of a terminal report (to be released shortly) on this research program.

3.3 NUCLEAR SAFETY PILOT PLANT
(AEC Activity 04 60 80 01 1)

L. F. Parsly

Work on topical reports covering the spray experiments done in the Nuclear Safety Pilot Plant during the past three years continued during the reporting period. No significant new information was developed. Two reports were submitted for editing; one covered I_2 removal experiments and the other is an annotated bibliography on methyl iodide. Preparation of a report covering particle removal experiments was started.

3.4 RADIATION AND THERMAL STABILITY OF SPRAY SOLUTIONS (AEC Activity 04 60 80 01 1)

H. E. Zittel

Hydrogen Evolution from Paint Coatings

The carbon steel primer coat used on many reactor containment interiors contains various amounts of zinc. Although some studies have been carried out on the effect of the various proposed spray solutions on the physical appearance of paints over these primer coats, no thorough investigation has been made of the chemical reactivity. Therefore a study was initiated on a variety of paints obtained from various vendors to determine the consequences of exposing such paints and primers to the rather severe physical conditions expected to exist in an accident situation. The area of prime interest is hydrogen evolution due to reaction between the zinc in the primer coats and the spray solutions. All samples were exposed at 130°C in air. The results of the initial studies are given in Table 3.1. These were intended to be scoping experiments, and the conditions were more severe than would exist in the real case. It is apparent, however, that there was fairly large generation of hydrogen from each sample studied. These samples were 1 × 2-in. coupons obtained from the various paint vendors. Each coupon has a specified primer coat, with or without a paint cover, as noted. One or more of these coupons was immersed in the spray solution contained in a small autoclave at a temperature of 130°C, and the solution was stirred during the complete experiment. The pressure rise was monitored throughout these scoping tests, and a run was terminated when the pressure seemed to have reached a more or less constant value. A sample of the gas was then taken and analyzed with a gas chromatograph.

While it is realized that no hard and fast conclusions may be drawn from the limited data, the following points can be made: (1) in all cases appreciable amounts of hydrogen evolved, (2) in all cases the amount of hydrogen evolved was a large fraction of the theoretical amount, and (3) the presence of a paint top coat decreased the hydrogen generation, but in no case could the hydrogen generation be considered insignificant.

Table 3.1. Hydrogen Evolution from Various Coatings

Sample	Exposure Time (hr)	Solution	Hydrogen Evolved (cc/cm^2)	Theoretical Yield[a] (cc/cm^2)
Galvanized ASTM A525	100	0.15 *N* NaOH with 3000 ppm B	10.1	13.2
A-1				
1.5-mil primer coat	24	Same	3.2	3.7
1.5-mil primer coat	48	Same	3.3	3.7
A-2, 2-mil primer coat	24	Same	4.4	4.9
A-3, 3.5-mil primer coat	24	Same	4.4	8.5
A-1, primer and top coats	48	Same	2.6	3.7
A-2, primer and top coats	48	Same	3.1	4.9
A-3, primer and top coats	24	Same	2.7	8.5
B-1, 3.5-mil primer and 3.5-mil top coats	24	Same	4.0	7.3
B-1	24	1 wt % $Na_2S_2O_3$, 0.15 *N* NaOH, and 3000 ppm B	3.3	7.3
B-1	24	3000 ppm B	4.2	7.3

[a]Theoretical yeild based on vendor's statement of zinc content of primer coat.

It is apparent that this area deserves and requires much more thorough study, which may not be possible under present conditions of manpower and funding.

Radiolytic Hydrogen Generation

Work continued on the study of sodium metavanadate ($NaVO_3$) as a possible means of curtailing radiolytic hydrogen production in the spray solution. Previous studies showed that $NaVO_3$ is quite effective in reducing $G(H_2)$ in the borated NaOH spray solution but not at all effective in the base-borate-thiosulfate spray solution. A study was carried out to define the pH effect on the ability of $NaVO_3$ to reduce the production of

radiolytic hydrogen production. The test solution was 2×10^{-3} *M* $NaVO_3$ with 3000 ppm B and sufficient NaOH to give the desired pH. The solution was at ambient temperature and contained in a capsule. It was given a dose of 1×10^8 rads at a rate of 4×10^6 r/hr. All the $G(H_2)$ values given below are averages of three runs:

pH	Apparent $G(H_2)$
5.8	0.12
6.5	0.08
7.0	0.05
7.5	0.03
8.0	0.03
8.5	0.04
9.0	0.03
9.5	0.04
10.9	0.22
12.1	0.27

It may be seen that the $NaVO_3$ is most effective in lowering $G(H_2)$ in the mid-pH range; that is, between pH 6 and 10.

Tests are being conducted on $NaVO_3$ effectiveness in the dynamic-loop radiation facility. These tests are as yet incomplete, but preliminary data indicate that the $G(H_2)$ lowering seen in the capsules also occurs in the loop. The spray solutions under study are the base-borate, the 3000-ppm B solution, and distilled H_2O.

3.5 CORROSION STUDIES IN SPRAY SOLUTIONS

(AEC Activity 04 60 80 01 1)

J. C. Griess G. E. Creek

A program to investigate the corrosive effect of low pH (4.5 to 7.5) spray solutions on materials of construction was initiated. The program involves nine design-basis-accident transient-type loop tests and three long-term storage tests. The facilities are those previously used in the spray program.[1] The corrosion tests with low pH (4.5, 7.5) refueling water solutions, described in the preceding report in this series, are now under way and the first results are expected soon. The loop tests at high temperatures (285°F for 24 hr and 212°F for 168 hr) are 75% complete, and the first long-term test (additional two months at 180°F) is soon to be completed.

Reference

1. J. C. Griess and A. L. Bacarella, Design Consideration of Reactor Containment Spray Systems — Part III. The Corrosion of Materials in Spray Solutions, USAEC Report ORNL-TM-2412, Oak Ridge National Laboratory, December 1969.

4. HTGR SAFETY PROGRAM

4.1 STUDIES OF REACTIONS OF GRAPHITE WITH STEAM

(AEC Activity 04 60 10 01 1)

C. M. Blood S. H. Freid
H. J. de Nordwall* A. P. Malinauskas*

The reactions of steam with various graphites are being studied to develop methods for calculating the effects of steam on the core of an HTGR and the rates of hydrogen and carbon monoxide production. Laboratory investigations are centered on the determination of rate constants and the understanding of the reasons why the observed rate of reaction varies with the extent of reaction. The in-pile program is devoted to testing the validity of the synthesis of laboratory data under realistic conditions.

Laboratory Investigations of Steam-Graphite Reaction

Samples of H-327 graphite received from two sources, Great Lakes Carbon Corporation (GLC) and Gulf General Atomic (GGA), were exposed to steam. Although the experimental data have not yet been analyzed sufficiently to present quantitative results, the differences noted previously (see preceding report in this series) in reactivity of the samples persist; for example, the GLC material is about ten times more reactive than the specimens obtained from GGA, even though no discernable differences in physical characteristics have been found. However, differences in chemical composition of the samples were detected that could account for the observed disparity in reactivity, although both materials are within the specified chemical composition.

Table 4.1 compares the compositions of one sample of each of the source materials. In addition to the differences in ash content, unmistakable differences also exist in iron and vanadium content. Both these elements are known to promote the attack of graphite by steam.

---

*Part time.

Table 4.1. Chemical Composition of H-327 Graphite Samples Received from Two Different Sources

Components	Content (ppm by weight)	
	GGA Graphite	GLC Graphite
Ash	<100	360
Al	<0.3[a]	0.5[a]
B	0.7	0.7
Ca	5	2
Cr	2	20
Cu	3	0.3
Fe	20	150
K	5	5
Mg	6	6
Na	5	5
Ni	5	10
P	0.2	0.2
Si	30	30
V	<0.2	10
Cl	20	20

[a]at. ppm.

In-Pile Experiments

The operational portion of the first in-pile experiment was completed. The purpose of this experiment was to commission the entire facility and to yield information on the resistance to steam of UC_2 fuel coated with SiC. The commissioning experiment took longer than anticipated because of the necessity of correcting several inadequacies in the facility, which was described in a previous report.[1]

During this experiment the fuel was cycled four times into and out of the region of high-neutron flux. During the in-core portion of these cycles the temperature of the graphite casing ranged from 730 to 900°C and the fuel center-line temperature ranged from 840 to 1040°C. The graphite casing containing a bonded bed of fuel particles was exposed to 4% steam in helium during the last two cycles, which lasted a total of about 30 hr. During this time, some 25% of the carbon in the binder and the

casing was removed — not necessarily at a uniform rate. The experimental casing has now been removed from the ORR and disassembled in a hot cell. Evaluation of the data is still incomplete, but the following preliminary conclusions may be drawn:

1. Oxidation of the carbon binder of the fuel stick was almost complete. During hot cell disassembly the loose fuel was poured out of the graphite casing (see Fig. 4.1). The end plug, which originally had been cemented into the can, was easily removed. Removal of the fuel binder during the operational portion of the experiment was indicated by the halving of the thermal conductivity of the fuel piece. Noble-gas release was fairly high during the experiment and tended to increase during steam exposure, indicating significant fuel coating fractures or the exposure of regions of coatings containing ^{235}U. Initial examination of the loose fuel showed both cracked coatings and bare kernels (see Fig. 4.2).

2. The steam oxidized approximately 20% of the graphite casing. This is far more than would be removed in any one HTGR accident. The oxidation occurred, however, by a pitting mechanism (see Fig. 4.3), and easy access of steam to the fuel was possible through sizable holes. Figure 4.4 shows a closeup of a slice through the graphite casing.

3. Radiolytically induced corrosion was insignificant or below the limit of detection at all temperatures used in this experiment.

4. Preliminary analysis of the distributions of fission products after the experiment indicated that in spite of broken coatings and the presence of steam, fission-product release from the fuel was extremely low, even for ruthenium, which is known to have volatile oxides. Table 4.2 shows the fractional distributions of several fission products within the experimental assembly.

The analysis of the data is continuing. The experimental program will continue as soon as a final quality-assurance program is established for the in-pile portion of the apparatus. In future experiments fuel and surface temperatures will be kept constant. Also a new batch of H-327 graphite will be used that does not seem to exhibit the severe pitting type of corrosion found in this experiment. Reasons for different batches corroding in different ways are being explored with assistance from Great Lakes Carbon Corporation, the manufacturers of H-327.

Table 4.2. Distribution of Fission Products After In-Pile Steam-Graphite Experiment SG-1

Component	Fraction of Fission Product Found in a Given Component[a]					
	^{131}I	^{89}Sr	^{140}Ba	^{141}Ce	^{95}Zr	^{103}Ru
Fuel	0.986	0.998	0.999	0.999	0.999	0.993
Graphite casing	2×10^{-3}	5×10^{-4}	6×10^{-4}	4×10^{-4}	5×10^{-4}	6×10^{-4}
Reaction chamber and ceramics[b]	3×10^{-3}	1×10^{-3}	7×10^{-4}	1×10^{-3}	9×10^{-4}	6×10^{-3}
Lower stainless steel tube and filter	9×10^{-3}	3×10^{-4}	5×10^{-5}	1×10^{-5}	2×10^{-5}	1×10^{-5}
Remainder of experimental assembly[c]	6×10^{-7}	1×10^{-6}	3×10^{-6}	1×10^{-6}	$\leq 10^{-7}$	$\leq 10^{-7}$

[a]Fraction of fission product found is defined as atoms of nuclide i in a component divided by atoms of nuclide i found in the whole system at a given time.

[b]Includes a thermocouple that penetrated the fuel bed.

[c]Comprises gas lines to junction box.

Fig. 4.1. Coated Particle Fuel Poured from Model Fuel Element After Exposure to Steam (Experiment SG-1).

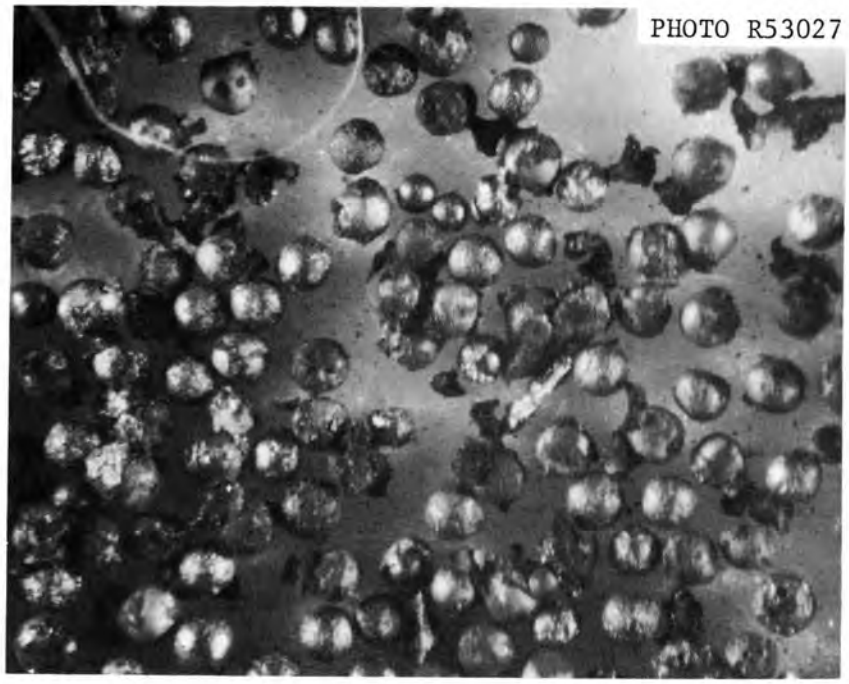

Fig. 4.2. Coated Particle Fuel from Experiment SG-1 Showing Damage to Fuel Coatings and Remnants of the Fuel Stick Matrix.

PHOTO R53034

Fig. 4.3. Graphite Casing of Model Fuel Element Used in Experimental SG-1 After Exposure to Steam.

PHOTO R53037

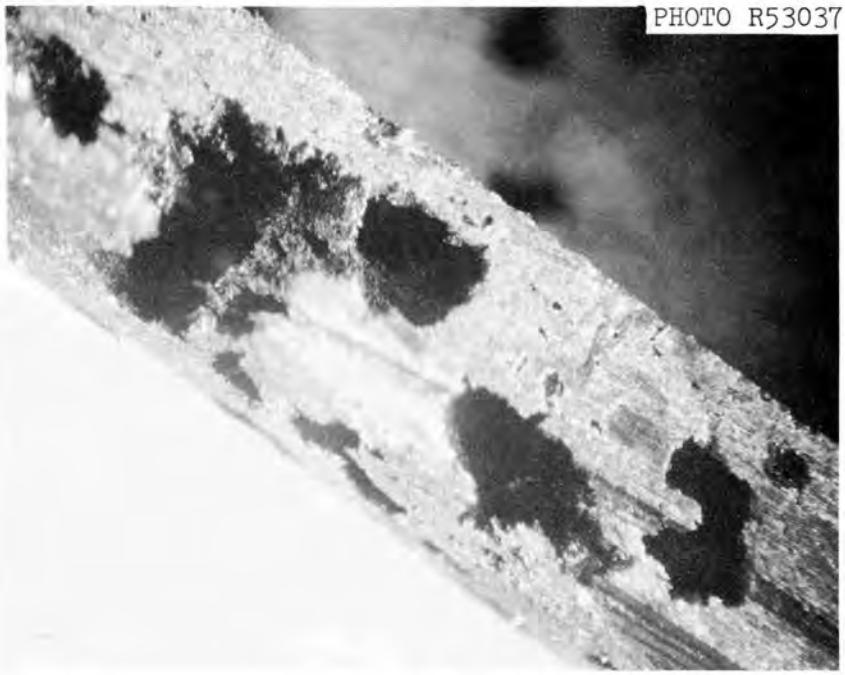

Fig. 4.4. Section Through Part of the Graphite Casing of the Model Fuel Element Used in Experiment SG-1 After Exposure to Steam. Note extent of selective oxidation within the fuel element wall.

Reference

1. S. H. Freid et al., Nuclear Safety Program Ann. Progr. Rept. Dec. 31, 1968, USAEC Report ORNL-4374, p. 299, Oak Ridge National Laboratory.

4.2 FUEL INTEGRITY AND FISSION-PRODUCT RELEASE

(AEC Activity 04 60 10 01 1)

M. T. Morgan R. L. Towns
C. D. Baumann

The reasons for the failure of fuel-particle coatings when temperatures and temperature gradients exceed those to be expected during normal operations are being investigated. A knowledge of when a fuel element is likely to fail after a perturbation is necessary for the design of engineered safety features and the proper analysis of the risks involved from fission-product release.

Fission-Product Release from Coated Fuel Particles in a Bonded Bed During Postirradiation Anneals

The B-51 bonded bed from B9-41, which released 25% of the cesium during an anneal at 1250°C for 2500 hr (see preceding report in this series), was disintegrated in 2.5 *M* HNO_3 by an electrolytic method, and the coated particles were examined under a 30× microscope. Although some of the sacrificial coatings were cracked, none of the cracks appeared to extend into the outer coatings of the particles. The matrix and the coated particles are being analyzed for cesium and strontium.

Diffusion of Cesium in Pyrolytic-Carbon Coatings

The first multiple-tube annealing experiment was completed. Five BISO-coated UO_2 particles from B9-42 were heated simultaneously at 1400°C in separate tungsten tubes. The cesium activity deposited on each tube during the anneal was analyzed periodically to obtain a release versus annealing-time graph. Diffusion coefficients were calculated from the time it took for the cesium to come through the coatings at 1400°C. The cesium released during 72 hr of annealing varied from 0.5 to 32%. No ^{85}Kr was released, and thus no coating failures were indicated. The diffusion coefficients and the cesium release are given in Table 4.3. A diffusion coefficient could not be calculated for coated particle No. 8, which was the one that had the exceptionally high cesium release. The intercept with the annealing time axis indicated that cesium had already

Table 4.3. Cesium Release and Diffusion Coefficient Obtained from BISO-Coated Particles Annealed at 1400°C

Coated Particle No.	Cesium Release in 72 hr (%)	Diffusion Coefficient (cm^2/sec)
		$\times 10^{-11}$
1	0.5	2.6
2	2.6	12
3	4.6	7.0
4	6.2[a]	6.5
5	7.2	8.4
6	15	12
7	17	13
8	32	

[a]Extrapolated from cesium release at 42 hr.

penetrated the coating at the beginning of the anneal, although these coated particles were irradiated at approximately 600°C and no cesium migration would be expected through intact coatings. This particle will be examined further.

Cesium Release Through TRISO Coatings at High Temperatures

Investigation of SiC layers that failed to retain cesium during post-irradiation anneals of TRISO-coated UO_2 particles at temperatures of 1800°C and above was continued. "Fax-film" replicas were made of the surfaces of the exposed SiC layers of apparently intact coated particles that had released cesium, and these were examined under the scanning electron microscope. One-third to one-half the surfaces of four such coated particles were explored at magnifications up to 5000×, and no evidence of cracks was found.

In a previous study, eight of ten coated particles annealed for 10 min at 2200°C had released cesium, and photomicrographs showed all eight to be cracked, while the two that did not release cesium were not cracked. This was not conclusive, since the cracks seen in the photomicrographs

could have been caused during the grinding and polishing preparations. In a calculation of stresses developed within these coated particles, it was shown that the SiC layer could have failed without simultaneous failure of the pyrolytic-carbon outer coating. These calculations are described below.

Scanning electron micrographs of fragments of SiC from one coated particle that released cesium revealed apparent porosity. Porosity could not be found, however, in subsequent micrographs of SiC layers of other coated particles from the same sample, which had also released cesium.

These investigations indicate a high probability of cesium being released through cracks in the SiC layers of TRISO coatings during the anneals at high temperatures, but optical and electron microscope studies failed to reveal such cracks. The investigation is to be continued with electron micrographs of the SiC coatings that were shown to be cracked in the photomicrographs in order to be sure what a crack looks like in the electron micrographs. Also, more coated particles with the outer coatings burned off, some of which have released cesium and some which have not, will be annealed. If the SiC is cracked, the coated particles should burst open at a lower temperature than if it is not cracked.

Failure Model Analysis of Irradiated OR-818 TRISO-Coated Particles

The Walther Stress 2 computer code* was used to analyze the failure of irradiated OR-818 coated fuel particles, as indicated by ^{137}Cs release during postirradiation anneals. The fully enriched UO_2 kernels were coated with a low-density buffer layer, a thin high-density pyrolytic-carbon sealer layer, an SiC layer, and a high-density outer pyrolytic-carbon coating. The coated particles had been irradiated in the ORR B9-41 experiment at 630°C to a burnup of 20% FIMA at a fast-neutron (>0.18 Mev) fluence of 2.38×10^{20} neutrons/cm^2. The coated particles were then annealed for 10 min at 1300 to 2200°C in 100°C increments. The ^{95}Zr and ^{137}Cs activities of each coated particle were measured after annealing.

*Code obtained from Dragon Project under USAEC-Dragon Project exchange agreement.

X-ray radiographs and metallographic micrographs were made, and from these the average dimensions of the components of each coated particle were obtained.

The Walther Stress 2 code for calculating the in-pile performance of a coated particle was modified for use on the ORNL computers by Hall Roland.* The values for the tangential rupture stress of the sealing layer, SiC, and outer pyrolytic-carbon coating were adjusted until the code gave a reasonable description of the performance of the particles as indicated by the ^{137}Cs release fraction. It is necessary to proceed in this manner because there is not much data on the mechanical properties of the materials used in coated particle manufacture as functions of temperature, fast-neutron dose, and structure; and it is difficult to be sure that the samples of the various materials used in obtaining data were identical with the materials in a given batch of fuel or, in particular, a given particle. Thus the value of the design code in this application is that it permits a semiquantitative discussion of the results and permits exploration of the relative significance of parameter changes. Extrapolation beyond experimental conditions must be done with great care.

Table 4.4 lists the results of the calculations when the rupture stresses of the sealer, SiC, and outer pyrolytic-carbon coating were 45,000, 160,000, and 50,000 psi, respectively. While these results are not exactly replicative of the particle performance indicated by ^{137}Cs release, they are qualitatively correct. Even though the assumed values of the rupture stresses are reasonable [Price[1] gives a value of $(135 \pm 16) \times 10^3$ psi for SiC], there are probably other combinations of different values of the rupture stresses that would describe the performance just as well or perhaps better. Additional trial and error calculations will be made to determine better combinations of rupture stresses. However, it would probably require the successful description of many more than ten particles before any unique set of rupture stresses could be considered valid. Hence the need for representative independently determined coating properties is indicated.

---

*Consultant, University of Tennessee.

Table 4.4. Failure Model Analysis of Irradiated OR-818 TRISO-Coated Particles[a]

Particle No.	Measured ^{137}Cs Release (%)	Calculated Conditions for Coating Fracture			Ratio of Core Volume to Buffer Volume
		Sealer Coating Annealing Temperature (°C)	SiC Coating Burnup (%)	Outer Coating Annealing Temperature (°C)	
1	<1	(b)	(b)	(b)	0.54
2	1	(b)	(b)	(b)	0.60
3	47	(b)	19.6	(b)	0.94
4	43	(b)	18.9	(b)	0.98
5	45	(b)	19.1	(b)	1.03
6	45	2000	17.0	(b)	1.13
7	50	1900	17.3	(b)	1.13
8	58	2000	17.1	(b)	1.16
9	59	2000	16.8	(b)	1.20
10	64	1500	16.3	2000	1.25

[a]Assumed rupture stresses: sealer, 45,000 psi; SiC, 160,000 psi; outer coating, 50,000 psi.

[b]Computations indicated that this coating would not have broken under the test conditions.

It was found that a rather simple geometric parameter, the ratio of the core volume to the buffer volume (which roughly corresponds to the internal gas pressure), results in a surprisingly good qualitative description of particle performance (see Fig. 4.5). Apparently the reason for this is that the variation in the thickness of the SiC and outer pyrolytic-carbon coatings was much less than the variation in the core-to-buffer volume ratio.

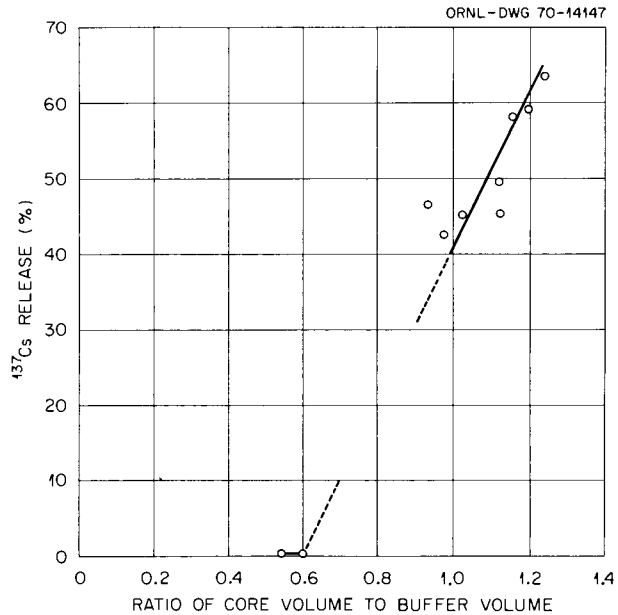

Fig. 4.5. ^{137}Cs Release During Postirradiation Anneal Versus Core-to-Buffer Volume Ratio.

Reference

1. R. J. Price, Structure and Properties of Pyrolytic Silicon Carbide, USAEC Report GA-8883, Gulf General Atomic, Inc., Oct. 22, 1968.

4.3 FISSION PRODUCTS IN HTGR COOLANT CIRCUITS

(AEC Activity 04 60 10 01 1)

F. F. Dyer* J. Kolb
H. J. de Nordwall*

The distribution, nature, and behavior of fission products in the primary coolant circuit are being studied under accident conditions. Laboratory experiments are under way to obtain the data needed to carry out a satisfactory analysis of the release and transport of radiologically important nuclides. This requires an understanding of the chemical species normally present in the coolant gas, either as a gas or adsorbed on circulating particles. It also requires further information on the mechanisms for deposition of these forms of fission products on surfaces within the circuit and subsequent reentrainment during an accident.

Coolant circuit chemistry, particularly of iodine and iron iodides, and deposition and reentrainment of dust from flowing gas are presently being investigated. Earlier progress reports in this series indicated the significant developments on the chemistry of the coolant circuit, and the studies of dust deposition and reentrainment and the measurement of fission products in the circuit of an operating HTGR are the subjects of this report.

Dust Dynamics

Deposition and reentrainment of dust from turbulently flowing gas is being studied as a function of surface and hydrodynamic conditions. The first experiment will be in straight-channel geometry. The main effort during this report period was on preliminary aerosol generation tests, equipment selection, and instrument calibration for the dust deposition facility (DDF). A summary of the dust deposition facility operating characteristics, as described in detail in the previous bimonthly report, is given below:

---

*Part time.

Type of aerosol generator	Carbon arc with air purge
Minimum aerosol age	3 min
Deposition region section	3 × 1/4 in.
Flow medium	Dried "instrument" air
Volumetric flow available	>75 scfm
Average flow velocity	240 ft/sec at 75 scfm
Channel Reynold's number	57,800 at 75 scfm
Friction pressure drop (smooth surface)	0.56 in. H_2O/ft at 75 scfm
Radioactive tracer	27-d ^{51}Cr

Aerosol-generation rate tests are under way in a glass mockup of the final aerosol generator. Effects of air purge rate and spark gap on generation rate are being determined. A continuously recording condensation nuclei counter has been put in service to monitor the aerosol number concentration.

A preliminary investigation of the comparative reentrainment conditions in the dust deposition facility and the Fort St. Vrain HTGR was made. Flow conditions for helium at 700 psia and 1450°F were estimated in the 2-ft circular ducts connecting the core and steam generators. The wall shear stress was used to estimate the relative fluid dynamic force on the same particle deposited on the wall of the DDF and the HTGR duct. The Blasius friction factor formula was used to calculate the friction velocity, μ, for smooth surfaces. The wall shear stress is then given by $\tau_0 = \mu^2\rho$, where ρ is the fluid density. The air flow required in the DDF for equal wall shear stress with smooth surfaces is about 48 scfm, which will be well within the air flow rate available to the DDF. With 75-scfm air flow, the wall shear stress in the DDF is 2.15 times the wall shear stress in the Fort St. Vrain duct. However, for roughened surfaces, more flow is required in the DDF than with a smooth surface for the same relative wall shear stress. This situation results because the roughened-surface friction factor levels out rather than decreases with increasing Reynold's number. For example, the same wall shear stress is obtained in the DDF and the reactor duct for 75-scfm flow with relative sand roughness below 507. Therefore air flows in excess of 75 scfm will be used in reentrainment experiments with roughened surfaces.

Fission-Product Surveillance Program

Peach Bottom Measurement Procedures

Although it is planned to measure short-lived fission gases in the primary circuit of the Peach Bottom HTGR by absorbing and counting the gases on charcoal, an alternative approach by direct examination of the flowing primary circuit helium by gamma spectrometry will also be attempted. This possibility arose during a recent visit to Peach Bottom. A 1.5-in.-diam pipe conducts primary circuit helium from a circulator to the hot gate valve for cooling, and about 1 ft of the pipe is accessible during reactor operation. It will therefore be possible to place an appropriately shielded Ge(Li) gamma detector within about 1 in. of this pipe and perhaps measure the short-lived gases directly. The necessary counting equipment will be taken to Peach Bottom within the next few weeks to test the direct-counting method.

It is estimated that about 100 cm^3 of primary circuit helium can be measured with a counting efficiency that is approximately 0.1 of that obtainable with a charcoal trap sample. Measurements of the expected count rates and detection limits obtained for several of the short-lived gases by both methods have been compared. Because of the probable long delay times, it was assumed that most gases on charcoal traps would be measured by counting their longer lived daughters. It was also assumed that gas collection times would not exceed two weeks, and under these conditions the count-rate estimate indicates that for gases with very long-lived daughters (e.g., ^{137}Xe-^{137}Cs) direct counting would be the most sensitive method. In those instances in which the daughters have half-lives of a few weeks or less the charcoal absorption method would be about 100 times more sensitive than direct counting.

If later in the project a 4096-channel γ analyzer can be made available for use on the spot, shorter-lived γ-emitting daughters could be counted for all mass chains of interest, with gains in sensitivity, speed, convenience, and additional information. The design of gas samplers is proceeding.

Aerosol from Peach Bottom HTGR

In a previous report in this series an examination of samples of particulate matter from a diffusion probe and an aerosol filter from the Peach Bottom HTGR was described. These samples were provided by Gulf General Atomic, Inc. Some additional information has been obtained from further electron microscopy.

Inspection of samples stripped from the diffusion probe body (2DP-3) and of replicas of the probe's surface yielded little new information. The denser deposits were found to contain many very small particles; some were as small as 0.01 μm in diameter. The composition of this deposit was essentially that previously reported; namely, metal oxides and carbon, which is either not crystalline or present only in small particles; but some x-ray lines have been reassigned (see below).

Electron micrographs of replicas of the diffusion probe (2DP-3) showed regions where reaction was taking place that corresponded to the thicker sections of the films observed to be covering the surface when polished sections were examined optically. These islands were wrinkled, irregular, and pock-marked. Figure 4.6 shows a boundary between a smooth region and a wrinkled one that is typical of stainless steel exposed to impure hot helium. However, a third structure was also observed, shown in Fig. 4.7, which looks like a local development of porosity or local melting and resolidification. Irregularly shaped particles such as the one in the center of Fig. 4.7 were sometimes congruently associated with these "porous" areas. Whether these areas represented the sites of reaction or were merely artifacts is not clear, nor can it be proved that a particle had originated from all such zones. Since it is thought that these processes are of greater interest with respect to carburization and oxidation processes in the primary circuit, these observations have been reported to Gulf General Atomic, Inc.

In the previous report, it was stated that x-ray powder analysis had revealed a compound "FeC." This material (ASTM Index Card No. 3-0410) has a diffraction pattern similar to that of graphite.[1] Further comparison of the x-ray diffraction pattern of the material from the diffusion probe filter (sample 3DP-F) with that of graphite suggested that graphite

PEM-200-11744

Fig. 4.6. Replica of Part of Diffusion-Probe Body. Type 304 stainless steel exposed to helium coolant of Peach Bottom HTGR for about 150 power days at 690°C. 12,000×. Note two different regions.

PEM-200-11747

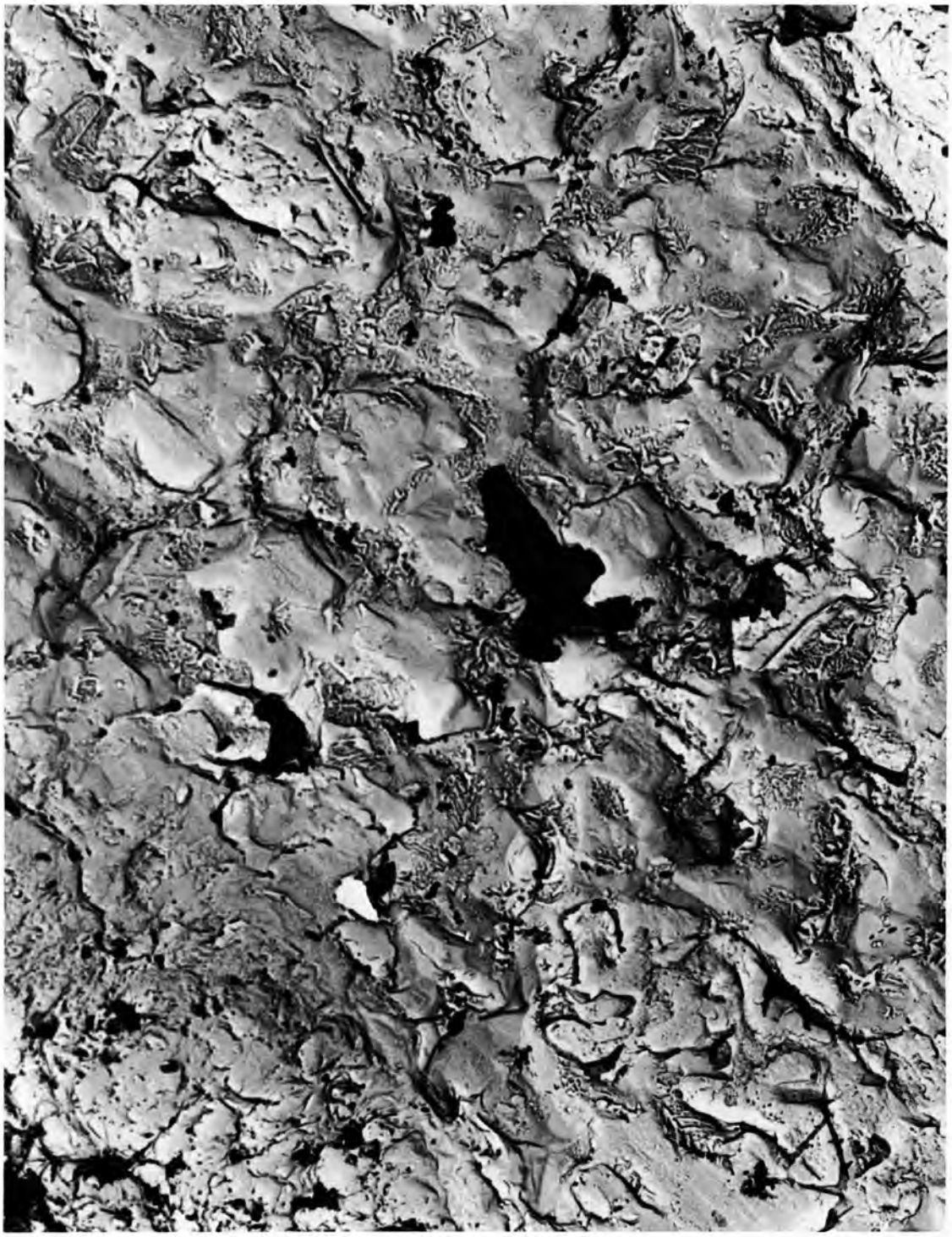

Fig. 4.7. Replica of Part of Diffusion Probe Body. Type 304 stainless steel exposed to helium coolant of Peach Bottom HTGR for about 150 power days at 690°C. 12,000×. Note small apparently porous or pockmarked regions and association of congruent particles with such regions.

was a more reasonable assignment for these lines. Only one line known to be of low intensity was lacking, while eight were observed.

Fe_2C, which was also found, is known to be formed on the iron-based catalysts that are used in the synthesis of hydrocarbons from carbon monoxide and methane.[2,3] Above 400°C all carbides of empirical formula Fe_2C, or thereabout, decompose to cementite, Fe_3C, and carbon. Fe_2C was not found in the hot part of the probe. While Fe_2C is well documented, Konobejewski's[1] FeC is not believed to represent more than a sample of graphite containing an iron impurity, although there is another "FeC" described by Eckstrom and Adcock[4] (ASTM Index Card 6-0686) that does differ markedly from graphite. This is believed by Herbstein and Snyman[5] to be Fe_7C_3 and was not observed in these specimens.

The previous conclusion that carbon deposition and carburization had occurred on the probe is still valid. The presence of a diffraction pattern for graphite is consistent with the environment; namely, a graphite-moderated reactor and the previously reported graphite whiskers.

Assistance was provided in this work by H. W. Dunn and T. E. Willmarth of the Analytical Division and J. H. DeVan of the Metals and Ceramics Division.

References

1. S. Konobejewski, A Solid Solution of Iron in Graphite, *Zeit Krist.*, 72: 381 (1929).

2. G. H. Barton and B. Gale, The Structure of a Pseudo-Hexagonal Iron Carbide, *Acta Cryst.*, 17: 1460 (1964).

3. L. J. E. Hofer, E. M. Cohn, and W. C. Peebles, The Modifications of the Carbide, Fe_2C; Their Properties and Identification, *J. Amer. Chem. Soc.*, 71: 189 (1949).

4. H. C. Eckstrom and W. A. Adcock, A New Iron Carbide in Hydrocarbon Synthesis Catalysts, *J. Amer. Chem. Soc.*, 72: 1042 (1950).

5. F. H. Herbstein and J. A. Snyman, Identification of Eckstrom-Adcock Iron Carbide as Fe_7C_3, *Inorg. Chem.*, 3(6): 89 (June 1964).

5. PRESSURE-VESSEL AND PIPING TECHNOLOGY

5.1 HEAVY-SECTION STEEL TECHNOLOGY PROGRAM
(AEC Activity 04 60 80 03 1)

F. J. Witt

The civilian nuclear power industry has progressed rapidly in the last few years, as attested to by the some 100 nuclear power stations now in operation, under construction, or on order. Capacities of plants under construction are exceeding 1100 Mw(e), and the walls of the reactor pressure vessels are approaching 12 in. in thickness, with design pressures up to 2500 psi. The design temperature ranges up to 650°F.

The Heavy-Section Steel Technology (HSST) program is one of the major USAEC-sponsored safety programs specifically oriented to assess the safety of the pressure vessels. Since all steel vessels are assumed to contain flaws (nonhomogeneities or discontinuities) of some size, the effects of such flaws on the fracture behavior of pressure vessels are of primary interest. The development of a quantitative technology to make the necessary safety assessments, together with an understanding of the factors (including irradiation) that degrade or change the anticipated behavior of the steel, is a primary objective of the HSST program.

The HSST program is divided into 12 tasks under which all the activities fall. These tasks are discussed below.

Task A. Program Administration and Procurement

A technical report[1] and a technical manuscript[2] were published, and a progress report was distributed.[3] Also, two technical reports, one documentary report, and three technical manuscripts were reviewed prior to publication. The HSST Program Review Committee met at ORNL on October 26 and 27.

Fabrication of the intermediate vessels is continuing. The delivery date has been set back because unexpectedly high strength values were found for the cylindrical test courses. A deadline of December 1 has been set for resolution of this problem.

Task B. Material Inspection and Control

Careful monitoring of the fabrication history of the intermediate vessels continues. This is proving especially helpful in investigating the high strength values of the cylindrical courses.

Task C. Material Characterization

A final report on this activity is being written.

Task D. Variability in Plates, Heat-Affected Zones, Welds, and Forgings

A *Data Trac* instrument was set up to study the factors that affect the properties of pressure vessel steels and steel product forms. This instrument is currently being used in the properties investigation of the intermediate vessels.

Task E. Transition-Temperature Investigations

No work is currently in progress under this task.

Task F. Fracture Mechanics Investigation

The investigation of dynamic fracture toughness was completed by Westinghouse Electric Corporation and a final report is being written. Work continues on the gross strain and crack arrest investigations. Final reports were written on the fracture-toughness characterization of HSST 12-in.-thick steel plates.

Negotiations were completed with Westinghouse Electric Corporation for obtaining K_{Ic} in the transverse direction at temperatures perhaps as high as 100°F. Tests will also be made on a variety of specimens at temperatures where valid K_{Ic} values cannot be obtained. Some tests will be performed at 550°F. The results of these tests will be used in evaluating data from both two- and three-dimensional elastic-plastic finite-element computer programs developed under the HSST program.

Task G. Fatigue and Crack Propagation

The cyclic testing portion of 2-in.-thick side-notched compact tension specimens in an environment of high-temperature high-pressure water is continuing. Fourteen specimens were prepared for stress corrosion studies being conducted by the General Electric Company.

Task H. Irradiation Effects

The investigations of irradiation effects on HSST plate (ASTM A 533, grade B, class 1) and weldments at Westinghouse Electric Corporation, Naval Research Laboratory, and ORNL were completed.

The main emphasis at the Naval Research Laboratory has been on the investigation of irradiation effects on dynamic-tear specimens. Some results from quarter thickness and surface specimens are shown in Figs. 5.1 and 5.2. The orientation was transverse, and the irradiation temperature was less than 300°F. The half-energy transition shift may be seen to vary between 260 and 310°F for these conditions. The shelf energies are reduced by around 40%. Similar studies (the data are not yet available) at 550°F have shown that the percent reduction in Charpy shelf energy with irradiation is comparable to the percent reduction in 5/8-in.-thick dynamic-tear specimen shelf energy.

The emphasis of the work at ORNL has been on Charpy V-notch and tensile data. The most recent investigations have been on weld metal. The effects of an irradiation fluence ($E > 1$ Mev) of approximately 1×10^{19} neutrons/cm^2 at about 550°F on submerged-arc and electroslag weld metal are shown in Figs. 5.3 and 5.4, where shifts in the temperature at which the energy transition occurs of from about 50°F for the electroslag weld to 200°F for the submerged-arc weld may be seen. The shelf of the electroslag weld was virtually unchanged, while for the submerged-arc weld the shelf was reduced by about 40%.

An extensive study has been under way, mainly at Hanford Engineering Development Laboratory, to determine the feasibility of irradiating and testing 4-in.-thick compact tension specimens. A completely satisfactory set of conditions has not been found and the investigations are continuing.

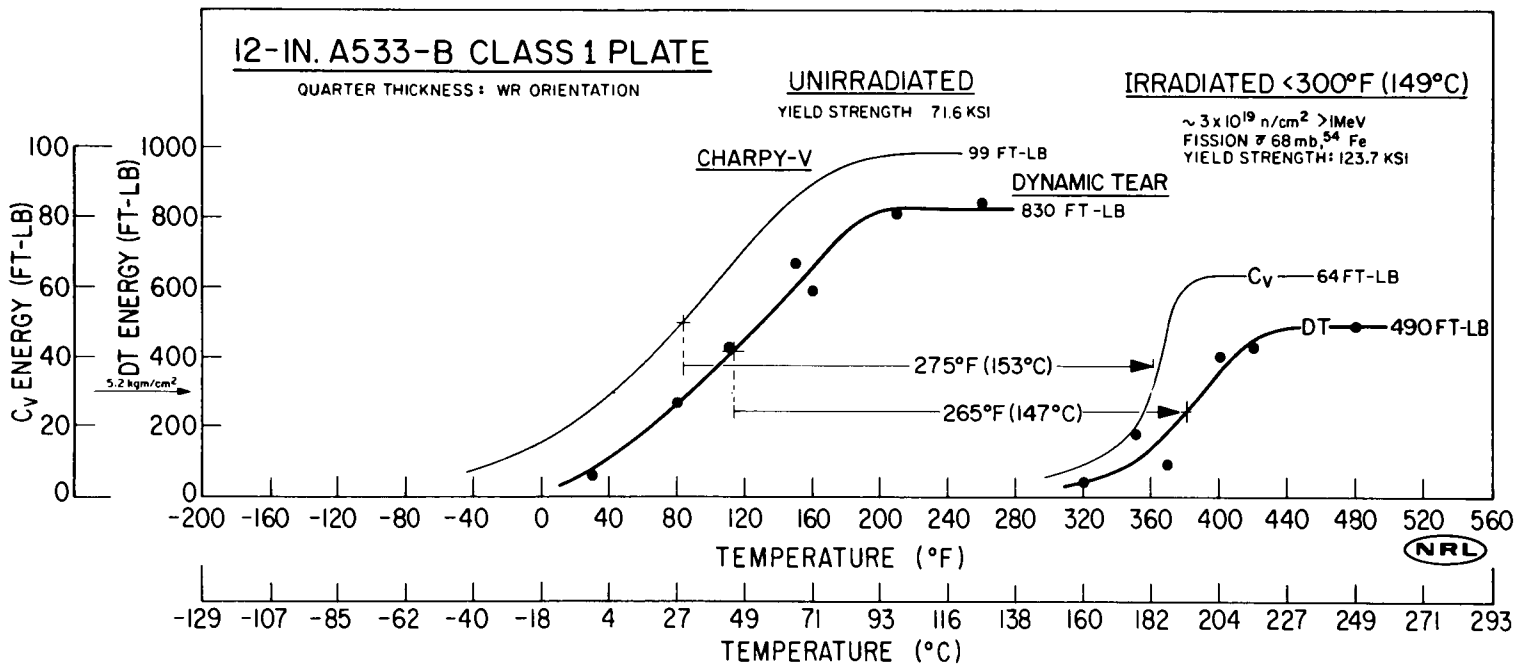

Fig. 5.1. Experimental Comparison of the Charpy-V and Dynamic-Tear Test Performance of Thick-Section A 533, Grade B, Class 1 Steel Plate After Irradiation at Less Than 300°F; Quarter Thickness Material; WR Orientation (NRL).

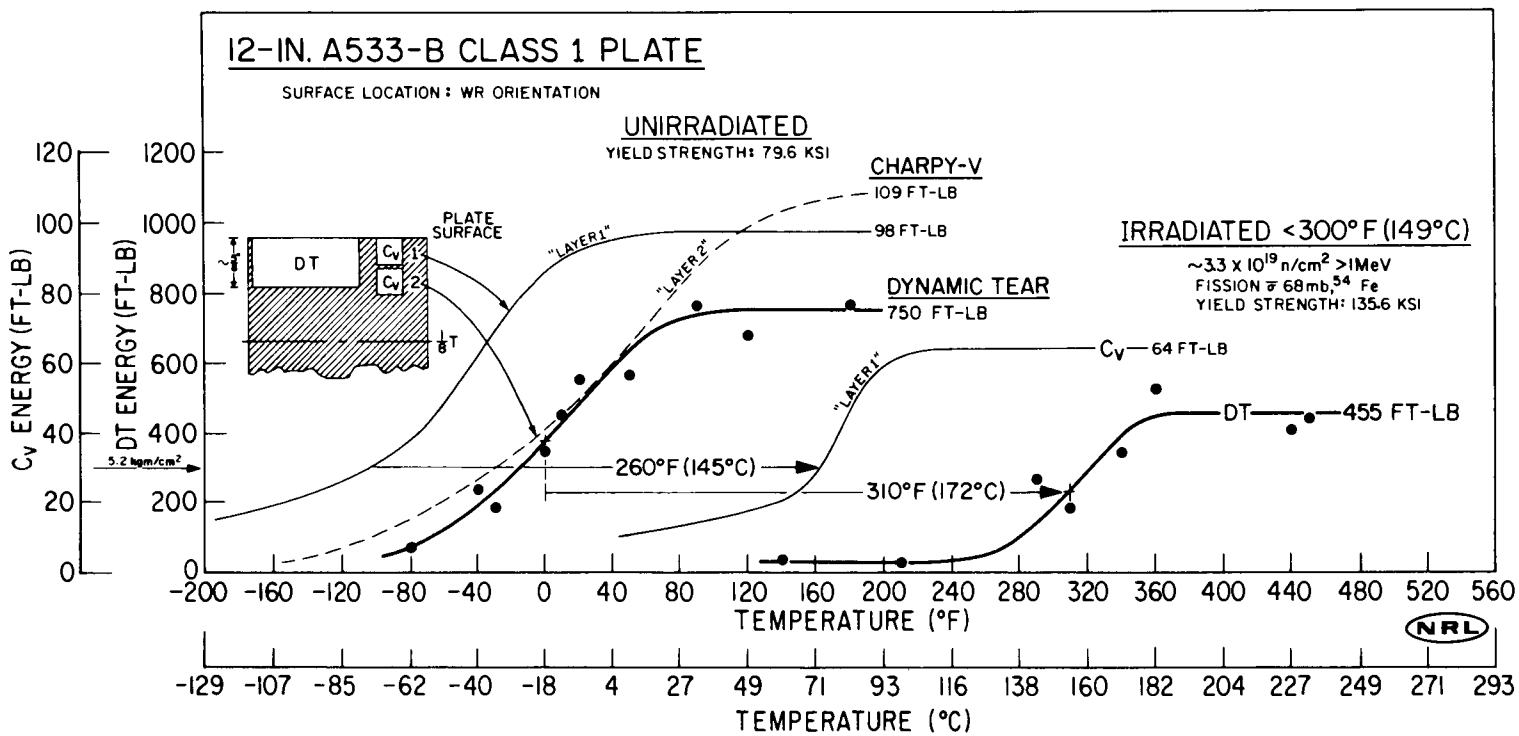

Fig. 5.2. Experimental Comparison of the Charpy-V and Dynamic-Tear Test Performance of Thick Section A 533, Grade B, Class 1 Steel After Irradiation at Less Than 300°F; Surface Material; WR Orientation (NRL).

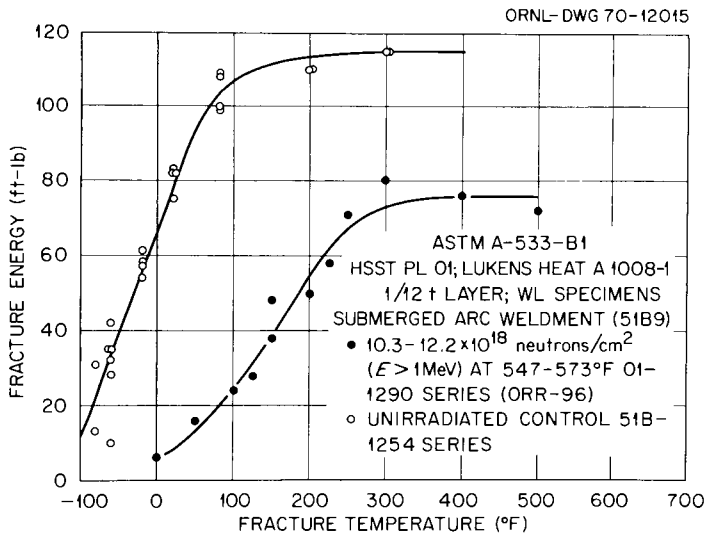

Fig. 5.3. Comparison of Pre- and Postirradiation Charpy V-Notch Toughness of 12-in.-Thick Submerged-Arc Weldment.

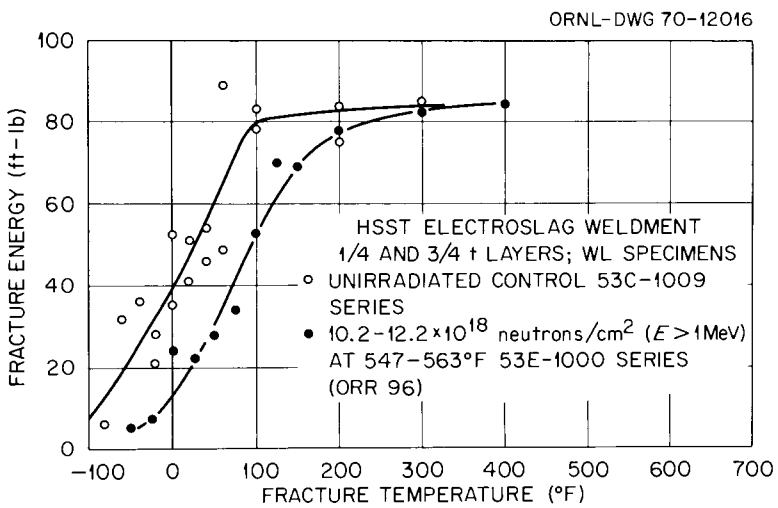

Fig. 5.4. Comparison of Pre- and Postirradiation Charpy V-Notch Toughness of Electroslag Weldment.

Task I. Complex Stress State

Fabrication of a series of small pressure vessels is nearing completion. Once flaws are produced in the vessels, testing will start immediately.

A procedure for locally fatiguing a crack by means of pressure has been developed. Crack growth resulting from applying the procedure to a machined notch is shown in Figs. 5.5 and 5.6. A crack grown 0.18 in. from a tapered notch at room temperature is shown. This growth was accomplished in about 25,000 cycles at 17,000 psi. Essentially, a seal is formed around a machined notch, and pressure is applied cyclically to the notch. The crack growth is monitored ultrasonically. A crack being grown in a large tensile specimen is shown in Fig. 5.7. Cracks were prepared in two such specimens by this procedure (24,000 cycles at 19,000 psi), and the specimens were tested at Southwest Research Institute (see later discussion, Task K). The fatigue cracks obtained extended between 3/8 and 1/2 in. from the root of the machined notch, except very close to the surface.

PHOTO Y101817

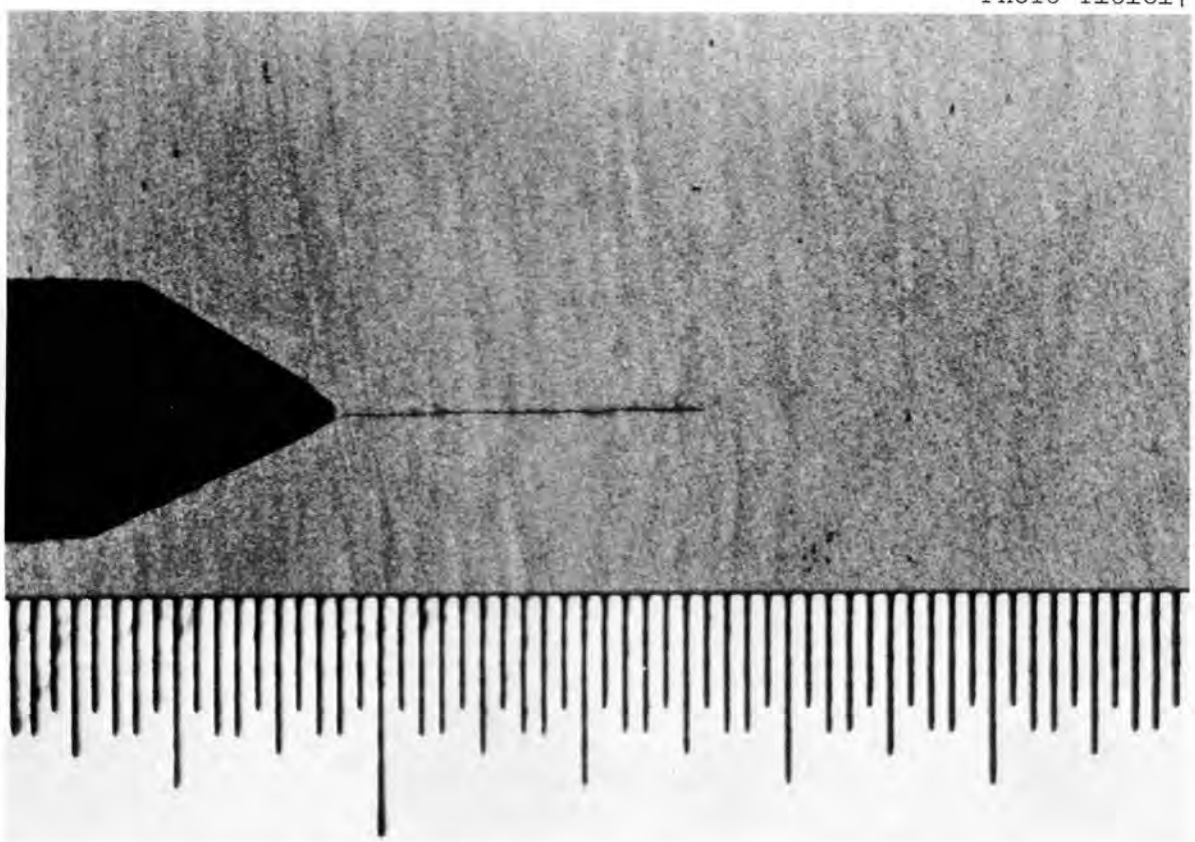

Fig. 5.5. A Fatigue Crack 0.18 in. Deep Grown from a Machined Notch at Room Temperature in 25,000 Cycles.

PHOTO Y102210

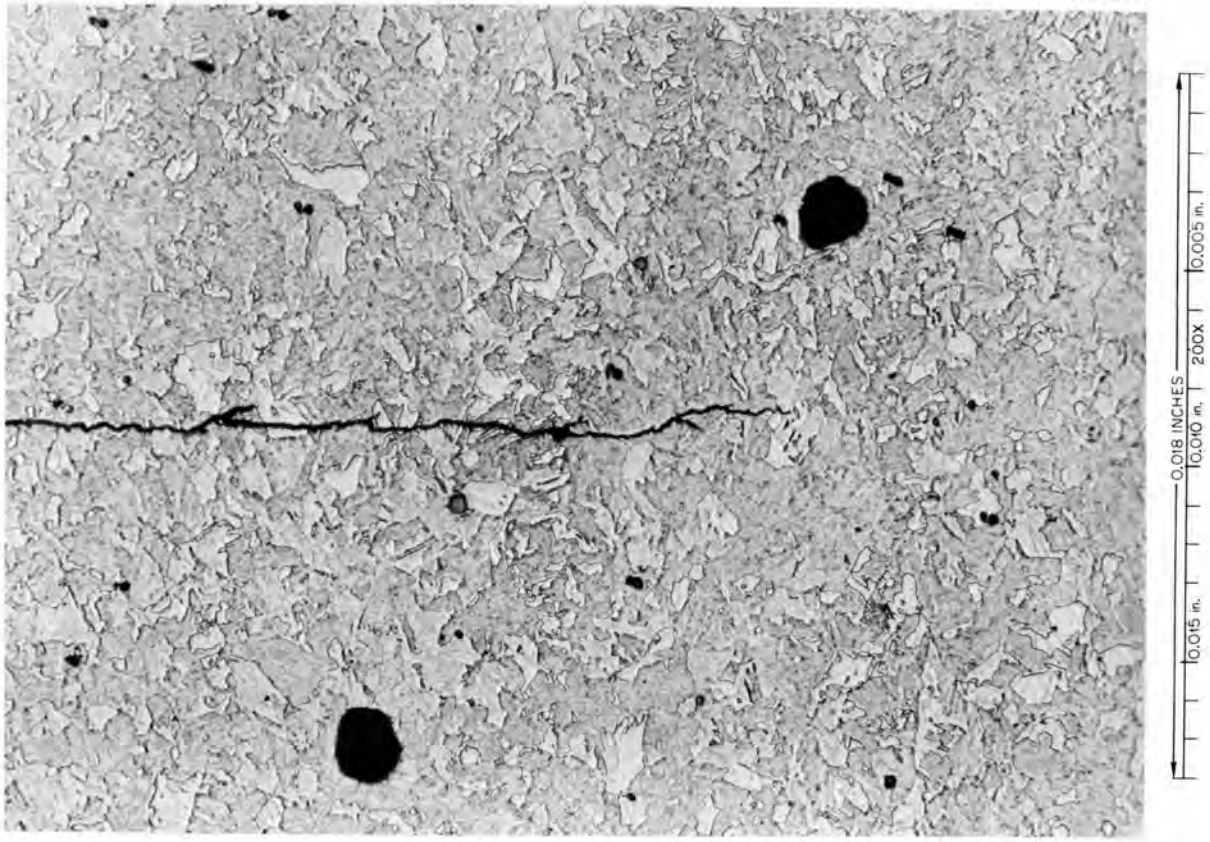

Fig. 5.6. Crack Grown by Local Fatigue. 200×

Task J. Periodic Proof Testing and Warm Prestressing

No work is currently in progress under this task.

Task K. Simulated Service Test

The fourth, fifth, and sixth large tensile specimens were tested at Southwest Research Institute. Five of the six fracture surfaces are shown in Fig. 5.8. The surface from the first specimen, which was also tested at about 220°F, is not shown. Essentially flat fracture occurred at 50 and 75°F and in one of the specimens tested at 100°F. The results for the other specimen tested at 100°F and the one tested at 220°F were very similar as far as load and strain are concerned. Supposedly, the two

Fig. 5.7. Crack Being Grown by Local Fatigue in a Large Flawed Tensile Specimen.

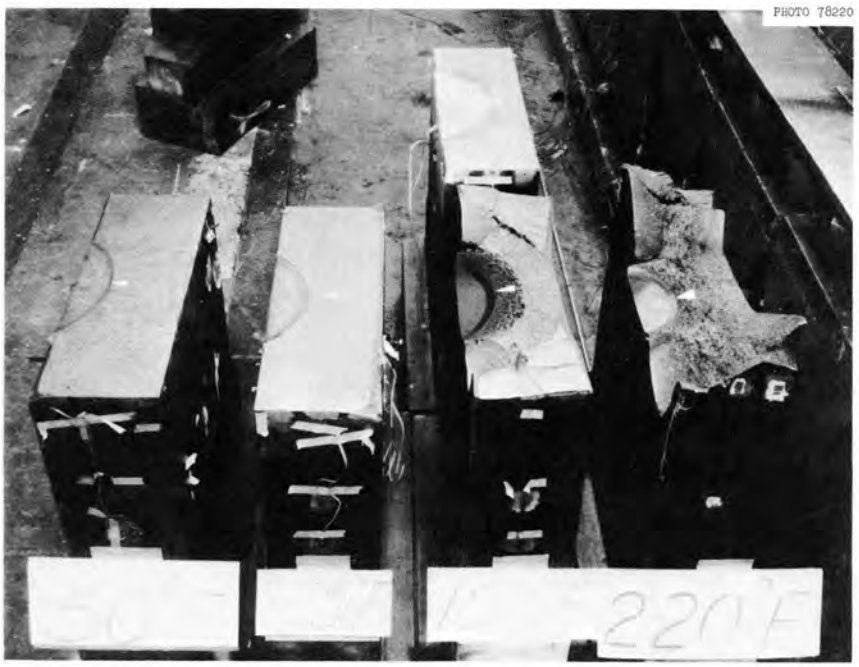

Fig. 5.8. Fracture Surfaces of Five Large Tensile Specimens 18 in. Long and 6 in. Thick Tested at Temperatures Between 50 and 220°F.

specimens tested at 100°F differed only in flaw size, with the one exhibiting flat fracture having a flaw about 3 1/2 in. deep, while in the other the flaw was about 2 1/8 in. deep. The 1/2-in.-deep fatigue crack grown by the method discussed above is easily identified by the arrow on the specimen tested at 75°F.

The results for the two specimens tested at 100°F appear to be somewhat anomalous, and the reasons for this are being further investigated.

The equivalent energy method was applied to the testing of these specimens. With the exception of the specimen tested at 100°F, which behaved in a very tough manner, the behaviors of the remaining five specimens were very accurately predicted by the equivalent energy method. The calculated energy dissipations for the five specimens were within the scatter range of the data obtained from symmetrically placed strain gages. If the yield strengths of the actual specimens had been accurately known, load calculations would have been accurate to within ±2%. Further evaluation and collection of the test results are in progress.

Task L. Specific Safety Research

A draft copy of the final report of the correlation study of impact and fracture toughness data was received and being reviewed. A final report on the thermal-shock study was completed except for one appendix. Both reports should be in the process of being published within the next six weeks.

References

1. T. R. Mager, Heavy Section Steel Technology Program Technical Report No. 9, Post-Irradiation Testing of 2T Compact Tension Specimens, Report No. WCAP-7561, Westinghouse Electric Corporation, August 1970.

2. D. A. Canonico, Transition Temperature Considerations for Thick-Wall Nuclear Pressure Vessels, USAEC Report ORNL-TM-2114, Oak Ridge National Laboratory, October 1970.

3. F. J. Witt, Heavy-Section Steel Technology Program Semiannual Progress Report for Period Ending February 28, 1970, USAEC Report ORNL-4590, Oak Ridge National Laboratory, October 1970.

5.2 EXPERIMENTAL AND ANALYTICAL INVESTIGATIONS OF NOZZLES

(AEC Activity 04 60 70 01 1)

W. L. Greenstreet J. P. Callahan

The intersection of a nozzle with a large pressure vessel is a highly stressed region when either the vessel is subjected to internal pressure or the nozzle is subjected to moment or thrust loadings. The development of analytical procedures together with experimentation to substantiate these procedures, has been undertaken in order to accurately predict magnitudes and locations of these stresses. Included in the studies are single nozzles radially and nonradially attached to a spherical shell, perforated flat plates and spherical shells, nozzles attached in clusters to flat plates and spherical shells, and single nozzles attached to cylindrical shells. Factors to be investigated by these studies include (1) the effect of superposition of various loadings on the nozzle, (2) mutual interactions between adjacent openings and nozzles, and (3) the general magnitude of stresses in nonradial (or hillside) nozzles in order to establish their potential limitations.

These investigations are conducted in close cooperation with subcommittees of the Pressure Vessel Research Committee (PVRC) of the Welding Research Council. The results are being used to establish rules for both industrial and AEC-RDT standards and to provide analyses and design methods capable of assuring that reliability and safety requirements are being met. The information is made available in the form of computer programs and design charts and tables based on parametric studies or empirical correlations.

Project Management

As a member of the Pressure Vessel Research Committee, ORNL has been assigned the task of coordination, review, and evaluation of the research program for the PVRC Subcommittee on Reinforced Openings and External Loadings. This management function consists of (1) direction of AEC-sponsored work, including the work both at ORNL and under subcontract, (2) generation of parameter studies in support of various evaluation and correlation

studies being conducted at Battelle Memorial Institute, (3) reporting to the PVRC subcommittee on non-AEC-sponsored projects and making recommendations concerning those projects, and (4) soliciting comments and recommendations from the PVRC subcommittee concerning AEC-sponsored work. Two PVRC meetings were held in New York in September — a meeting of the Subcommittee on Reinforced Openings and External Loadings on September 28, and a meeting of the Design Division on September 29. Oral reports on current progress of the various projects were made at both meetings.

Single Nozzles in Spherical Shells

Models with individual nozzles radially and nonradially attached to steel hemispherical shells are being subjected to experimental stress analysis at the University of Tennessee. One model has a 7.875-in.-OD nozzle attached radially, and a second model has two 2.625-in.-OD nozzles attached at oblique angles of 22 1/2 and 45°, respectively. Currently tests are being conducted on the 22 1/2° nozzle model having a 0.0625-in. wall thickness.

Single Radial Nozzles in Cylindrical Shells

A report containing results of the plastic collapse test of a large thin-walled tee ($d/D = 0.5$, $D/T = 23$, $s/S = 0.51$)* under internal pressure loading is being prepared at the University of Tennessee.

At ORNL, analyses are being made of nozzle-to-cylindrical shell attachments by using closed-form types of solutions for the equations. The results of the analyses will be compared with available experimental results for internal pressure loading and out-of-plane bending moment loading. Thus far comparisons have been made between analytical and experimental results for internal pressure loading of Westinghouse Research Laboratories' photoelastic model WC-2AY.[1] The model parameters are

---

*d, D = outside diameter of nozzle, shell
t, T = nozzle, shell thickness
s, S = membrane stress in nozzle, shell due to internal pressure
ρ_0, R = nozzle, shell mid-surface radius

$\rho_0/R = 0.117$, $\rho_0/t = 14.8$, and $R/T = 29.6$, where ρ_0 is the nozzle mid-surface radius, R is the shell mid-surface radius, t is the nozzle thickness, and T is the shell thickness. Comparisons of analytical predictions and experimental results for the 0° plane are shown in Figs. 5.9, 5.10, 5.11, and 5.12. Although the experimental data do not fall exactly on the theoretical curves, good agreement is generally observed. A report describing this work is being prepared.

Clusters of Nozzles

At Auburn University two extensively strain-gaged hemispherical shell models are being tested. One of the steel vessels was used to measure stress distributions around four separate clusters of holes under internal pressure. The vessel has an outside diameter of 40.901 in. and a wall thickness of 0.503 in. The model was divided into quadrants containing two-, three-, four-, and five-hole clusters arranged as shown in Fig. 5.13. All the holes are radial, with 1.572-in. diameters. The hole groupings were located at a vertical angle of 47° from the base of the model to avoid possible influence of the vessel flange on the strain field in the vicinity of the holes. The holes were sealed by pistons and O-rings, as shown in Fig. 5.14, in order to simulate a pressurized vessel.

Three-gage electrical-resistance strain-gage rosettes were attached to the vessel along radial stringers (designated as x-axis lines). The test consisted of subjecting the model to a static pressure of 200 psi. The strain gages were then read while the pressure was maintained constant by means of a dead-weight tester. Examples of the resulting plots of the ratios of measured stress to nominal stress are shown in Figs. 5.15, 5.16, 5.17, and 5.18 for the two-, three-, four-, and five-hole clusters, respectively.

The stress ratios were found to approach a value of three (the theoretical stress concentration for a single hole in a flat plate) in the case of only two stringers — stringer No. 1 of the two-hole clusters, Fig. 5.15, and stringer No. 7 of the four-hole cluster, Fig. 5.17. Generally a maximum stress ratio of 2 was recorded for most of the stringers. As could be expected a stress ratio of 1 was recorded at locations

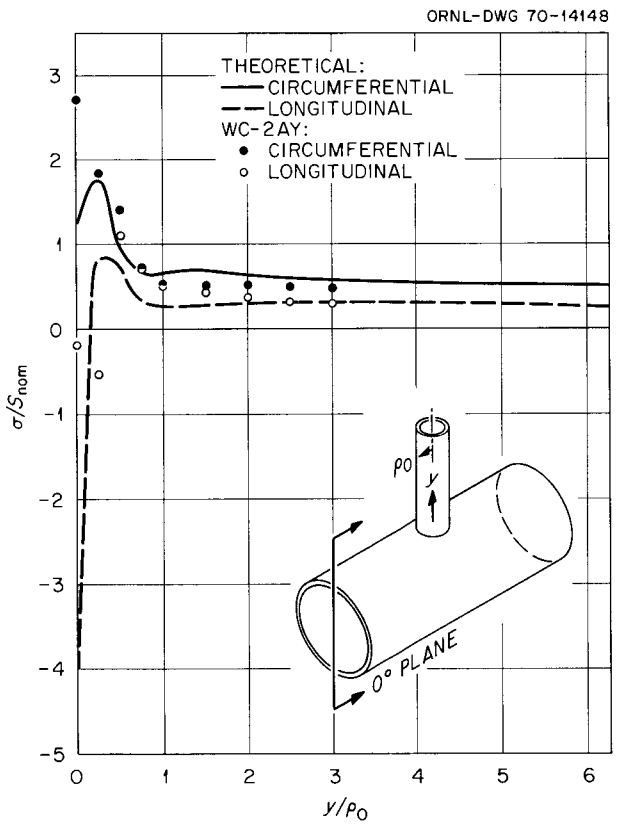

Fig. 5.9. Comparison of Analytical and Experimental Results for Nozzle Inner Surface, 0° Plane.

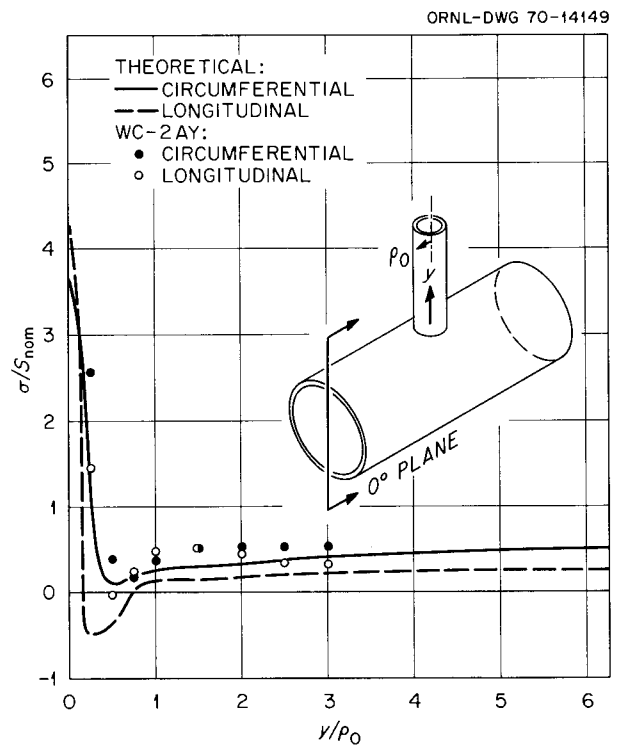

Fig. 5.10. Comparison of Analytical and Experimental Results for Nozzle Outer Surface, 0° Plane.

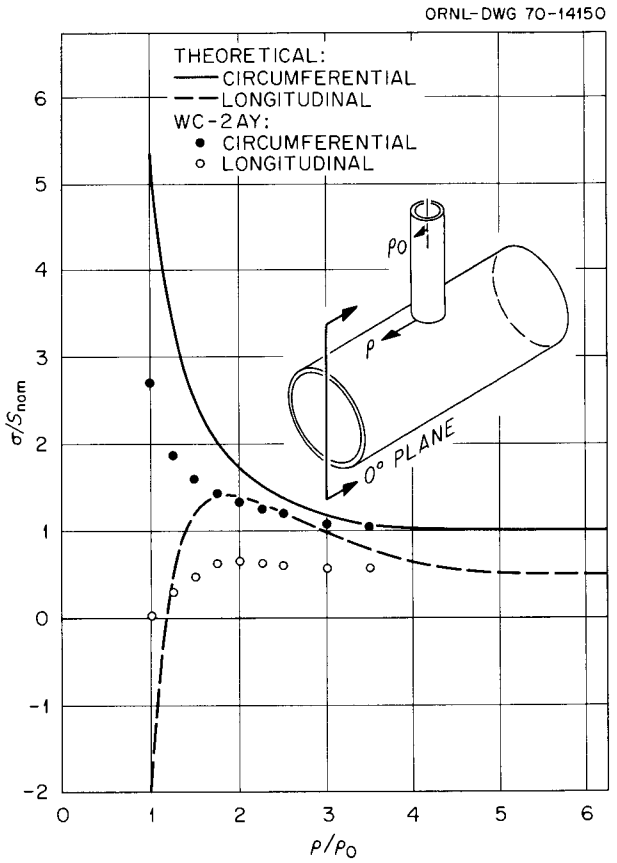

Fig. 5.11. Comparison of Analytical and Experimental Results for Shell Inner Surface, 0° Plane.

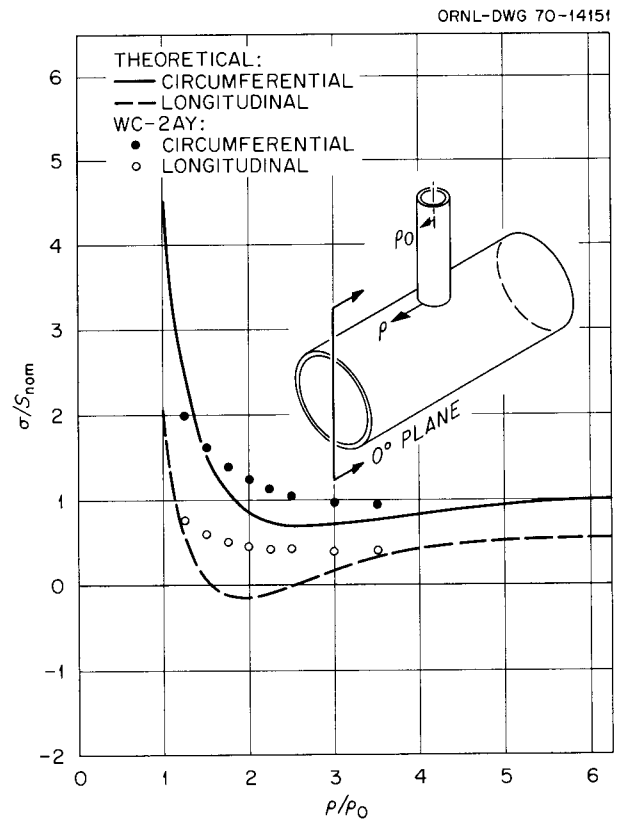

Fig. 5.12. Comparison of Analytical and Experimental Results for Shell Outer Surface, 0° Plane.

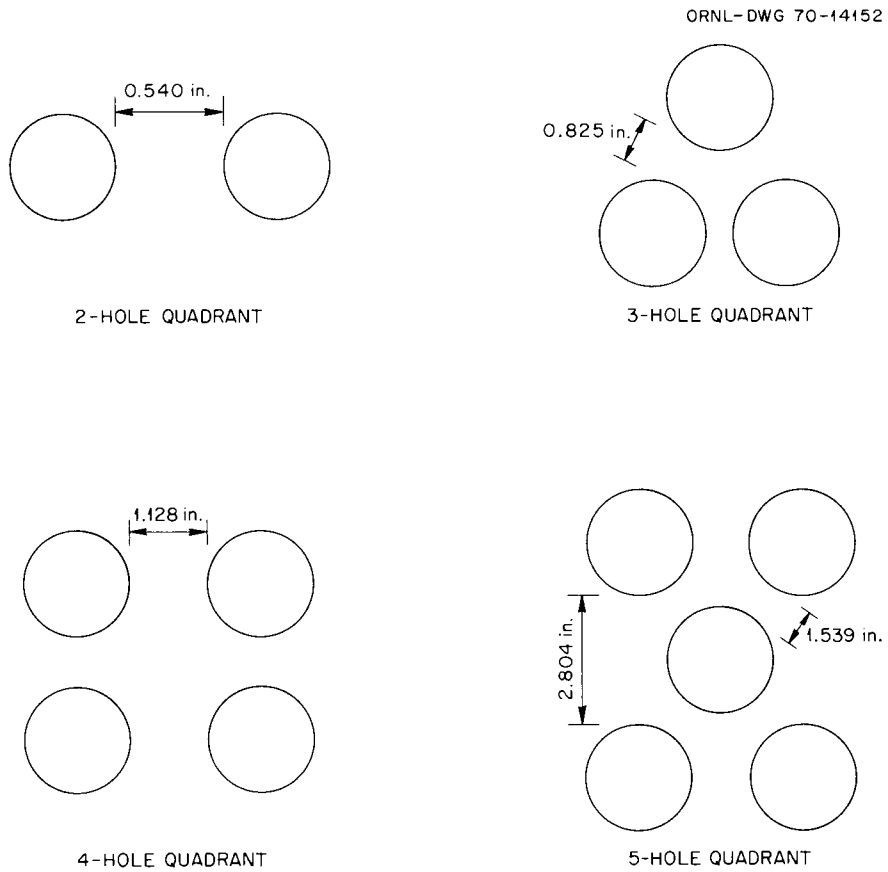

Fig. 5.13. Hole Arrangement in the Auburn Hemispherical Vessel Model.

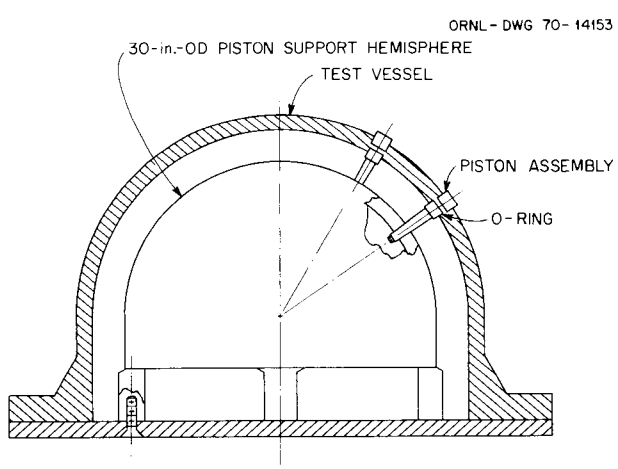

Fig. 5.14. Piston Support Assembly for Sealing the Holes in the Auburn Hemispherical Vessel Model.

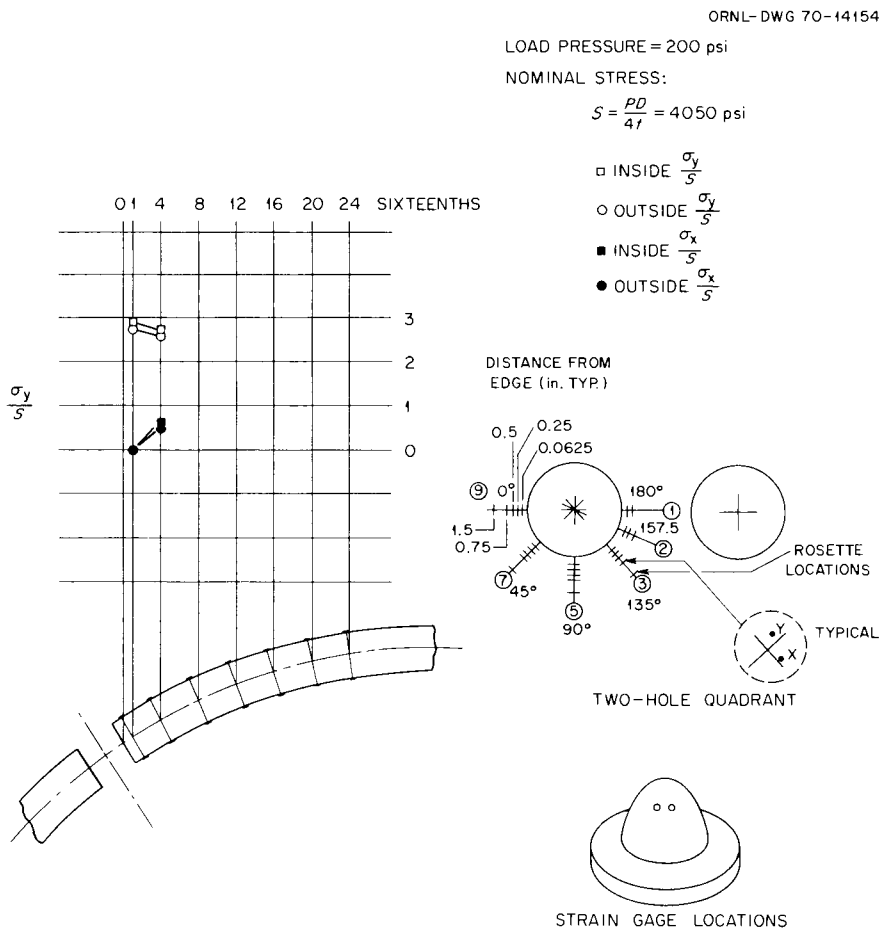

Fig. 5.15. Strain-Gage Results for Stringer No. 1 of the Two-Hole Quadrant.

relatively remote from the holes. The O-ring seals were found to have an insignificant effect on the stress distributions, as was indicated by the low measured values of radial stress near the edges of the holes. A report is being prepared on the results of this experiment.

A report has also been prepared at Auburn University of the results of an experimental analysis of a hemispherical model containing two closely spaced 7.002-in.-OD radial nozzles.[2] The report is currently being reviewed at ORNL prior to release.

Tests have been initiated at Auburn University on clusters of nozzles attached to flat plates. The loading frame for this study was designed and

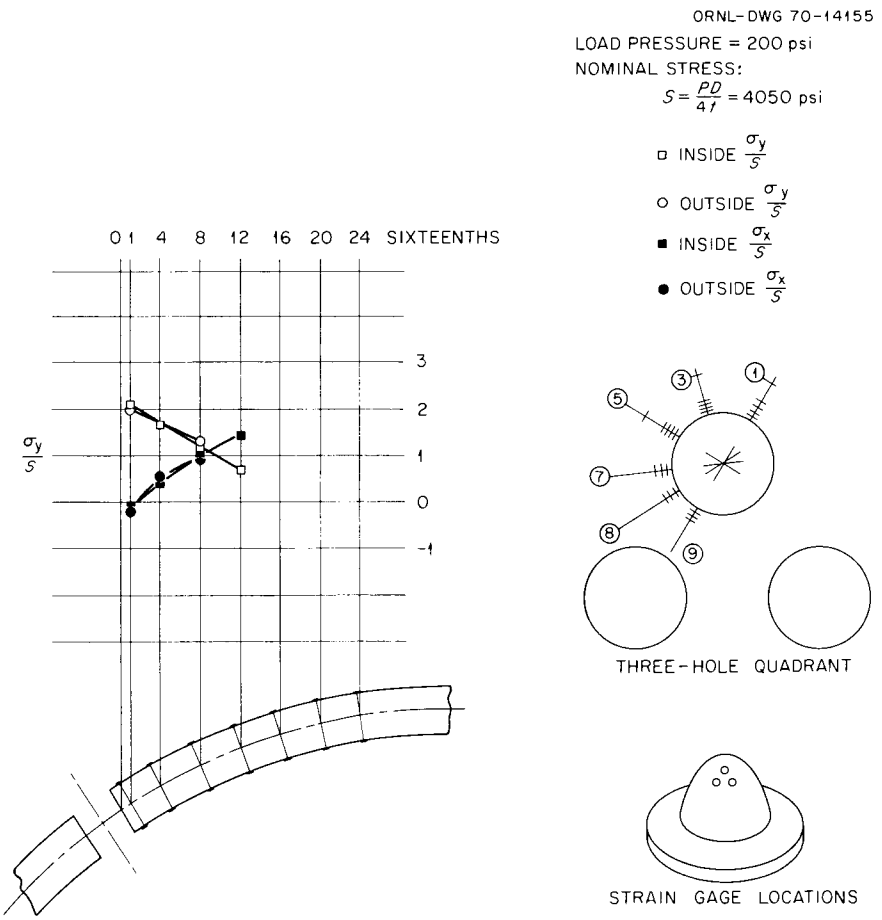

Fig. 5.16. Strain-Gage Results for Stringer No. 9 of the Three-Hole Quadrant.

fabricated at ORNL and has now been assembled at Auburn University. Testing of an unpierced flat plate is now under way. The plate was instrumented at ORNL with 17 three-gage strain-gage rosettes and is being used to determine whether the loading frame can satisfactorily produce the required biaxial stress fields. The flat-plate single nozzle model, the first nozzle model in this series, was strain-gaged at ORNL and shipped to Auburn for testing.

Experimental investigations of stresses around clusters of holes in flat plates resulting from uniaxial and biaxial loadings are being conducted at the University of Tennessee. A report containing the results of uniaxial and biaxial testing of the plate containing two holes was completed and is currently being reviewed at ORNL.[3] Reports are also being written on the three- and five-hole plate tests.

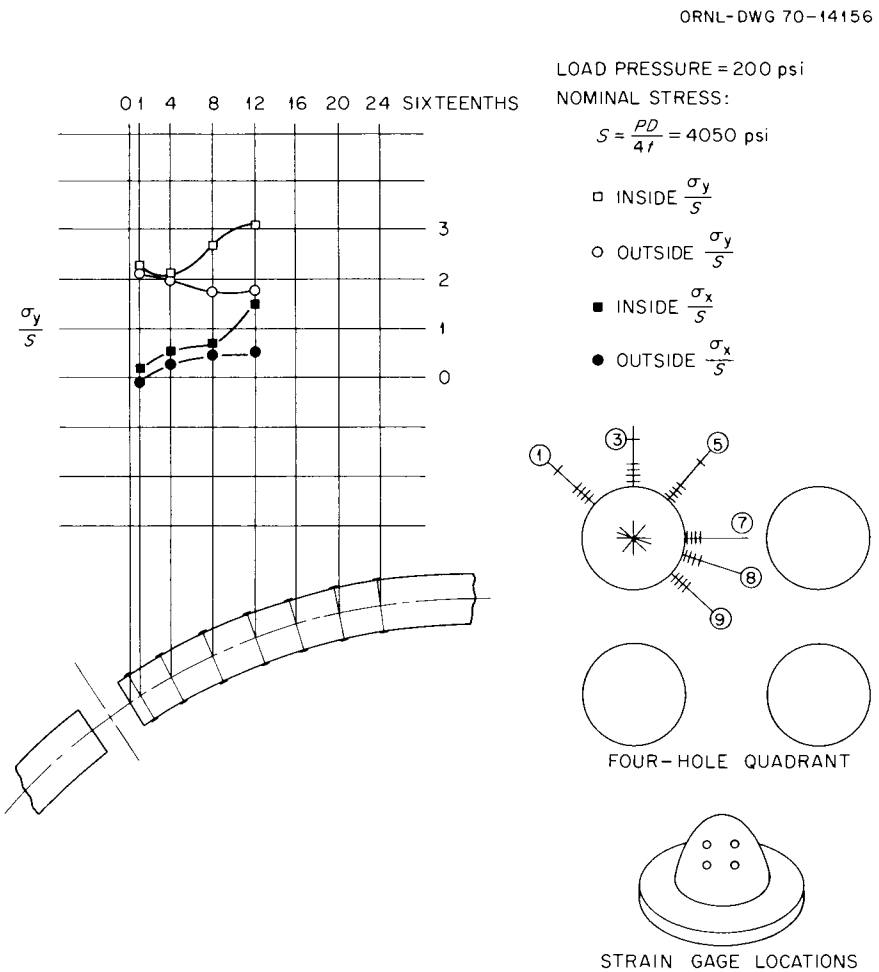

Fig. 5.17. Strain-Gage Results for Stringer No. 7 of the Four-Hole Quadrant.

The second draft of the Battelle Memorial Institute report describing the computer codes for analysis of perforated plates and plates with clusters of nozzles is being reviewed at ORNL.[4] This report will also serve as a user's manual for the computer codes.

Reinforcement Studies

Finite-element analyses are being performed for a nozzle-to-spherical-shell structure with parameters of $D_i/T = 72$, $d_i/D_i = 0.20$, and $s/S = 0.99$. D_i and d_i are inside diameters of the shell and nozzle, respectively. According to Section III of the ASME Boiler and Pressure Vessel Code the

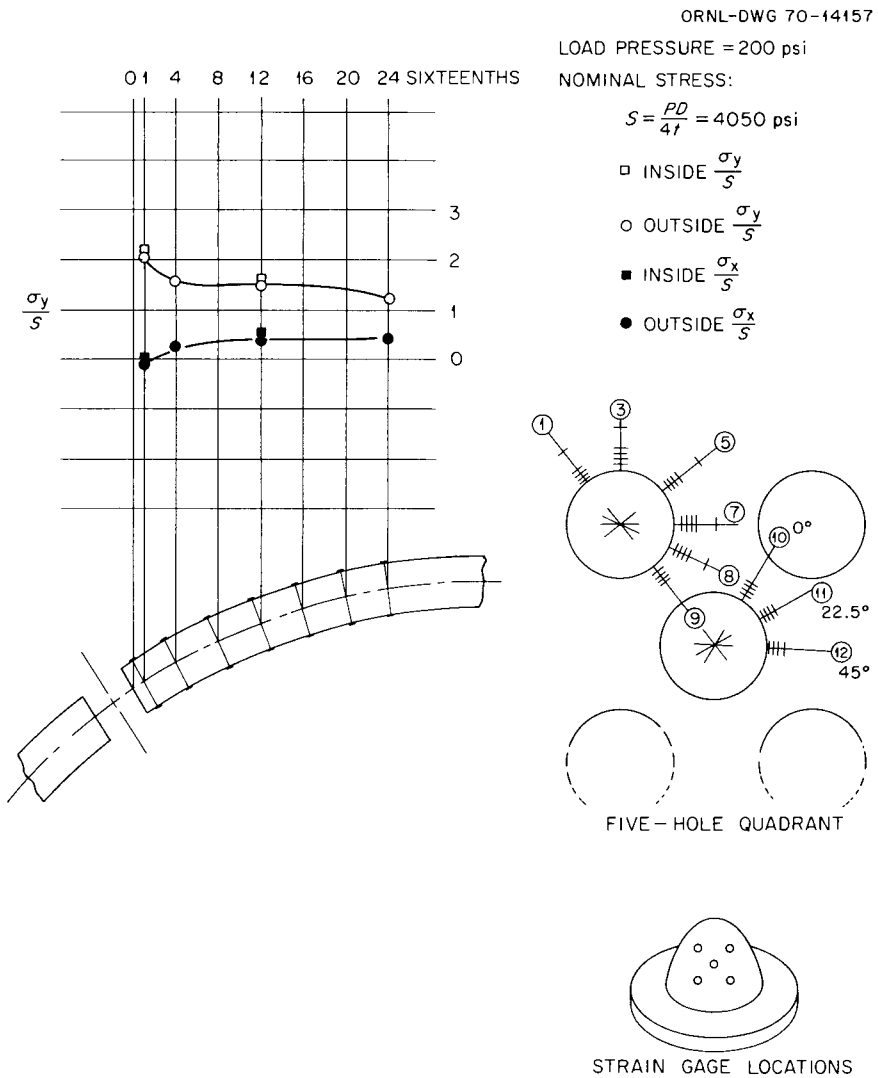

Fig. 5.18. Strain-Gage Results for Stringer No. 9 of the Five-Hole Quadrant.

percentage of reinforcement is calculated as a fraction of the area A_r, where $A_r = dT \cos \phi$, and $\phi = \sin^{-1} d/D$. The studies consider various percentages of reinforcement, as well as various configurations.

Thus far, the peak circumferential (σ_θ) and longitudinal (σ_ϕ) stresses have been examined for the unreinforced case and for two configurations of outside and inside reinforcement. In Figs. 5.19, 5.20, and 5.21 are shown examples of original undeformed and deformed shapes of a cross section of the finite-element models subjected to an internal pressure of 548 psi (resulting in a membrane stress of 10,000 psi). The unreinforced case is shown

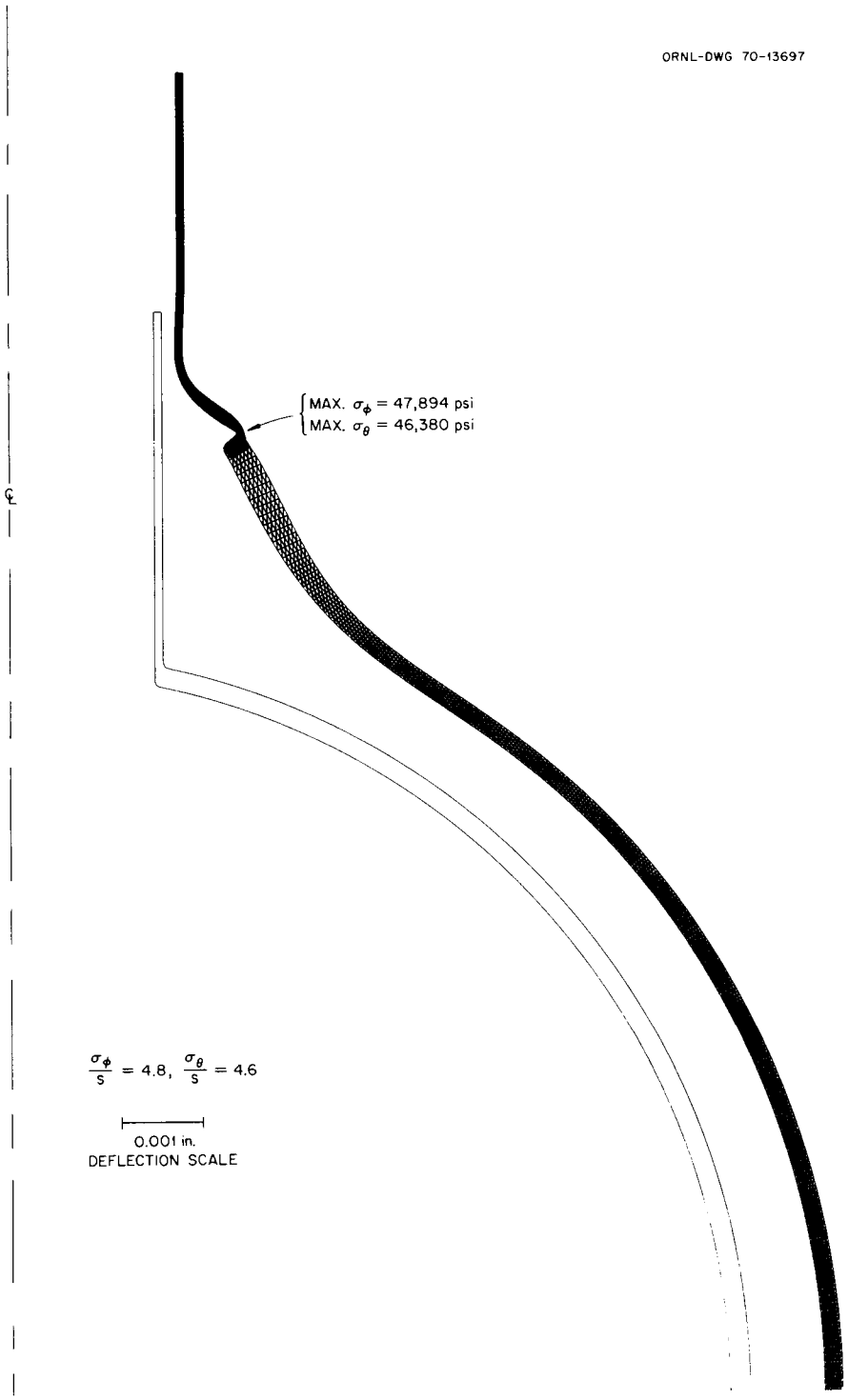

Fig. 5.19. Finite-Element Analyses of an Unreinforced Nozzle-Shell Model for an Internal Pressure of 548 psi.

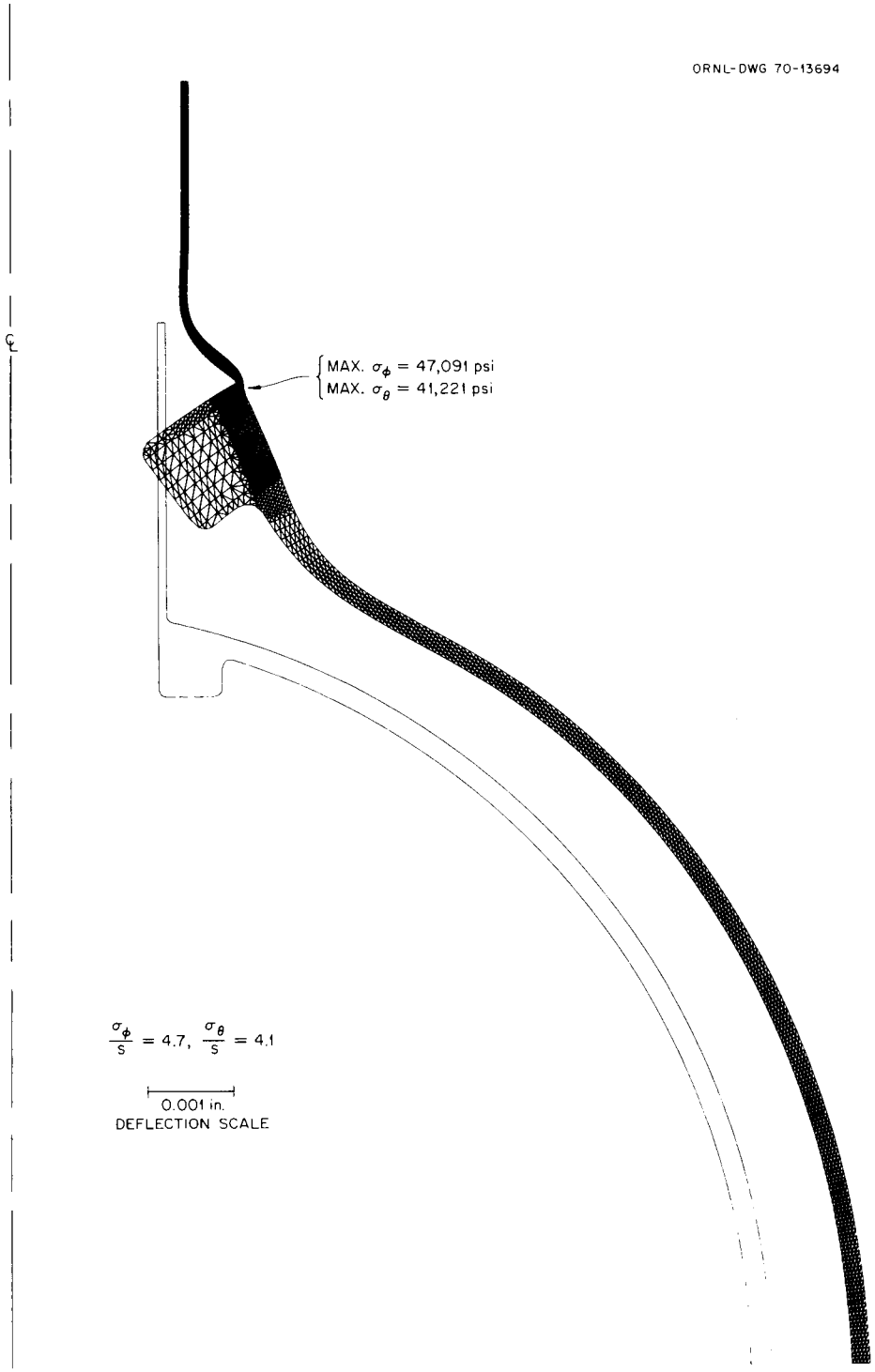

Fig. 5.20. Finite-Element Analysis of 100% Internally Reinforced Nozzle-Shell Model for an Internal Pressure of 548 psi.

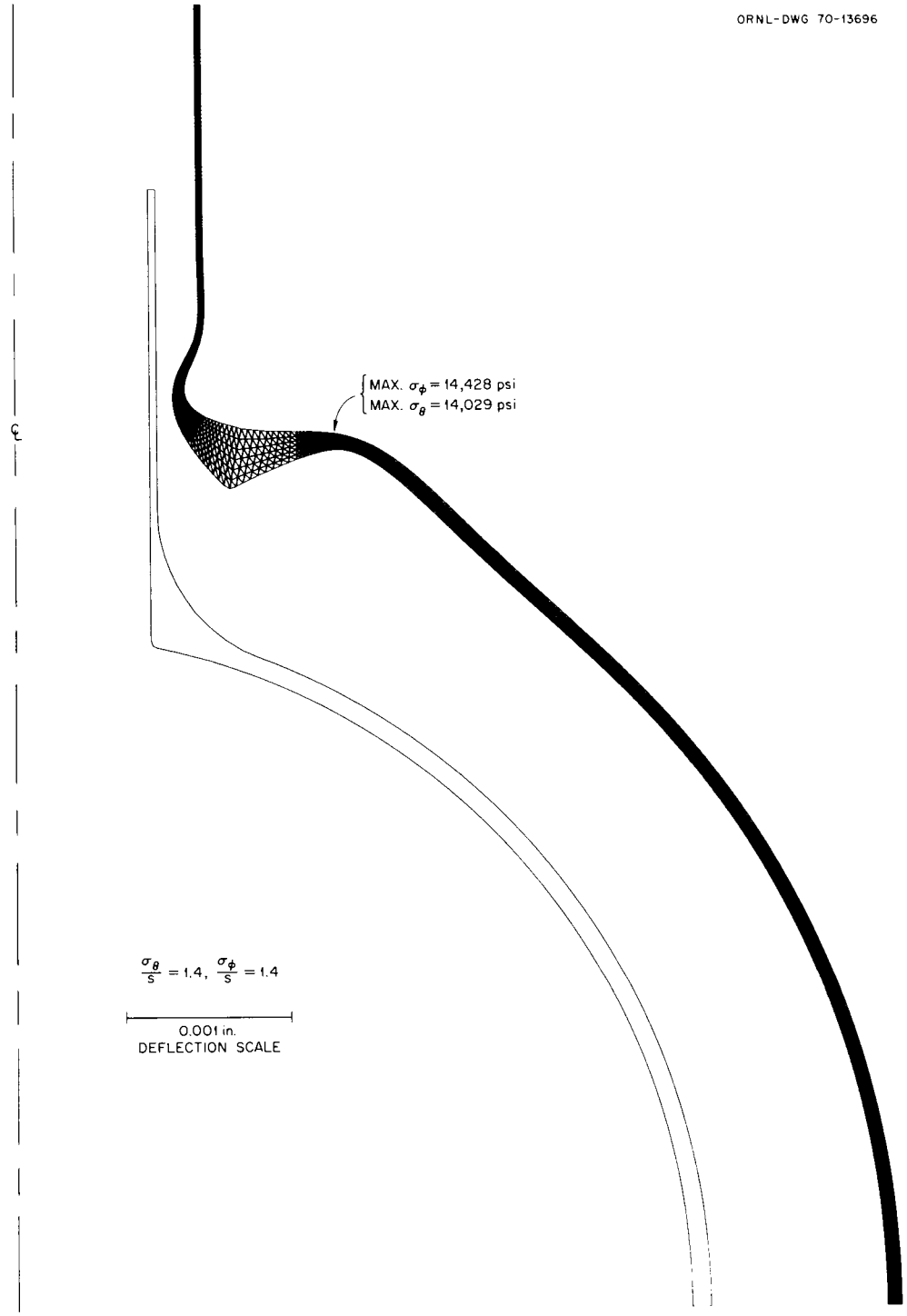

Fig. 5.21. Finite-Element Analysis of 100% Externally Reinforced Nozzle-Shell Model for an Internal Pressure of 548 psi.

in Fig. 5.19, and cases of inside and outside reinforcement of 100% are shown in Fig. 5.20 and 5.21, respectively. The deformed shapes shown in the figures have been exaggerated to indicate clearly the direction of rotation, which is entirely different for the two types of reinforcement. The resulting stress concentration factors are also indicated. It should be noted that for the same percentage of reinforcement, the stress concentration calculated for the internal reinforcement is approximately three times that of the external reinforcement.

References

1. M. M. Leven, Photoelastic Determination of Stresses in a Reinforced Steam Charging Connection with a Thermal Sleeve, Report 69-9D7-PHOTO-R1, Westinghouse Research Laboratories, Jan. 14, 1969.

2. R. W. Aderholdt and W. F. Swinson, Experimental Stress Analyses of Spherical Pressure Vessels with Closely Spaced, Large Radial Nozzles Attached, Technical Report ME-UC-2670-1, Auburn University Engineering Experiment Station, March 1970 (to be published).

3. A. Mathews and R. B. Michaels, Experimental Stress Analysis of Clusters of Holes of Equal Diameters in Flat Plates, Part II, Two Holes, Report EM 70-2, Department of Engineering Mechanics, The University of Tennessee, June 1970 (to be published).

4. L. E. Hulbert, A. T. Hopper, and E. F. Rybicki, Second Annual Report on The Stress Analysis of Perforated Plates and Plates with Single and Clustered Nozzles, Battelle Memorial Institute, Oct. 9, 1970 (to be published).

5.3 DESIGN CRITERIA FOR PIPING, PUMPS, AND VALVES
(AEC Activity 04 60 80 03 1)

W. L. Greenstreet S. E. Moore

Basic structural information and design data are being developed for assuring the continued adequate and safe design of piping systems for nuclear service. The ORNL work is primarily concerned with piping components and is part of a larger AEC-Industry cooperative program for developing piping, pumps, and valve design criteria. Through this program, factors urgently needed for use in both industry and AEC-RDT codes and standards are being developed that delineate design practices commensurate with meeting reliability and safety requirements of modern nuclear power plants.

Primary tasks to be carried out under the ORNL Piping Program are accurate, thorough experimental and analytical stress analyses of pipe fittings. At present, the experimental work is confined to tees, branch connections, and elbows, while analytical studies are planned for all standard pipe fittings. From the analyses and companion studies, data correlations and evaluations will be made; design charts, graphs, and tables will be prepared; and code rules will be drafted for use by the various code bodies. Data will be presented in terms of stress indices and flexibility factors for direct use. Overall interpretive reports will also be written on work sponsored under this program plus that done by others.

In support of the ORNL management responsibility for the AEC-funded portion of the joint AEC-Industry cooperative program, ORNL has been charged with keeping the AEC and industry fully informed through the Pressure Vessel Research Committee (PVRC) of the Welding Research Council. Periodically, subcommittees of the PVRC and working task groups of the subcommittees meet to discuss the various research tasks. A meeting of the Design Division of the PVRC was held in New York on September 29, 1970, at which oral and written progress reports were presented. These reports will be included in the minutes of the meetings, which are distributed quarterly to the PVRC membership.

I. Survey Reports

There is nothing to report this period.

II. Structural Analysis of Tees

The structural analysis of ASA B16.9 tees is one of the more complex portions of the ORNL program on piping components. Essentially no directly applicable information exists in the published literature that can be used to develop stress indices and flexibility factors for combined loadings. Consequently, a development program consisting of analytical and experimental stress analysis and fatigue testing has been undertaken. Fifteen tees representing the "standard product" of three different manufacturers are being tested and analyzed, as outlined in the latest Annual Progress Report.[1] Currently, portions of the work are being done at Oak Ridge National Laboratory and under subcontract at the University of California, Southwest Research Institute, Combustion Engineering, Inc., and Westinghouse Research Laboratories.

In addition to the work on "standard" tees, experimental and analytical work is being conducted at ORNL on thin-shell idealized tee models (cylindrical nozzles in cylindrical shells), and analytical studies on small branch connections are being conducted at Auburn University.

The task effort progress accomplished at the various facilities is described below.

Elastic Response and Fatigue Tests on 12-in. Tees

Five 12-in. ASA B16.9 tees are being experimentally stress analyzed and fatigue tested at Southwest Research Institute (SwRI). They are:

Tee No.	Nominal Size	Material
4	12 × 12 × 12-in., sched. 80	A 106, grade B, steel
6	12 × 12 × 12-in., sched. 80	A 106, grade B, steel
7	12 × 12 × 12-in., sched. 160	Type 304L stainless steel
8	12 × 12 × 6-in., sched. 40	Type 304L stainless steel
15	12 × 12 × 6-in., sched. 40	Type 304L stainless steel

During the current reporting period T-8 was retested for elastic response with a torsional bending load applied to the branch pipe (referred to as loading M3Y). Analysis of the data from the initial series of tests on T-8 had shown what appeared to be nonlinear response from a large number of strain-gages for the M3Y loading, whereas the remaining loadings all showed a linear response. Further analysis of the data, and consultations with Southwest Research personnel, indicated that the apparent nonlinearities were caused by a small unbalanced force in the loading setup. The data from the retest have been analyzed, and they show the expected linear behavior. T-8 will now be fatigue tested with an out-of-plane force loading applied to the branch pipe.

Currently T-7 is being fatigue tested with a constant internal pressure of 3240 psi and an alternating in-plane force loading on the branch pipe. The fatigue tests of both T-7 and T-8 are to be completed during the next reporting period.

Elastic Response and Fatigue Tests on 24-in. Tees

The four 24-in. ASA B16.9 tees of A 106, grade B, steel identified below are being experimentally stress analyzed and fatigue tested at Combustion Engineering, Inc.:

Tee No.	Nominal Size
10	24 × 24 × 24-in., sched. 40
11	24 × 24 × 24-in., sched. 160
12	24 × 24 × 10-in., sched. 40
13	24 × 24 × 10-in., sched. 160

Fabrication of the test assemblies for all four tees is essentially complete, and T-10 is currently being tested.

All 12 elastic-response test loadings were completed, and the strain-gage data were analyzed and accepted from the subcontractor. The tee is currently being fatigue tested with a constant internal pressure of 1025 psi and an alternating in-plane bending moment applied to the branch pipe.

The fatigue test of T-10 should be completed during the next reporting period. T-11 will then be put in the loading frame, and the elastic-response tests will be started. Because of the present tight budget

situation, it will be necessary to delay the scheduled tests for T-12 and T-13 until next fiscal year.

Photoelastic Tests on Models of 12-in. Tees

Frozen stress photoelastic analyses of one-half-scale models of the four 12-in. tees listed below are being conducted at Westinghouse Research Laboratories:

Tee No.	Nominal Size	Loading
6	12 × 12 × 12-in., sched. 80	Applied moment
7	12 × 12 × 12-in., sched. 160	Internal pressure
8	12 × 12 × 6-in., sched. 40	Applied moment
9	12 × 12 × 6-in., sched. 160	Internal pressure

All four models have been fabricated, assembled, and tested with the appropriate loading. Both surface stresses and stress distributions through the walls will be determined from slices and subslices cut from the models. The surface stress determinations have now been completed for the T-7 and T-9 models. These models were loaded with internal pressure, and maximum stresses for both models occurred on the inside corner of the branch-run intersections.

Currently the surface stresses are being determined for the photoelastic models of T-6 and T-8. Both models were loaded with an out-of-plane bending moment applied to the branch pipe extension. Figure 5.22 shows the T-8 model in the loading frame prior to the stress freezing operation.

Finite-Element Stress Analysis of 12-in. Tees

A finite-element computer code with three-dimensional elements is being developed at the University of California for the elastic stress analysis of ASA B16.9 tees. Three of the tees being tested at Southwest Research are also being analyzed at the University of California as one means of optimizing the computer code for accuracy and economical

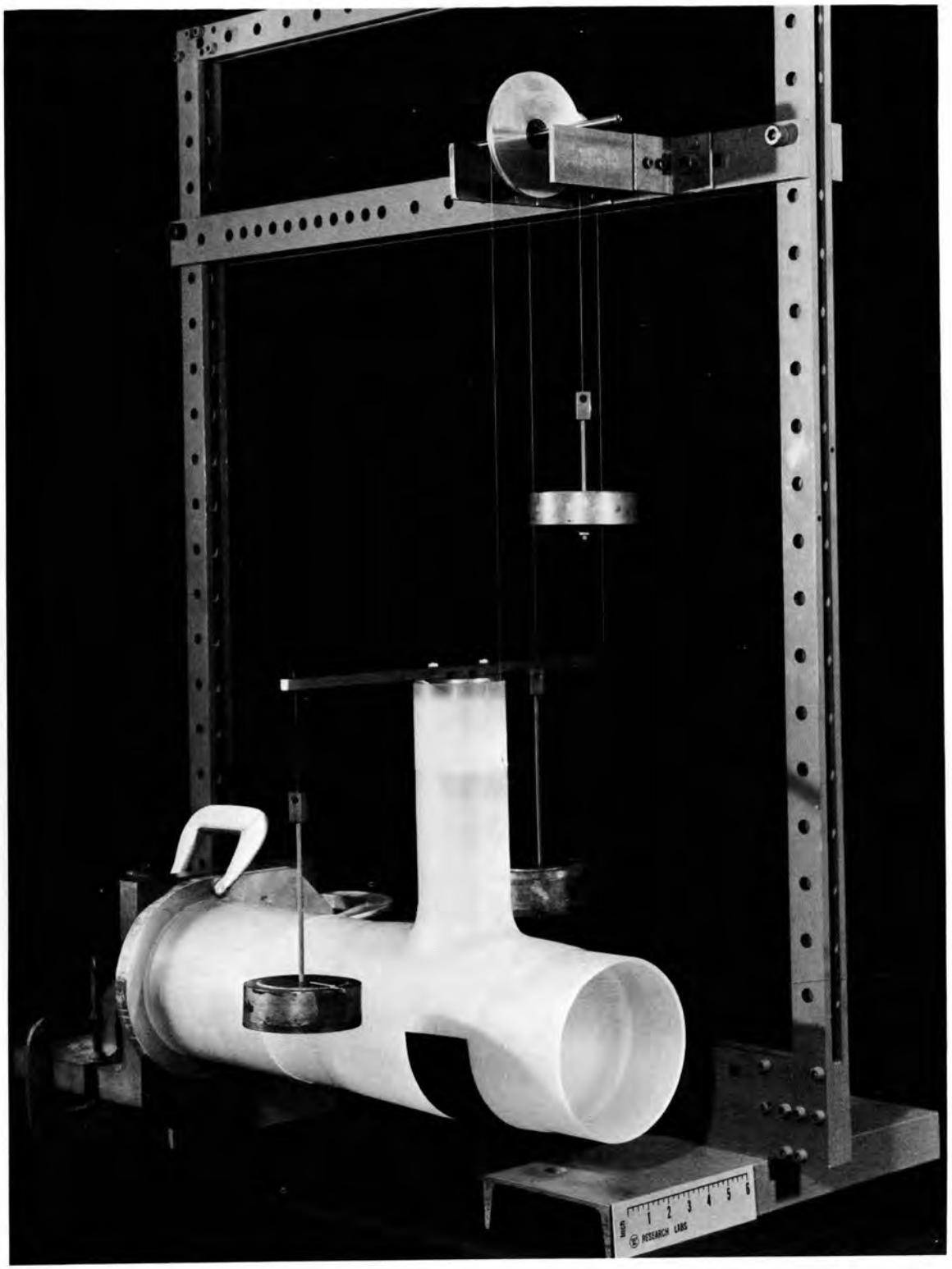

Fig. 5.22. One-Half-Scale Model of 12 × 12 × 6-in. Sched.-40 ASA B16.9 Tee No. T-8 Loaded with an Out-of-Plane Bending Moment on the Branch Pipe.

operations. The tees being analyzed are listed below:

Tee No.	Nominal Size
6	12 × 12 × 12-in., sched. 80
7	12 × 12 × 12-in., sched. 160
8	12 × 12 × 6-in., sched. 40

During the current reporting period finite-element calculations were made for T-8 with the new computer program. This program used an improved eight-node finite element with five degrees of freedom at each node. Results for the case of out-of-plane bending moment load on the branch pipe were compared with the experimental results, and excellent agreement was found. Results from other loading conditions are currently being plotted for comparison.

Studies of Thin-Walled Tees and Small Branch Connections

As reported earlier in this series of reports, a series of finite-element studies of small branch connections is being conducted at ORNL and Auburn University by using the computer program JØINT. Stresses were to be calculated for the eight models listed in Table 5.1 to provide analytical information to supplement the experimental data used as the basis for proposed design rules for small branch connections.[2] Loadings to be considered were internal pressure and three mutually perpendicular force and bending moments applied to both the branch and run pipes. Comparisons between the finite-element results and photoelastic results were to be made for model 1 for internal pressure loading.

The calculations have now been completed for the first three models for all 13 different loading cases by using a fine finite-element mesh. Comparisons have also been made between the photoelastic internal pressure results for model No. 1 and finite-element results obtained by using three different sized element layouts. A report has been written on the results from the comparisons.[3]

Table 5.1. Branch Connection Models for Analytical Parameter Study

Model No.	Dimensionless Parameters[a]				
	D/T	d/D	t/T	s/S	r/T
1	59.4	0.115	0.235	0.49	0
2	20.0	0.02	0.02	1.00	0
3	20.0	0.08	0.473	0.169	0
4	20.0	0.32	1.00	0.322	0
1F	59.4	0.115	0.235	0.49	0.60
2F	20.0	0.02	0.02	1.00	1.00
3F	20.0	0.08	0.08	1.00	1.46
4F	20.0	0.32	0.32	1.00	3.34

[a]D and d are the diameters of the run pipe and branch pipe, respectively; T and t are the wall thickness of the run pipe and branch pipe, respectively; s/S is the ratio of membrane stress in the nozzle to the membrane stress in the run pipe due to internal pressure loading, in terms of other parameters, $s/S = d/D \times T/t$; and r/T is the ratio of the reinforcement fillet radius to the wall thickness of the run pipe.

III. Structural Analysis of Elbows, Curved Pipe, and Miters

Elastic-Response Analysis of Machined Elbows

The test assembly for the first in a series of four machined 10-in. elbows fabricated with controlled dimensional distortions (described previously) was fabricated and is currently being strain-gaged. The model will be gaged with a total of 77 three-gage strain rosettes by using both 62- and 125-mil gages. The instrumentation is to be completed during the next reporting period.

A finite-element computer program is also being prepared for the analysis of the four machined-elbow test assemblies. The computer program JØINT is being modified for this purpose, and an input data preparation package is being written to facilitate conducting parameter studies. The programming work should be completed during the next reporting period.

Limit Load Tests of 6-in. Elbows

The series of plastic limit-load tests for 6-in. elbows listed in Table 5.2 was completed. The test assemblies were fabricated by welding pipe extensions of the same nominal size to the elbows; and the assemblies were loaded with an applied force near one end, while the other end was rigidly fixed at a heavy flange. For those cases where an internal pressure is indicated in the table, the assembly was pressurized to the noted design pressure, and then the moment loading was superimposed. Loads were applied until a significant amount of plastic deformation was obtained, as indicated by plots of load versus pipe-deflection data. In addition to the carbon steel elbows listed, one 6-in. type 304L stainless steel elbow

Table 5.2. Results of Plastic Limit-Load Tests on 6-in. Elbows

Elbow			Loading Conditions			
			Moment			
Number[a]	Wall Thickness (sched.)	Bend Radius (in.)	In-Plane[b] $+M_z$	In-Plane[b] $-M_z$	M_y, Out-of-Plane	P, Pressure
PE-1	40	9	X			
PE-2	40	9		X		
PE-3	40	9			X	
PE-4	40	9	X			X
PE-5	40	9		X		X
PE-6	40	9			X	X
PE-7	80	9	X			
PE-8	80	9		X		
PE-9	80	9			X	
PE-10	40	6	X			
PE-11	40	6		X		
PE-12	40	6			X	
PE-13	40	6	X			X
PE-14	40	6			X	X

[a]The letters PE stand for plastic collapse, elbow.

[b]A positive in-plane moment ($+M_z$) causes the elbow to close, whereas a negative in-plane moment ($-M_z$) causes the elbow to open.

assembly was tested with an in-plane bending moment. The data are currently being analyzed to obtain representative limit load values for elbows.

In addition to the ORNL data, previously unreported plastic-limit load data obtained at Tube Turns, Division of Chemetron, Inc., some 20 years ago were made available for use in developing stress indices. The Tube Turns data were analyzed and will be used in developing proposed design rules for code use.

References

1. W. L. Greenstreet, S. E. Moore, and R. C. Gwaltney, Progress Report on Studies in Applied Solid Mechanics, USAEC Report ORNL-4576, Oak Ridge National Laboratory, August 1970.

2. E. C. Rodabaugh, Stress Indices for Small Branch Connections with External Loadings, USAEC Report ORNL-TM-3014, Oak Ridge National Laboratory, August 1970.

3. N. Krishnamurthy, Comparison of Results from Finite Element Analysis and Photoelastic Tests of a Cylinder-Nozzle Attachment, Auburn University (to be published).

6. RDT STANDARDS PROGRAM

M. Bender, Project Director

6.1 PROGRAM OBJECTIVES AND ACTIVITIES
(AEC Activity 04 60 80 03 1)

W. F. Ferguson R. A. Schmidt

The prime responsibility for organizing, developing, preparing, and distributing engineering standards was undertaken by the Oak Ridge National Laboratory at the request of the AEC Division of Reactor Development and Technology. These standards provide sound bases from which nuclear reactors and related facilities that are under the guidance of RDT can be planned, designed, constructed, and operated. The RDT standards program at ORNL is responsible for the preparation of standards applicable to water-cooled reactor systems, as well as for standards covering liquid-metal-cooled systems. The standards for the liquid-metal-cooled systems are prepared in cooperation with the Liquid Metal Engineering Center (LMEC), which has the prime responsibility for standards applicable to these systems. The RDT standards program is a source of proven engineering practices for designers, builders, and operators of nuclear reactors and related facilities that will improve quality assurance, reactor safety, and functional reliability.

Current activities include (1) analyzing RDT project needs for standards; (2) planning and developing program schedules, goals, and details; (3) preparing and distributing new standards and revising and updating existing standards; (4) providing assistance in application of standards to reactor projects under the direction of RDT; (5) maintaining close liaison with the LMEC standards office; (6) directing and reviewing the participation of subcontractors and engineering consultants in the standards program; (7) participating in committee and task group activities of recognized voluntary codes and standards agencies; (8) consulting with reactor designers, builders, operators, AEC agencies, and contractors; (9) analyzing and preparing periodic summaries of RDT incident reports; (10) preparing guidelines for format, definitions, titling, and numbering; and (11) writing and distributing reports, indexes, and tabluations pertaining to the program.

A paper describing the RDT standards program at ORNL was presented at the Argonne National Laboratory Reactor Quality-Assurance Institute, and detailed discussions were held relative to the preparation and application of RDT standards and RDT quality-assurance practices.

A paper entitled "Pressure Relief Devices for Water-Cooled Nuclear Reactor Systems" was presented at the ANS Power Conference in Williamsburg, Virginia.

Ninety-one tentative standards are currently available for use, and 93 draft standards are awaiting approval by RDT. The ORNL mailing list for tentative standards now contains 272 addressees, including AEC installations and contractors, codes and standards organizations, architect-engineers, consultants, nuclear component manufacturers, and electrical utilities, who receive a total of 520 copies.

In response to telephone and memo requests, 849 copies of RDT standards and 11 copies of the standards index were mailed to 50 organizations, five of which were added to the distribution list to receive future issues of the standards or the quarterly index.

Organization, Scheduling, and Manpower

The existing manpower and subcontract estimates were reviewed and adjusted and the schedules and assistance requirements for current projects were reviewed for the fiscal year. Increased effort was directed toward expediting instrumentation, electrical, quality assurance, valve, and heat exchanger standards; providing review of standards being prepared; and summarizing review comments received by ORNL. Subcontract work at Franklin Institute Research Laboratories (FIRL), MPR Associates, and Teledyne Materials Research (TMR) proceeded as planned.

Activities

ORNL is updating a list of engineering standards needed for the design and construction of nuclear facilities. Additional information being factored into the compilation was obtained from the ANSI list of "78 most needed" standards, LMFBR standards development plans, and AEC Regulatory guides, as well as current RDT project activities.

A meeting was held with LMEC to revise the draft of RDT C6-1, NaK Transmission High Temperature Pressure Transmitter for Liquid Metal Service, to resolve common problems, and to establish closer working relationships in standards activities.

Members of the standards group met with representatives from several suppliers and prospective suppliers of materials to RDT standards. Discussions centered around the rationale, intent, and interpretation of specific requirements in the standards and acceptable methods for meeting the requirements.

Meetings were held with a manufacturer, an architect-engineer, and LOFT to obtain current practices and establish project needs for preparation of a standard for containment piping penetrations. A detailed discussion of valve standards was the subject of other meetings at LOFT.

Participation continued in the work of Subcommittee ANS-7 on Reactor Component Criteria, ASTM A-10 Subcommittee IV-408 on Stainless Steel Corrosion, ANSI N45-3.0 Subcommittee on Nuclear Quality-Assurance Standards, N45 ad hoc committees 3.4, 3.5, 3.6, 3.7, and 3.8, and ASME Boiler and Pressure Vessel Working Group on Core Support Structures (SC-III).

Standards Issued, Drafted, Reviewed, or Renumbered

The following approved tentative standards were issued.

C 9-1T	Single-Point Strip-Chart Recording Potentiometer
C 9-2T	Multipoint Strip-Chart Recording Potentiometer

The following standards were prepared and submitted to RDT for approval.

C 6-1	NaK Transmission High Temperature Pressure Transmitter for Liquid Metal Service
*E 1-6	Automatic Spring-Loaded Safety Valves
*E 1-14	Power-Actuated Pressure Relief Valves
*E 1-23	Stainless Steel Throttling Valves, 1/2" Through 2", Power Operated
*E 1-31	Carbon Steel Isolation Valves
*E 3-6	Horizontal, Electric Motor Driven, Single-Stage Centrifugal Pump

*Approval to be processed by LOFT.

*E 3-8	Horizontal, Electric Motor Driven, Multi-Stage Centrifugal Pump
E 4-2	Water-to-Water Heat Exchanger, Reactor Coolant
E 9-1	Air Filter, HEPA, for High Humidity, High Temperature Application
E 9-2	Air Filter, HEPA, General Purpose
M 16-3	HEPA Filter Media, Glass Fiber

RDT numbers were assigned for 19 new standards, and previously assigned titles for 6 standards were revised as follows.

†C 4-4	Venturi Tube for Liquid Sodium Service (title revised)
†C 6-3	Liquid Metal Pressure Measurement System, Flush Mounted, Eddy Current Type, Inductive, Absolute or Gage (title revised)
†C 8-1	Manufacturing Requirements for a Sodium Plugging Meter (title revised)
†C 8-2	Liquid Sodium Bearing, Film Thickness, Variable Reluctance Proximity Measurement System (title revised)
C 15-3	Wide Band Width Current Amplifier for Use with Pulse Fission Chambers
C 15-4	In-Core Neutron Flux Detector (number changed, previously C 14-1)
†C 15-5	Low-Level Fission Type Neutron Detector, Prototype
E 1-32	Check Valves, 1/2" thru 2" (INC)
E 1-33	Gate Valve, Manual, Pneumatic or Electric Motor Operated, 1" to 6" (INC)
†E 4-5	Cold Trap Assemblies for Removal of Sodium Impurities (title revised)
E 4-18	Air Cooled Heat Exchanger for Nuclear Steam Supplied Systems (INC)
†E 6-25	FFTF, Control Rod Pin Assembly
†E 6-26	FFTF, Control Rod Disconnect Drive Line
†E 6-27	FFTF, Control Rod Cladding
†E 6-28	FFTF, Control Rod End Caps
†E 6-29	FFTF, Control Rod Wire Wrap
†E 6-30	FFTF, Control Rod Boron Carbide

---

*Approval to be processed by LOFT.

†LMEC is responsible Standards Office.

*E 6-31	FFTF, Control Rod Insulator
*E 6-32	FFTF, Control Rod Reflector
*E 6-33	FFTF, Control Rod Assembly
*E 8-10	FFTF, Core Restraint Mechanism for Sodium Cooled Reactors
*E 8-11	FFTF, Closed Loop In-Reactor Assembly for Sodium Cooled Test Reactors
*E 8-12	Surveillance and Inservice Inspection Equipment for the Reactor Vessel, Reactor Guard Vessel, and Reactor Vessel Head (title revised and number changed)
*E 13-15	Fuel Assembly for Pressurized Water Reactors
*P 4-1	Electrical Immersion Heater (WADCO)

Considerable effort was directed during this period toward the continuing activities of reviewing and commenting on draft standards prepared by others and of evaluating comments received from outside reviewers on drafts prepared by ORNL.

RDT E 3-10, Supplement to Pump and Valve Code, and C 6-5, High Temperature Ni-Mo-Cr Alloy Pressure Transmitter, were reviewed.

A work session was held with RDT to discuss the content and redraft work for Sections 1, 2, and 3 of RDT F 2-5, Quality-Assurance Program Guidelines.

The following drafts were reviewed, and comments were prepared and submitted to LMEC:

C 6-3	Flush Mounted, Eddy Current Type, Inductive, Liquid Metal, Absolute or Gage, Pressure Measurement System
C 8-2	Liquid Sodium Bearing Film Thickness, Variable Reluctance Sensor, Proximity Measurement System
M 12-4	Reflective Insulation

RDT C 2-2, Leakage Testing for Instrumentation, was reviewed, and comments are being prepared for submittal to LMEC.

The comments received on the following documents are being evaluated for incorporation into the standards.

E 4-3	Heat Transfer Equipment Design
F 2-5	Quality Assurance Program Guidelines

---

*LMEC is responsible Standards Office.

M 1-16T	Zirconium & Zirconium Alloy Bare Welding Rods (ASTM B351 with Additional Requirements)
M 2-9T	Zirconium & Zirconium Alloy Forgings and Extrusions (ASTM B356 with Additional Requirements)
M 3-8T	Zirconium & Zirconium Alloy Tubes (ASTM B353 with Additional Requirements)
M 5-6T	Zirconium & Zirconium Alloy Plate, Sheet, and Strip (ASTM B352 with Additional Requirements)
M 7-9T	Zirconium & Zirconium Alloy Bars, Rod and Wire (ASTM B351 with Additional Requirements)
M 10-1T	Zirconium & Zirconium Alloy Ingots (ASTM B350 with Additional Requirements)

Drafts of the following standards were distributed for review and comments.

C 7-15	Thermocouple Connectors and Thermocouple Connector Panels
C 7-16	Thermocouple Assembly, Magnesium Oxide Insulation, Stainless Steel Tube Sheathed
E 5-2	Electric Heater and Connector Assembly for Pressurizer for Pressurized Water Reactors

The preliminary draft of the Piping Design Guide (E 7-1) was reviewed, and comments were submitted to TMR.

6.2 REACTOR COOLANT SYSTEMS AND EQUIPMENT STANDARDS

(AEC Activity 04 60 80 03 1)

J. W. Anderson
H. G. Arnold
W. A. Bush
D. D. Cannon
R. W. Dehoney
W. R. Gall
D. L. Gray
T. L. Hudson
L. F. Parsly
T. H. Row

Valves, Rupture Disks, Piping, and Piping Penetrations

The following standards, which were prepared for use by LOFT in the procurement of valves, were completed and submitted to RDT for approval.

E 1-6	Automatic Spring-Loaded Safety Valves
E 1-14	Power-Actuated Pressure Relief Valves
E 1-23	Stainless Steel Throttling Valves
E 1-31	Carbon Steel Isolation Valves

Three additional valve standards have been requested for this project.

Work was begun on preparation of a standard for containment piping penetrations. Visits were made to Tube Turns, a supplier of these assemblies, to discuss their standard product line and their capability to perform to RDT standard quality levels, to Sargent & Lundy to obtain recommendations for specifying penetrations, and to LOFT to determine project requirements.

A meeting was held at MPR Associates to resolve the comments received from the review of RDT E 1-17, Design Evaluation Guide for Rupture Disk Assemblies Used in Pressurized Water and Boiling Water Reactors. The major unresolved problem area is the fatigue analysis procedure for reverse-buckling-type rupture disks.

Pumps

Work continued at FIRL on the COPATS computer program for stress analyzing complex pump casings. To assure smooth transition in the utilization of the finite-element code COPATS from FIRL to ORNL, a trip was made to FIRL to discuss the mesh-generation-code portion. The required programming at FIRL, the validation run at ORNL, and the Theory Manual and COPATS Input Guide are expected to be completed and delivered as scheduled.

RDT E 3-8, Horizontal, Electric Motor Driven, Multi-Stage Centrifugal Pump, was mailed to LOFT for use in the procurement of emergency core cooling system pumps and for RDT approval through LOFT application. This standard reflects the input derived from reviews and comments received from LOFT and RDT while applying the reactor coolant pump standard (E 3-3) during procurement.

A bid package for RDT E 3-3, Vertical, Shaft-Sealed, Motor-Driven, Single-Stage, Centrifugal Reactor Coolant Pump, was submitted for approval by INC for LOFT.

Heat Exchangers

RDT E 4-2, Water-to-Water Heat Exchanger, Reactor Coolant, was completed and submitted to RDT for approval.

Preparation of RDT E 4-3, Heat Transfer Equipment Design, continued with comments being reviewed and evaluated for incorporation into the revised draft.

Nuclear Code Supplements

RDT E 3-10, Supplement to Pump and Valve Code, was reviewed, and comments received are being resolved. To date, three code supplement standards are awaiting approval by RDT.

Pressurizers

RDT E 5-1, Pressurizer for Pressurized Water Reactors, and E 5-2, Electric Heater and Connector Assembly, for Pressurizer for Pressurized Water Reactors, were incorporated into a bid package by INC for the LOFT project and submitted for approval.

Radioactive Waste Systems

Initial planning was started with MPR Associates in an effort to define the role of RDT standards in radioactive waste applications.

Containment Spray Systems

A proposal outlining a standard covering the design requirements of reactor containment spray system tanks, pumps, valves, piping, and spray nozzles as they relate to heat extraction and fission-product removal was completed. This standard will include process, mechanical, safety, and reliability considerations and requirements that must be dealt with when designing and specifying a spray system.

6.3 INSTRUMENTATION, CONTROLS, AND ELECTRICAL EQUIPMENT

(AEC Activity 04 60 80 03 1)

A. E. G. Bates
H. E. Cochran
J. T. DeLorenza
T. L. Hudson
C. S. Lisser
H. J. Metz
P. Rubel
J. A. Russell
R. A. Schmidt
O. M. Thomas

Instrumentation

RDT C 2-2, Leakage Testing for Instrumentation, was reviewed at ORNL, and comments are being prepared for submittal to LMEC.

The draft of RDT C 2-3, Time Response Test for Sheathed Thermocouples, was prepared and is to be issued for review.

RDT C 6-1, NaK Transmission High Temperature Pressure Transmitter for Liquid Metal Service, was submitted to RDT for approval. At a meeting at LMEC, the scope of this document was expanded and modified to fit project requirements. LMEC will prepare the final standard and submit it to RDT as part of a procurement specification.

RDT C 9-1T, Single-Point Strip-Chart Recording Potentiometer, and C 9-2T, Multipoint Strip-Chart Recording Potentiometer, were issued as tentative standards.

Preparation of the draft of RDT C 15-3, Wide Band Current Amplifier for Use with Pulse Fission Chambers, is in progress.

An ORNL review of RDT C 6-5, High-Temperature Ni-Mo-Cr Alloy Pressure Transmitter, is in progress.

During a visit to RDT, a discussion was held on RDT C 13-1, General Purpose, Stored Program, Digital Computer. Since several reviewers felt that the draft standard prepared by ORNL and based on a computer bought by ORNL was too detailed and specific, it was recommended that a suitable procurement standard be developed from USAEC Report BNWL-1378, Process Control Computer System Specification Guideline, which would be more appropriate than the original ORNL draft standard.

Electrical

In a meeting at RDT it was decided to temporarily discontinue preparation of RDT P 2-4, Criteria for Auxiliary Power Systems, and to concentrate effort on the preparation of the requirements for the emergency power system. Work on this new standard, RDT P 2-3, Supplementary Criteria and Requirements for Class IE Electrical Systems for RDT Reactors, was started.

6.4 PROGRAMMATIC AND PROCEDURAL STANDARDS

(AEC Activity 04 60 80 03 1)

J. W. Anderson
H. G. Arnold
C. A. Burchsted
N. E. Dunwoody
F. L. Hannon
L. F. Lieber
T. W. Pickel
J. A. Woodley

Quality Assurance

RDT F 2-5, Quality Assurance Program Guidelines, is being revised to incorporate comments received from reviewers. Upon completion of draft 3 of this standard, it will be submitted to RDT and to the RDT Quality-Assurance Working Group for review.

A meeting of the Quality-Assurance Working Group was held at RDT to discuss quality-assurance organizations and programs at the various AEC sites, the status of RDT F 2-5, experience with RDT standards at the various sites, and application of RDT standards in procurement. This meeting was also attended by representatives of Atomics International, Westinghouse, and General Electric who are working on the LMFBR Demonstration Plants.

ORNL continued to contact maintenance groups at current projects, such as the FFTF, in an effort to verify the applicability of RDT F 4-1, Maintenance Program Requirements.

Seismic Standards

Meetings were held at AEC Headquarters to discuss the proposed seismic standard for design. It was agreed that the entire nuclear system should be covered, including interactions between parts of the system, and that first efforts are to be directed to the major structures and equipment that constitute the containment and primary pressure boundaries. A revised proposal for the seismic standards program is being prepared and will be resubmitted to RDT.

Cleaning Standards

Specific provisions of proposed RDT standards F 5-2, 5-5, and 5-6 covering cleanliness control and cleaning of nuclear components and systems during fabrication and construction were discussed with LOFT, WADCO, TVA, and J. A. Jones-Fabrication. These drafts are being used for establishing program requirements and, in one case, requirements for a clean room to be used for the fabrication of FFTF components.

Air Cleaning

RDT E 9-1, Air Filter, HEPA, for High Humidity, High Temperature Application; E 9-2, Air Filter, HEPA, General Purpose; and M 16-3, HEPA Filter Media, Glass Fiber, were revised and submitted to RDT for approval.

6.5 MATERIALS AND FABRICATION

(AEC Activity 04 60 80 03 1)

J. W. Anderson
R. O. Carden
R. M. Fuller
F. L. Hannon
J. N. Robinson
J. A. Woodley

A visit was made to Allegheny-Ludlum Steel Corporation, Watervliet, New York, to observe fabrication and inspection of seamless pipe and tubing in compliance with RDT standards that were applied in materials processing.

Work continued on the preparation of a number of materials and fabrication standards. Meetings were held with two material manufacturers to review and discuss the requirements of these standards.

7. GENERAL NUCLEAR SAFETY STUDIES

7.1 HTGR SAFETY PROGRAM OFFICE
(AEC Activity 04 60 70 01 1)

S. I. Kaplan W. E. Browning, Jr.

The HTGR Safety Program Office (HTGR-SPO) observes and evaluates research that contributes to the safety of High-Temperature Gas-Cooled Reactors (HTGRs) and prepares analyses and recommendations on this topic for the guidance of the AEC Division of Reactor Development and Technology (DRDT). It also is responsible for preparing a long-range plan for the HTGR Safety Program.

The HTGR-SPO represented DRDT at a meeting involving AEC Regulatory personnel and members of Gulf General Atomic, Inc. (GGA), and Public Service Company of Colorado (PSC). The meeting took place at the Bethesda offices of DRL on September 10 and comprised a series of informal discussions on safety behavior of the Fort St. Vrain reactor in connection with DRL's final evaluation of that plant relative to granting an operating permit. The major topics reviewed included fuel failures, failed fuel fraction due to manufacture, primary coolant fission-product inventory, reactivity transients, xenon transients, hydrolysis, steam leaks, radiation waste system, meteorology, calculation of doses, rapid depressurization accident, premanent loss of forced circulation, and safe shutdown cooling. The reaction of the AEC and ACRS personnel to the GGA presentation was generally favorable; future meetings will probably be held to consider other aspects of the design.

7.2 LOFT ASSISTANCE PROGRAM
(AEC Activity 04 60 60 05 1)

G. W. Parker W. J. Martin

The ORNL-LOFT assistance program is an engineering-scale study of the deposition behavior of fission products, including the chemical changes in radioiodine, in a containment atmosphere under simulated loss-of-coolant accident conditions. The present series of tests concerns only radioiodine behavior with respect to the effect of the organic coating of the containment walls on the deposition process and the conversion of radioiodine to persistent forms.

In the current reporting period, the fifth test in the radioiodine series was completed, and the sixth and final test is in progress. These two, which conclude the series in the original Amercoat liner, extend the study of the iodine mass-concentration effect to concentrations of 125 and 1000 $\mu g/m^3$. The preceding four runs, already reported, involved iodine mass concentrations from 0.1 to 35 $\mu g/m^3$. [In one run, only pure methyl iodide (CH_3I) was used.] In the fifth run (No. 120), the concentration of 125 $\mu g/m^3$ is comparable to a very modest iodine release from a modern power reactor but nonetheless far exceeds the present design level for LOFT, except in the event an enriched or seeded release test should be conducted. In the final test, the concentration of 1000 $\mu g/m^3$ represents the design conditions of emergency core coolant safety features of relatively low specific power reactors.

The experimental characteristics of the fifth run included provision for the total containment heating cycle to be performed with the use of low-pressure steam, which was released inside the containment vessel until the tank interior and walls reached a uniform design temperature of 115°C. This procedure (eliminating electric heating) provided a somewhat better simulation of the real containment wall thermal gradient and resulted in a significantly higher water content of the containment atmosphere (approaching 100% R.H.). The total volume of condensate collected (4666 ml) exceeded the average of the previous runs (2382 ml) by nearly a factor of 2. Similarly, the initial steam condensation rate also exceeded that in

previous runs by about a factor of 2. A compilation of the characteristics of five runs of this series is given in Table 7.1. The natural deposition curve for this run is shown in Fig. 7.1.

The activity distribution data for the fifth run show a marked change from the lower mass concentration runs in that nearly five times as much iodine was removed in the condensates. Since the condensation of steam

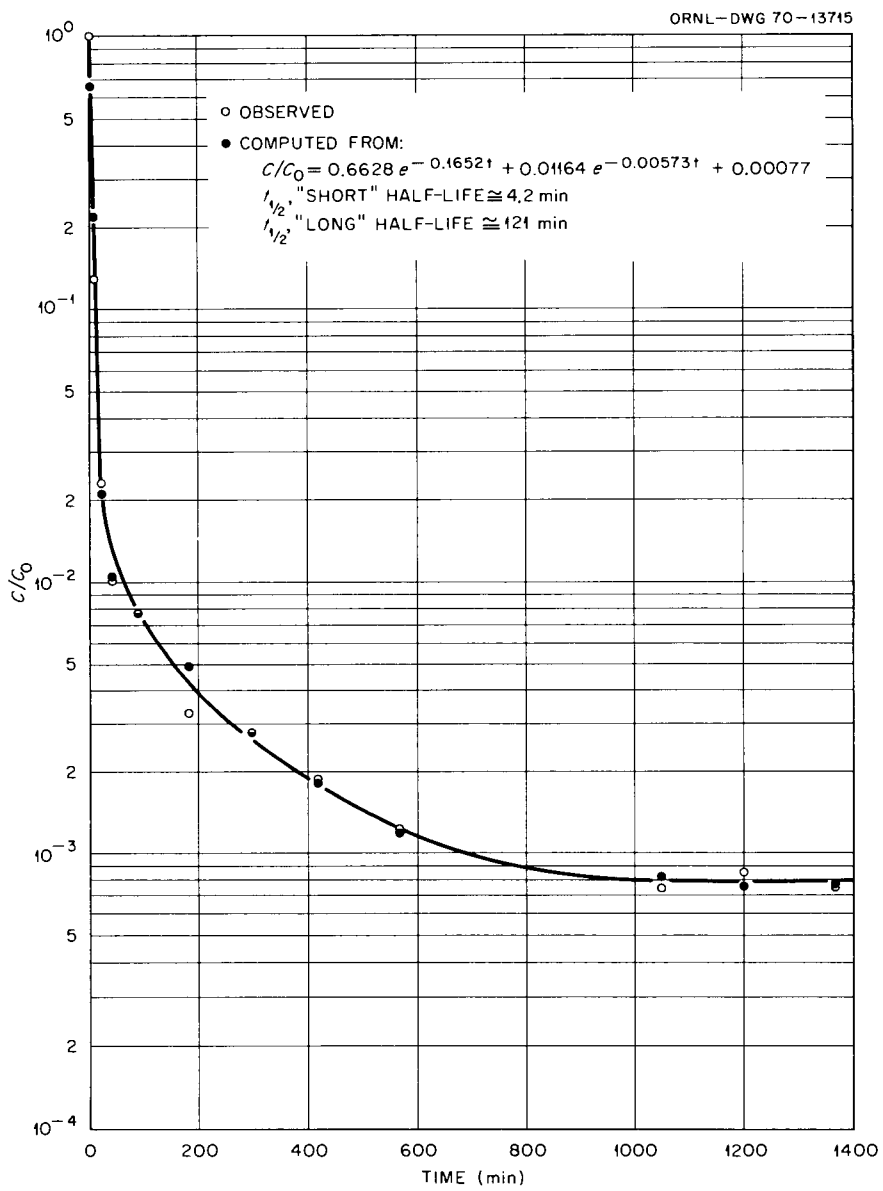

Fig. 7.1. Iodine Activity in CRI Containment Tank During Run CRI 120.

Table 7.1. Summary of Data Obtained in Tests in CRI

	Run 115	Run 117	Run 118	Run 119	Run 120
Iodine concentration in containment vessel, $\mu g/m^3$	0.1	5	5	35	125
Gas sample data, log of c/c_0 with time					
Short-life component, $T_{1/2}$, min	6	2.7	∿2.7	∿5	4.2
Long-life component, $T_{1/2}$, min	33	26	95	188	121
Constant term	0.036	0.018	0.012	0.0049	0.00077
Error mean square[a]	0.018	0.0058	0.0068		
Condensation (fraction in vapor phase) versus time					
$T_{1/2}$, min	292	568	353	251	215
Rate at time zero, ml/min	5.6	2.6	4.4	6.4	13.2
Total volume of condensate, ml					
Measured	2732	1776	2291	2527	4666
Computed	2630	2050	2270	2460	4570
Containment vessel temperature above ambient versus time, $T_{1/2}$, min	930	900	930	780	900
Deposition velocity, cm/sec					
From coupons		3.9×10^{-2}	3×10^{-2}	1.9×10^{-2}	8.2×10^{-2}
From containment vessel walls	0.68×10^{-2}	1.65×10^{-2}	1.84×10^{-2}		7.98×10^{-2}
Activity distribution, %					
On walls	92.8	95.6	91.8	94.4	73.9
In condensate	3.7	3.2	7.1	5.3	26.0
Pressure release	0.96	0.58	0.6	0.15	0.014
Recycle filter	0.99	0.38	0.3	0.15	0.05
Gas samples	0.15	0.08	0.2	0.02	0.015
CH_3I (% of inventory) after 1200 min	2.4	0.8	0.7	0.30	0.03

[a]Error mean square = $\left[\frac{(\text{Observed value} - \text{computed value})^2}{\text{Number of observations} - 2}\right]^{1/2}$; listed in the table to show how well an equation of two exponentials and a constant fits the data.

was much more rapid and produced much more water, this is not too surprising. The fact that the previous run (No. 119) did not show the effect, even though the mass concentration was higher than in the earlier ones, suggests that the steam condensation rate is more important than the mass effect.

An analysis of the behavior of radioiodine in relation to the Amercoat liner shows surprising uniformity over the range of iodine mass concentrations tested. The initial half-times for natural deposition have remained nearly constant, except for the initial run at the lowest mass concentration (0.1 $\mu g/m^3$). The major reason postulated for the difference is that the initial CH_3I composition of the iodine source may have comprised nearly one-third the preparation. It is also expected that the very low iodine concentrations may be more highly converted to CH_3I. Subsequent runs have shown a constant decrease in the percentage of iodine converted to CH_3I in a somewhat systematic relation, as shown in Fig. 7.2. The values used in

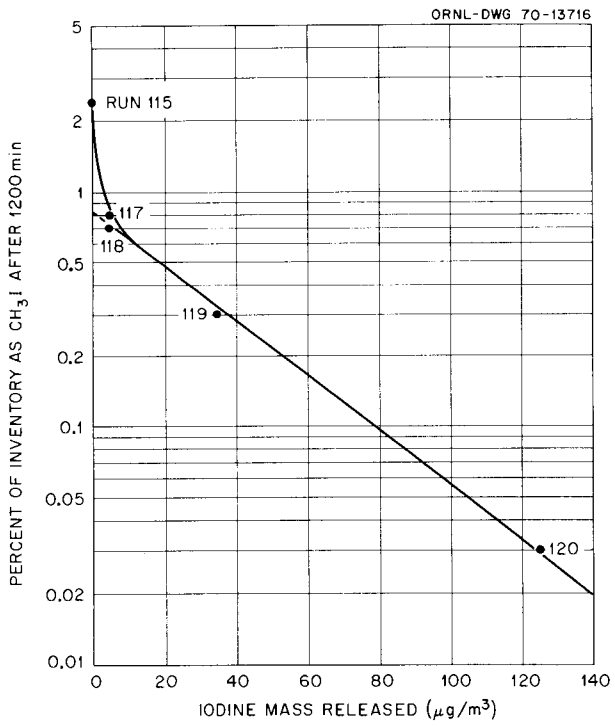

Fig. 7.2. Change in CH_3I Concentration in CRI Versus Total Iodine Released.

the graph were obtained by the moist-air elution method by which only that portion of the unreactive iodine that is rapidly desorbed from noniodized charcoal is considered as methyl iodide. This method tends to give a lower value than that obtained by categorizing all iodine which penetrates the HEPA filter and the silver membranes as CH_3I. The difference in the two values is presented graphically in Fig. 7.3 as a function of time, along with a corresponding plot of the precentage of iodine remaining airborne. In this run the change in the CH_3I fraction shows a positive slope, although in the previous runs it had always been negative. This variation in slope

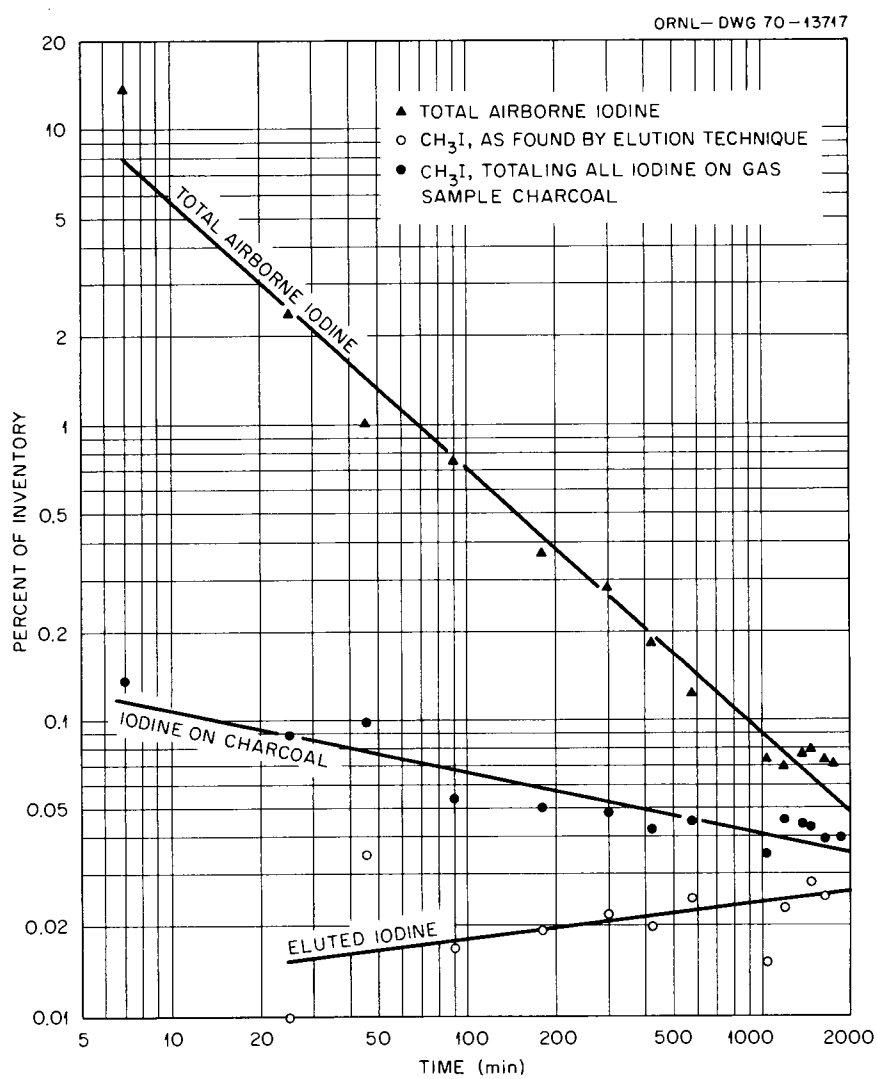

Fig. 7.3. Variation of CH_3I with Time in CRI Run 120.

is considered plausible, since the simultaneous processes of conversion by organic impurities and sorption in the Amercoat, while mainly sensitive to the effect of both iodine concentration and atmospheric impurities, is also affected by total steam condensation, water film thickness, etc. The rather sharp drop in the fraction of iodine converted to CH_3I suggests that another tenfold increase in iodine concentration for the last run will produce less than 0.01% as CH_3I. A least-squares fit to a straight line, with a limiting value of about 1% CH_3I at the end of the decay period (1200 min), gives

$$\% \ CH_3I = 0.83 \ e^{-0.0267C} ,$$

where C represents the initial iodine mass concentration in $\mu g/m^3$.

A single test of the rate of desorption of iodine from the painted liner was conducted at the end of the run (after washdown) by recycling 14.5 tank volumes of air through a test filter-absorber over a period of 18 hr. The total amount of iodine recovered was equivalent to 0.01% of that adosrbed in the paint (75% of total iodine). On the basis of a linear volume concentration for the 14.5 tank volumes, this would represent less than 1 part in 10^5 in the atmosphere over the washed paint surface.

The run now in progress at 1000 $\mu g/m^3$ will conclude the series and will provide a final test of the relation of iodine mass concentration to the amount converted to CH_3I. Following this run, the CRI containment liner will be replaced with a new Amercoat liner, and the planned tests of a cladding failure release with emergency core-coolant injection will be conducted.

7.3 REACTOR AIR-CLEANING SYSTEMS

(AEC Activity 02 04 20 90)

R. J. Davis J. Truitt
R. P. Shields

Air-cleaning systems are fequently employed in nuclear facilities either as a major element of a gaseous effluent discharge system or as an engineered safety device for use in accident situations. In either case the reliability of these air-cleaning systems under severe conditions is of concern. Two potential problems of current interest are (1) the ignition of charcoal adsorbers by fission-product decay heat and (2) the effect of velocity on the filter efficiency of "absolute" filter media for stainless steel oxide-UO_2 aerosols.

Ignition of Charcoal Adsorbers by Fission-Product Decay Heat

When considering the heat generation on charcoal adsorbers, there is a question of what fraction of the iodine produced as a daughter of the released tellurium should be considered as part of the heat source. Both iodine and tellurium are released to about the same extent,[1] but the tellurium may be adsorbed or react in a way that will preclude all the iodine produced by its decay from reaching the charcoal. Two cases have been considered: (1) the case where only the iodine released directly from the fuel reaches the charcoal and (2) the case where all the iodine, including that from tellurium decay, reaches the charcoal.

The calculation of the quantities of iodine available, based on either assumption, was done with the computer program called ORIGEN.[2] The calculation of the first case was based on a simple decay equation; an amount, $I_{0,i}$, of iodine isotope I_i is available at zero time; the amount decays accoring to the equation

$$I_i = I_{0,i}\, e^{-\lambda_i t} , \tag{1}$$

For the case in which the tellurium daughter products are included,

$$I_i = C_{1,i}\, e^{-\lambda_i t} + C_{2,i}\, e^{-\lambda_{2,i} t} . \tag{2}$$

Other assumptions were made in the calculations: (1) 25% of the iodine available in a 3000-Mw(t) reactor begins to deposit on the charcoal 10 min after reactor shutdown and (2) iodine is deposited on 2800 ft of charcoal adsorber 2 in. deep at a rate such that 95% of the total eventually deposited is deposited in about 100 min.

The results of the calculation are shown in Fig. 7.4; curve 1 was calculated by using the normal decay exponential given by Eq. (1), whereas curve 2 was calculated by using the normal decay exponential of Eq. (2); that is, all the iodine produced by decay of the tellurium released from the reactor was taken into account.

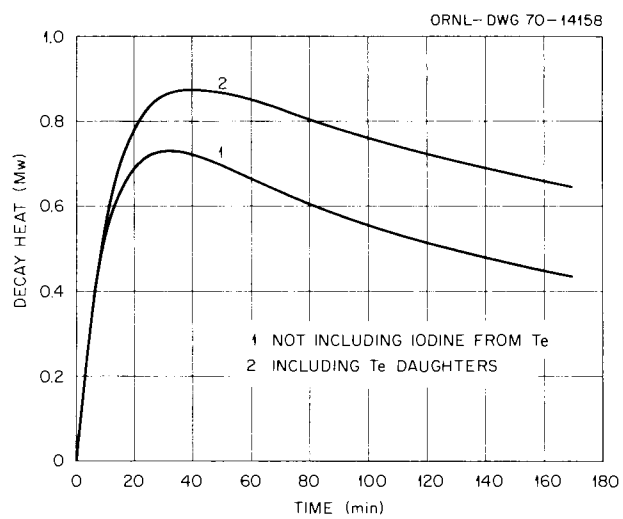

Fig. 7.4. Decay Power of Fission-Product Iodine from a 3000-Mw(t) Reactor Versus Time.

Previously reported[3] temperature rise (in charcoal bed) curves were not based on the total iodine (i.e., including tellurium daughters) and would, of course, have been increased by including the tellurium daughters.

Effect of Velocity on Filter Efficiency of Absolute Filter Media for Stainless Steel Oxide-UO_2 Aerosol

A program of measurements of filtration efficiency of commercially available absolute filter media for an electric-arc-generated aerosol of

stainless steel oxide-UO_2 particles was initiated. This aerosol is a good facsimile of anticipated reactor accident aerosols. The aerosol generation method, the particle-size distribution, the filter testing system, and the details of calculation of filter efficiency were described in connection with earlier work.[4] In principle, the method involves generating the aerosol in an arc to an irradiated stainless steel tube containing a UO_2 insert. The aerosol is filtered through a series of three filters at the face velocity of interest. The filter efficiency is defined as the ratio of the radioactive counts (due to ^{51}Cr in the irradiated stainless steel) in the first filter to the total counts on all three filters and assembly parts between filters.

The original system[4] was modified to operate at higher velocities, and some preliminary measurements on available media samples were made. These results are shown on Fig. 7.5 as a plot of penetration versus velocity. For orientation, the recommended velocity for operation of these filters is 5 ft/min, at which the nominal penetration is anticipated to

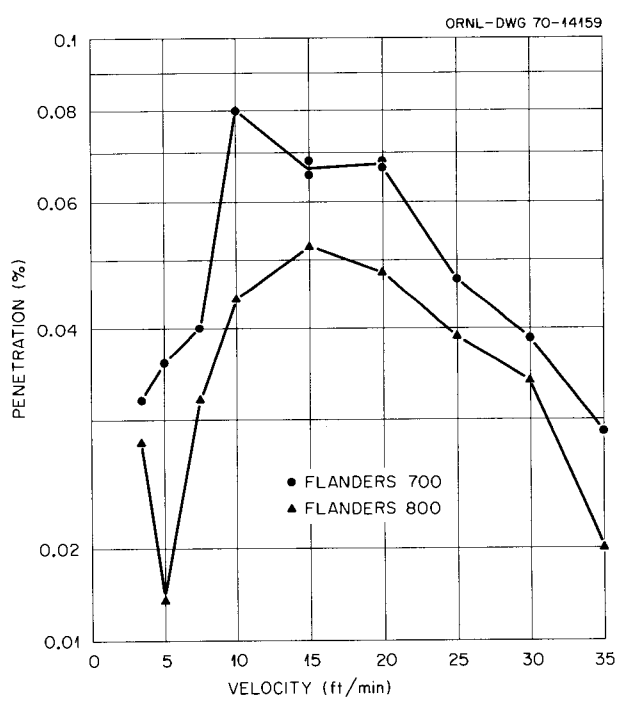

Fig. 7.5. Penetration of Filters as a Function of Face Velocity.

be 0.03%. As may be seen the nominally expected penetration occurred at 5 ft/min; there is a clear maximum in the penetration versus velocity curve in the range 10 to 20 ft/min. These tests will continue to include other commercial media.

References

1. W. E. Browning et al., Fission Product Behavior in Simulated Loss of Coolant Accident, p. 8, Nuclear Safety Program Semiann. Progr. Rept. June 30, 1965, USAEC Report ORNL-3843, Oak Ridge National Laboratory.

2. M. J. Bell, Chemical Technology Division Progr. Rept. May 31, 1969, USAEC Report ORNL-4422, pp. 89–94, Oak Ridge National Laboratory.

3. R. P. Shields, Ignition of Charcoal Adsorbers by Fission Product Decay Heat, paper presented at 11th AEC Air Cleaning Conference, Richland, Wash., Aug. 31–Sept. 4, 1970.

4. R. J. Davis, J. Truitt, J. S. Gill, and R. E. Adams, Removal of Radioactive Aerosols on High Efficiency Fibrous Filter Media, USAEC Report ORNL-4524, Oak Ridge National Laboratory, June 1970.

7.4 SEISMICITY AND THE SEISMIC RESISTANCE OF NUCLEAR POWER PLANTS

(AEC Activity 04 01 91 01 1)

G. D. Whitman J. Foster

The program of seismic research is concerned with supplying data that will contribute to (1) a more precise definition of earthquake conditions that must be considered in assessment of a site, (2) establishing the suitability of sites for reactors, and (3) improvement and verification of methods used in the design of nuclear power plants to withstand safely the effects of earthquakes. The principal activities during the reporting period were soils studies and analysis of data from blast-induced response testing of the experimental gas-cooled reactor plant and site.

An unsolicited proposal submitted to the AEC by Environmental Research Corporation is being reviewed. The document is titled "Proposal to Develop Design Seismic Input Criteria for the Siting of Nuclear Reactors." The ORNL review comments will be forwarded to AEC-DRDT in Washington.

EGCR Shaking Tests

An interim report on the blast tests conducted in July and August 1970 at the EGCR was prepared by UCLA. The primary objectives of these tests were to investigate the feasibility of using blast-induced vibrations as a method of determining the dynamic response of a nuclear power plant and to obtain experimental information on the nonlinear response of nuclear power plant structures and equipment due to high-force-level excitation. A preliminary review of the data indicates that significant results were obtained. The data from the tests are being analyzed in detail, and a final report will be prepared during the balance of the subcontract year ending in June 1971.

Soil Studies

Representatives of ORNL attended meetings in Washington with representatives of AEC-DRDT, DRL, and DRS to discuss and obtain comments on the

Shannon & Wilson—Agbabian Jacobsen Associates (SW-AJA) report, "Soil Behavior Under Earthquake Loading Conditions — Program Definition." Two consultants to ORNL under this program who were unable to attend the earlier review of this document in Oak Ridge during August attended the Washington meeting and supplied their written suggestions on the SW-AJA soil study subcontract work program. They were Professor R. F. Scott of the California Institute of Technology and Professor R. V. Whitman of the Massachusetts Institute of Technology. ORNL has sent SW-AJA a written commentary with suggested revisions for the proposed soils study program. The AEC groups have indicated that they will forward their comments to ORNL when they have completed their review. A meeting was scheduled with SW-AJA representatives at which to work out the required changes.

SW-AJA continued work on the literature review and state-of-the-art report on soil properties and behavior during earthquakes.

8. NUCLEAR SAFETY INFORMATION

8.1 NUCLEAR SAFETY INFORMATION CENTER
(AEC Activity 04 60 70 01 1)

J. R. Buchanan Wm. B. Cottrell

The Nuclear Safety Information Center was established in 1963 by the USAEC Division of Reactor Development and Technology to collect, evaluate, and disseminate nuclear safety information to governmental agencies, research and educational institutions, and the nuclear industry. The Center's basic computer file now contains abstracts of over 41,500 documents.

Computer Programming and Processing

Two additional CRT terminals were installed and placed in service during September, bringing the total number of scopes at NSIC to four. Their principal use is in adding abstracts, keywords, and bibliographic information to the computer storage file.

Modifications were made to all the teleprocessing programs in the NSIC system to improve the manner in which input/output machine errors are detected and handled when using direct-access devices.

In order to conserve direct-access storage and improve operational performance, the length of a document description is being changed from a maximum of 2496 characters to 1970. This change will necessitate the shortening of approximately 1% of the present records in the file. Because of the difficulty in processing records longer than a physical track on a direct-access device, the abstract and keywords were maintained on a separate file from the other data. Programming changes are being made to combine this information into a single file and have records no longer than that which can be accommodated on a track of an IBM-2321 Data Cell.

Nuclear Standards

The nuclear standards data base was increased by approximately 30% within the past two months. A new authority file for the organizations, committees, subcommittees, and tasks is being built in preparation for the next nuclear standards report. The use of this more comprehensive authority file has necessitated some modifications in the edit programs.

The output formats on the standards reports were altered slightly to enhance their use by nuclear standards personnel.

The sixth edition of the Compilation of National and International Nuclear Standards (Excluding U.S. Activities) was published as ORNL-NSIC-78 in October.

SDI Program

During this period 24 new SDI applicants were added to the program; there are now 1846 users. Eighty profiles were revised in this period.

Program and Project Information File Program

Three new users were added to the PPIF in this period, bringing the total number to 238. Two profiles were revised. This file now consists of a listing of 348 projects, or about 60% of the total expected to be included. During the past two months, the material under 117 of these projects was updated.

State-of-the-Art Reports

The report "Nuclear Reactor Siting Practice and Its Relationship to Population" is still undergoing final review.

Internal review of the report "Calculation of Doses Due to Accidentally Released Plutonium from an LMFBR" was completed, and a revised draft was submitted to AEC-RDT and selected Commission contractors for external review.

A state-of-the-art report on "Safety-Reliability of Reactor Systems" was drafted and is currently undergoing review.

Publications

NSIC reports published since the last reporting period are:

1. T. F. Lomenick and NSIC Staff, Earthquakes and Nuclear Power Plant Design, USAEC Report ORNL-NSIC-28, Oak Ridge National Laboratory, July 1970.

2. J. Paul Blakely, Compilation of National and International Nuclear Standards (Excluding U.S. Activities), 6th Edition, 1970, USAEC Report ORNL-NSIC-78, Oak Ridge National Laboratory, October 1970.

Summary of Information Activities

During the report period, the following requests were received and answered by NSIC personnel:

Technical inquiries (letter or telephone)	143
Specific NSIC reports and other nontechnical inquiries	165
Additions to NSIC reports distribution	3
Visits for consultation or use of reference material	16
Additions to SDI program	24
Additions to PPIF program	3

8.2 TECHNICAL PROGRESS REVIEW *NUCLEAR SAFETY*

(AEC Activity 14 02 01)

J. P. Blakely Wm. B. Cottrell

Nuclear Safety is a Technical Progress review that is prepared and edited at ORNL on a bimonthly schedule under AEC-DTI contract. The September–October 1970 issue (Vol. 11, No. 5, 78 pages, distributed September 18) contained articles by five authors from outside ORNL and by six authors from ORNL, including five *Nuclear Safety*/NSIC staff members. The lead article was an adaptation of the Minnesota oral presentation by Howard C. Brown, who pointed out that in the spring of 1969, the U.S. Atomic Energy Commission decided to take the case for nuclear power directly to the public by way of the town hall and the village square, the university symposium, and the speaker circuit. A factual approach has been useful in countering misinformation and in allaying unfounded fears, but the initial outings also demonstrated that the facts do not always speak for themselves because they are highly complex and occasionally challenged by small segments of the scientific fraternity. It has been necessary to translate technical jargon into everyday language and to learn to compete with the showmanship of critics. The need for nuclear electric power is increasingly recognized, but no substantial abatement in public concern for the environment is in sight. Larger segments of the public recognize that the solution to the environmental problem is neither to turn the clock back nor the light switch off, and they are prepared to pay a little more for a clean environment.

Other articles dealt with the water reactor safety program plan (by H. F. Bradburn, C. H. Cooper, and C. E. Gilmore, Idaho Nuclear Corporation), criteria and requirements for RDT plant protection systems (by C. S. Walker, ORNL), fission-product behavior in sodium (by A. W. Castleman, Jr., ANL), radioactive waste disposal by hydraulic fracturing (by Wallace de Laguna, ORNL), and a book review on safe operating of nuclear power plants (by W. R. Casto, ORNL). The issue concluded with the regular current-events-type features by W. R. Casto, A. W. Savolainen, H. B. Whetsel, and J. P. Blakely (all ORNL).

Makeup on the November—December 1970 issue (Vol. 11, No. 6) was delayed by preparation of the annual index for 1970, which is to be bound in the issue. Copy was sent to the printer in late October for distribution in mid-to-late-November.

External review was completed on the draft (ORNL-TM-3087) of the January—February 1971 issue (Vol. 12, No. 1). Comments and drafts were sent to authors for consideration and response, and revisions were transmitted to DTIE in late October. Distribution is scheduled for early January.

Future issues of *Nuclear Safety* through Vol. 12, No. 6 are in various stages of development.